AD-A034 047 BOSTON COLL CHESTNUT HILL MASS SPACE DATA ANALYSIS LAB F/G 9/2
NUMERICAL AND DATA ANALYSIS TECHNIQUES APPLIED TO SCIENTIFIC RE--ETC(U)
MAR 76 J E MARTINE, L F POWER F19628-73-C-0136

UNCLASSIFIED BC-SDAL-76-2 AFGL-TR-76-0091 NL

1 OF 2
AD
A034047

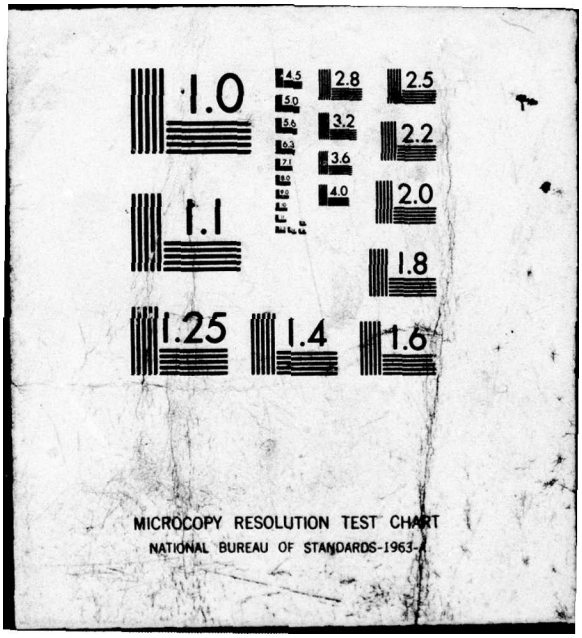
1.0
1.1
1.25
1.4
1.6
1.8
2.0
2.2
2.5
2.8
3.2
3.6
4.0
4.5
5.0
5.6
6.3
7.1
8.0
MICROCOPY RESOLUTION TEST CHART
NATIONAL BUREAU OF STANDARDS-1963-A

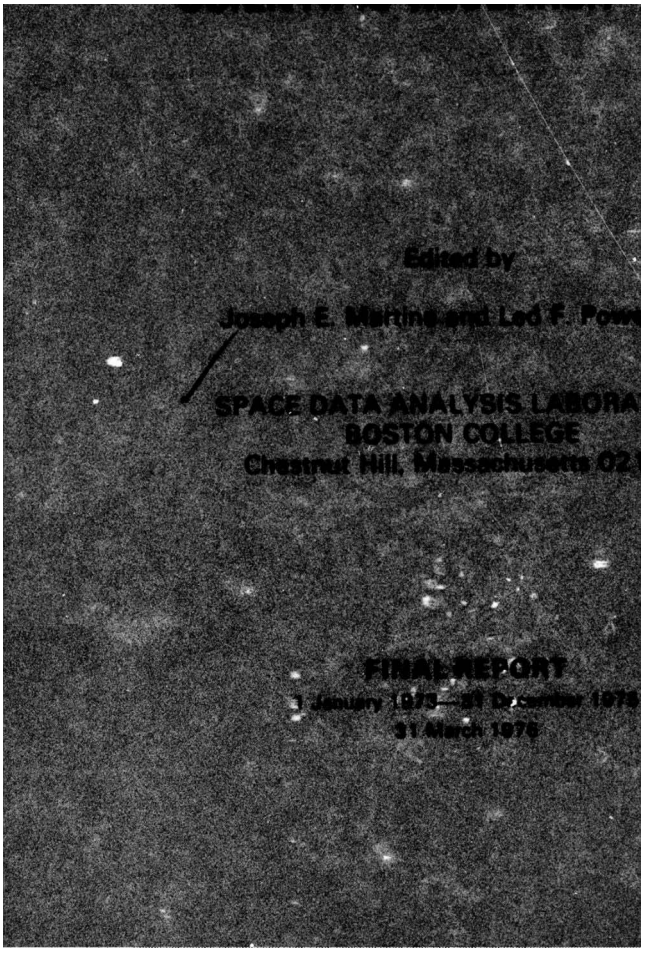
Edited by
Joseph E. Martine and Led F. Powe
SPACE DATA ANALYSIS LABORA
BOSTON COLLEGE
Chestnut Hill, Massachusetts 02
FINAL REPORT
1 January 1975—31 December 1975
31 March 1976

The program reads input from a packed magnetic tape generated at a prior

UNCLASSIFIED

SECURITY CLASSIFICATION OF THIS PAGE (When Data Entered)

REPORT DOCUMENTATION PAGE	READ INSTRUCTIONS BEFORE COMPLETING FORM
1. REPORT NUMBER: AFGL-TR-76-0091	2. GOVT ACCESSION NO.
3. RECIPIENT'S CATALOG NUMBER	
4. TITLE (and Subtitle): NUMERICAL AND DATA ANALYSIS TECHNIQUES APPLIED TO SCIENTIFIC RESEARCH, II.	5. TYPE OF REPORT & PERIOD COVERED: Scientific, Final rept. 1 Jan 73 - 31 Dec 75
	6. PERFORMING ORG. REPORT NUMBER: BC-SDAL-76-2
7. AUTHOR(s): Joseph E. Martine, Editor; Leo F. Power, Jr., Editor	8. CONTRACT OR GRANT NUMBER(s): F19628-73-C-0136
9. PERFORMING ORGANIZATION NAME AND ADDRESS: Trustees of Boston College, Chestnut Hill, Massachusetts 02167 (Sparse data analysis n/a)	10. PROGRAM ELEMENT, PROJECT, TASK AREA & WORK UNIT NUMBERS: 136p.
11. CONTROLLING OFFICE NAME AND ADDRESS: Air Force Geophysics Laboratory, Hanscom AFB, Massachusetts, Contract Monitor: Dr. Paul Tsipouras (SUYA)	12. REPORT DATE: 31 Mar 76
	13. NUMBER OF PAGES: 136
14. MONITORING AGENCY NAME & ADDRESS (if different from Controlling Office)	15. SECURITY CLASS. (of this report): Unclassified
	15a. DECLASSIFICATION/DOWNGRADING SCHEDULE

16. DISTRIBUTION STATEMENT (of this Report)

Approved for Public Release; Distribution Unlimited

17. DISTRIBUTION STATEMENT (of the abstract entered in Block 20, if different from Report)

1- A022 677 4- A030 285

3- A029 440

18. SUPPLEMENTARY NOTES

19. KEY WORDS (Continue on reverse side if necessary and identify by block number)

Numerical Analysis
Modelling
Data Analysis
Curve-fitting
Mathematical Analysis

20. ABSTRACT (Continue on reverse side if necessary and identify by block number)

This report describes selected mathematical analysis, numerical analysis, and computer programming problems performed under Contract F19628-73-C-0136.

Each problem selected is presented in capsule form and the analysis and computer techniques are outlined.

DD FORM 1 JAN 73 1473 EDITION OF 1 NOV 65 IS OBSOLETE

UNCLASSIFIED

SECURITY CLASSIFICATION OF THIS PAGE (When Data Entered)

403 460

PREFACE

The effort described in this report is a continuation in kind of that put forth under Air Force Contract F19628-70-C-0120. That effort was summarized in a Final Report dated 31 January 1973, titled Numerical and Data Analysis Techniques Applied to Scientific Research, AFCRL-TR-73-0433.

767607

The editors and contributors wish to express their thanks to Dr. Paul Tsipouras of the Air Force Geophysics Laboratory (AFGL) for his invaluable assistance in the development of solutions to many of the problems described herein. A similar debt of gratitude is owed to all problem Initiators from AFGL for providing the detailed background information regarding their particular problems.

Finally, our appreciation goes out to the support staff of this laboratory for their continual assistance in the program preparation of these problems and in particular to Miss Mary L. Kelly for typing this report.

LIST OF CONTRIBUTORS

Robert F. Boudreau

Neil J. Grossbard

Joseph E. Martine

Theodoros Persakis

Philip C. Powell

Frona B. Vicksell

TABLE OF CONTENTS

TABLE OF CONTENTS (Cont.)

DABOS Modification

Initiator: Mrs. I. Hussey

Problem No: 3018-3 Project No: 0001

The purpose of this work was to combine into one program two earlier versions of DABOS, which is an orbit determination and ephemeris computation program. From a mathematical point of view, the difference between the two earlier versions was that one used the Jacchia 1964 atmospheric density model and the other used the Standard Atmosphere Supplements 1966. These two density models are rather similar and it was possible to intertwine the formulae in a very efficient manner, allowing the user to select which model was to be used for a particular run.

Short-Term Power Spectra of Troposcatter Signals

Initiator: Mr. U. Lammers

Problem No: 30[illegible]3 Project No: 8682

This problem required the analysis of sets of equally spaced data (X(I)). A program was written which transformed the original input data (X(I)) as follows:

$$Y(I) = 10^{X(I)/20}$$

The resulting Y(I)'s were then Fourier analyzed using a Fast Fourier Transform and the results graphically displayed for the Initiator. In addition, the program was written with the option of analyzing various segments of the data and producing graphic displays of each segment.

Analysis of Electromagnetic Waves and Turbulence

Initiator: Dr. R. Fante

Problem No: 3026-7 Project No: 5635

This problem required the generation of four computer programs, each of which studied the behavior of electromagnetic waves in the ionosphere. The documentation titles for these four programs are:

1. Calculation of the Frequency Spectrum of a Laser Beam Propagating in Turbulence with a Von Karman's Spectrum.
2. The Frequency Spectrum of a Plane Wave Propagating in Turbulence with Constant Winds.
3. The Frequency Spectrum of a Plane Wave Propagating in Turbulence with Random Winds, and
4. The Frequency Spectrum of a Plane Wave Propagating in Turbulence with Random Winds varying along the Propagation Path.

The first program approximated $S_o(\Omega)$ where:

$$S_o(\Omega) = \frac{1}{\pi} \int_0^\infty dRo \cos(\Omega Ro) \; [FU(Ro)]$$

where:

$$FU(Ro) = 2S * (SIG*XKO*BLO)^2/(4\pi^2) \int_0^\pi \theta t \int_0^\infty dX \phi(X,Ro,\theta)$$

with:

$$\phi(X,Ro,\theta) = X \exp\left\{ \frac{P}{2} X^2 + \psi(Ro,X,\theta) \right\}$$

$$\psi(Ro,X,\theta) = \int_0^T dy \; F(y)$$

$$F(y) = [1.5Z^2 - 1.86Z^{5/3} - .254Z^{11/3}] \text{ if } Z < .7$$

$$= -1 + \frac{.489}{(Z)^{-3}}, \text{ if } .7 \leq Z \leq 1.5$$

$$= -1 + .994\sqrt{\frac{\pi}{2}}\, Z^{1/3}\, e^{-z}\left\{1 + \frac{2}{9Z} - \frac{7}{81Z^2} + \frac{175}{2187Z^3}\right\}, \text{ if } 1.5 < Z$$

where

$$Z = [Ro^2 + 2Xy\ Ro\ \cos\theta + X^2y^2]^{1/2}$$

$$SIG = .78 * XKO^2 * CN2 * \exp(\frac{5}{3}\ \ln(BLO))$$

$$\rho_2 = -(S*SIG^2/(4\pi)) + (\frac{\pi}{4XKO^2*S} + \frac{S}{(4\pi F^2)}) * T^2$$

$$+ SIG * S * T/(2\pi F))\ (XKO*BLO)^2$$

The integral $\psi(Ro,X,\theta)$ was evaluated by finding all the discontinuities in F(y) and using a Simpson's rule type, numerical integration technique, for each of the continuous line segments in F(y) for $o \leq y \leq T$. The integrals over θ and X used the technique described in reference 1. Here the X integration was performed from ϕ to XMAX, where XMAX is an input parameter, just as S, XKO, BLO and CN2.

The integration over Ro was performed from o to $N\Delta Ro$, where ΔRo and N are input parameters, where

$$\Omega_j = \frac{2\pi j}{NMAX*\Delta Ro} \text{ for } j=0,1, \ldots, \frac{NMAX}{2}$$

---

1 A New Adaptive Simpson Integration Routine, Neil Grossbard, Space Data Analysis Laboratory, Boston College, Chestnut Hill, Mass. 02167; AFCRL-70-0504, Scientific Report No. 1, September 1970.

The $S_o(\Omega_j)$'s were calculated by using a NMAX long Fast Fourier Transform to simulate a trapezoidal rule. Here NMAX = 2^{ℓ} (ℓ integer) and $2^{\ell-1} < 2N \leq$ NMAX.

The second program approximated $S_1(\Omega)$ where:

$$S_1(\Omega) = \frac{1}{\pi} \int_0^{\infty} du \cos(\Omega u) \left[e^{T(\phi(u)-1)}\right]$$

where

$$\phi(\eta) = 1 + 1.5\,\eta^2 - 1.86\,\eta^{5/3} - 0.254\,\eta^{11/3} \quad \text{if } 0 \leq \eta < .7$$

$$= \frac{.489}{(\eta)^{0.8}} \quad \text{if } .7 \leq \eta \leq 1.5$$

$$= .994\sqrt{\frac{\pi}{2}}\,\eta^{1/3}\,e^{-\eta}\left\{1 + \frac{2}{9\eta} - \frac{7}{81\eta^2} + \frac{175}{2187\eta^3}\right\} \quad \text{if } \eta > 1.5$$

As in the first program a set of Ωj values was obtained by using a Fast Fourier Transform on $\frac{1}{\pi}\left[e^{T(\phi u)-1)}\right]$.

The third program approximated $S_2(\Omega)$

$$S_2(\Omega) = \frac{2e^{-T}}{\pi\sqrt{2\pi}} \int_0^{\infty} du \cos(\Omega u) \int_0^{\infty} d\xi\, e^{-\xi^2/2} \left[e^{T\phi(\xi u)} - 1\right]$$

Here the ξ integration was performed from 0 to TMAX, an input parameter. The u integration was again performed using a Fast Fourier Transform to get a set of answers at points Ωj as in the first problem.

The fourth program approximated $S_3(\Omega)$ where:

$$S_3(\Omega) = e^{-T} \int_0^{\infty} dx \cos(\Omega X) \exp\left\{\frac{5}{6}\,T \int_0^{\infty} \frac{du\, J_0(xu^{1/2}) \exp\left[-u(10^{-6}+\frac{1}{6}X^2R)\right]}{(1+u)^{11/6}}\right\}$$

where J_0 is the Bessel Function of zero order. Here the u ingegration was performed from zero to TMAX, where TMAX = minimum (UMAX, $\frac{T\ell^2}{X^2}$, if $X \neq 0$). Here UMAX and $T\ell$ are input parameters. $T\ell$ is generally set to be the argument of the ℓ^{th} zero of the Bessel Function. The value of ℓ is also read in and the numerical integration starts with $4\ell + 1$ equally spaced values so that no oscillation of the Bessel Function will be missed. The X integration is again performed using a Fast Fourier Transform to get a set of answers at points Ωj as in the first problem.

These programs lead to very fast, fairly accurate answers (at least two significant figures). The Initiator indicated that these results were helpful in his analysis of electro-magnetic signals in the ionosphere.

Digicoder Presentation of Arrival Angle of Ionospheric Waveforms

Initiator: Dr. W. Pfister

Problem No: 3028-6 Project No: 7663

A technique for measuring drift motion and turbulence characteristics of various layers of the ionosphere consists of receiving reflected signals from the ionosphere at various pulse frequencies in the MHz ranges of closely spaced antennas and digitally recording the complex amplitudes of the echo pulses in the time domain. This is accomplished by use of a Complex Amplitude Multifrequency Scanner in conjunction with a digital ionosonde.

The time domain information can subsequently be spectral analyzed for power content, and the power per unit area can be presented graphically to represent characteristic ionospheric fluctuations.

The purpose of this problem is to reconstruct spectral information and to present a map-like display of reflected waveform axial projections by use of a digicoder printing device.

A digicoder display consists of a continuous printout containing 4 lines of data. Each line consists of 256 characters, allowing a 2-dimensional map of (256 x N) characters to be printed. A unique numerical character set, specific to the digicoder, allows 16 values of perceptive weight to be observed, thereby, adding the dimension of color density (white to black) to the numeric content of each printed character. Thus, the points in a peak of 2-dimensional data are presented as a darker area relative to background information, when observing the total map of, say, (128 x 256) points, yet, the specific value of each individual point is retained on any given scale of 16-point resolution.

Input to the computer program consists of Doppler Frequency-related Power, Coherence, and Phase spectra previously calculated from the Fourier Transform of the time domain raw data.

Basically, the phase relations are translated into angles in space, as functions of the recording hardware operating frequencies and the geometry of the receiving antenna orientations.

The locations of the reflecting regions are calculated from the cross-spectral phases between pairs of antennas, at those Doppler shifts characterized by peaks in the Power spectrum. The cross-spectral phase provides an estimate of the direction of the reflecting region. A band of width $\Delta\phi$ of the reflecting region is related to the given spectral coherency (COH) according to:

$$\Delta\phi = \pm \pi(1-\sqrt{COH})$$

The intersection of 2 bands from 2 antenna pairs provides a parallelogram area:

$$A = \frac{2}{\sqrt{3}} \frac{\lambda^2}{\alpha^2} (1-\sqrt{COH_1}) (1-\sqrt{COH_2})$$

where λ = the transmitter operating wavelength
and α = the length of the antenna pair baseline

The power density per unit area is defined as W/A, where W in this program is the average power from 3 receiving antennas at a particular Doppler frequency.

From the geometry of the 3 receiving antennas, three such parallelograms can be constructed, and from each parallelogram, trapezoidal areas can be projected onto X and Y axes oriented in the N-S and E-W directions. The sum of the heights of 3 projected trapezoidal areas on a given axis is proportional to the spectral density, W, and is indicative of the strength of the power content of the given region. The angular location of the reflecting region (see mathematics below) is given from the range over which each summed trapezoidal area extends on each projection axis. From the sums of the trapezoidal projections, then, two intensity modulated lines can be displayed on the digicoder, each as a function of Doppler frequency and arrival angle.

It should be noted that the program contains test criteria to avoid phase ambiguities in the reflected signals. It was desired that the range of the display correspond to the principal range of phase between 2 antennas, $-\pi$ to π radians. The test criteria are dependent upon the antenna pair chosen for observation and the projection axis.

Each digicoder output map is specific to a given time of recording, which is contained in a preface (identification) area preceding each power density display. In the digicoder printout, 128 points of Doppler frequency are presented along the vertical (length) of the display and 256 points (128 per N-S and E-W projection axis) along the horizontal (width). In addition, markers are presented every 16^{th} character along the horizontal in the preface area to assist in notation of scale. In the same manner, preface identification characters are presented every 16^{th} line along the left side of the vertical to denote the scale of the Doppler frequency.

Overall, for one subcase of time, four such (128 x 256) point maps are generated, each corresponding to a given height range gate on the recorder.

The program reads input from a packed magnetic tape generated at a prior stage of production processing. This program then generates digicoder information on packed magnetic tape, to be used at a later stage of data processing as digicoder input.

Mathematics

1 Location of reflecting areas on X- and Y-axis:

Antenna Pair	X Axis Location	Y Axis Location
12 , 23	$-\phi_{12} - \phi_{23} + 2\Omega/100$	$\frac{1}{\sqrt{3}}(-\phi_{12} + \phi_{23})$
23 , 31	$\phi_{31} + 2\Omega/100$	$\frac{1}{\sqrt{3}}(2\phi_{23} + \phi_{31})$
31 , 12	$\phi_{31} + 2\Omega/100$	$\frac{1}{\sqrt{3}}(-\phi_{31} + 2\phi_{12})$

where ϕ_{12}, ϕ_{23} and ϕ_{31} represent cross-spectral phase from antenna pairs 12, 23, 31.

and Ω = Doppler frequency under investigation.

2 Maximum Spectral Intensity projected onto trapezoidal areas along the E-W (Y) axis.

Area Reference No.	Intensity
2	$Q \cdot \frac{\sqrt{3}}{\Delta\phi_{12} + \Delta\phi_{23} + \lvert\Delta\phi_{12} - \Delta\phi_{23}\rvert}$
3	$Q \cdot \frac{\sqrt{3}}{2\Delta\phi_{23} + \frac{\sqrt{3}}{2}\Delta\phi_{31} + \lvert 2\Delta\phi_{23} - \frac{\sqrt{3}}{2}\Delta\phi_{31}\rvert}$

Area Reference No.	Intensity
1	$Q \cdot \dfrac{\sqrt{3}}{\frac{\sqrt{3}}{2}\Delta\phi_{31} + 2\Delta\phi_{12} + \left\lvert\frac{\sqrt{3}}{2}\Delta\phi_{31} - 2\Delta\phi_{12}\right\rvert}$

where $Q = \frac{W}{3}\frac{2\pi\alpha}{\lambda}$

W = average power at a particular Doppler frequency

λ = operating wavelength (meters)

α = antenna baseline (meters)

3 Maximum Spectral Intensity projected onto trapezoidal areas along the N-S (X) axis.

Area Reference No.	Intensity
2	$Q \cdot \dfrac{1}{\Delta\phi_{12} + \Delta\phi_{23} + \left\lvert\Delta\phi_{12} - \Delta\phi_{23}\right\rvert}$
1,3	$Q \cdot \dfrac{1}{2\Delta\phi_{31}}$

Doppler Shift/Ionospheric Reflection

Initiator: Dr. W. Pfister

Problem No: 3028-7 Project No: 8658

This program is part of a data processing project called DAASM (Doppler Angle of Arrival Spectral Measurement), for detailed study of the ionosphere. This particular effort involves the estimation of Doppler shift and the combining of three Fourier transforms. Signals generated in this case by a moving aircraft are reflected by the ionosphere and measured on the ground. The results are recorded on magnetic tape as a time series of digitized complex numbers. The computer program reads the magnetic tape, isolates samples about one minute long, calculates three overlapping Fourier transforms from each sample, and attempts to determine the Doppler shift of the strongest frequencies by looking for a consistent phase shift among the three transforms. Then the three transforms are combined, taking into account the Doppler shift. The results are written on two magnetic tapes, one in a format suitable for the Digicoder plotter, the other for input to other programs.

The raw data input tape is pre-positioned at the desired starting case. An input card is read specifying the number of consecutive cases to be processed. Each case occupies seven physical records on the input tape.

Each case is then handled as follows:

The first record is skipped. Prefaces are extracted from the remaining records and printed. Record numbers are checked. If normal sequence is broken, the program starts again from the current record. Data are packed into the array BUF. Then, taking one frequency and one antenna at a time, we obtain three Fourier transforms from the three interlaced complex data sets. (The three interlaced sets were all sampled the same way; sets 2 and 3 are just $\beta = 6/25$ of a step later than sets 1 and 2 respectively, where one step is the time between consecutive samples in one set, .25 seconds).

Each Fourier transform contains 256 complex points g_m, $m = 1,2,\ldots,256$, each point representing the summed contributions of a whole family of aliased

frequencies (m-1 + 256 n)/64 Hertz, n = 0, ±1, ±2,... The problem is to pick the n corresponding to the "best" (usually strongest) frequency in the original sampled signal. For this purpose we assume that a single value of n accounts for all the aliasing in the neighborhood of the best frequency. We divide the aliased frequency range into four equal segments and analyze each segment to see which best fits the model.

A displacement of Δt seconds in the time series sample causes phase shifts proportional to frequency in the Fourier transform. If we assume as above, that entry g_m in the transform is all due to one frequency, namely (m-1 + 256 n)/64 Hertz (n is a fixed but unknown integer), then a Δt displacement will cause a phase difference of $\Delta t \cdot (m-1 + 256\ n)/64$ cycles. And, if the same n applies to a sequence of g_m's, the phase differences between two interlaced transforms will be a linear function of m.

Let $\{g_{mk},\ m=1,2,\ldots 256\}$ be the transform of the k^{th} interlaced time series, k=1,2,3. The following expression uniquely defines p_{mk}:

$$g_{mk} = ||g_{mk}||\ \exp\ (2\pi i p_{mk}), 0 \leq p_{mk} < 1.$$

We have $\Delta t = .25\beta$ seconds, so, if our model were correct we would have:

$$(p_{m,k+1} - p_{mk})_{mod1} = (\beta[(m-1)/256+n])_{mod1}$$

or

$$c_{mk} \overset{def}{=} (p_{m,k+1} - p_{mk} - \beta(m-1)/256)_{mod1} = (\beta n)_{mod1}$$

In other words, the c_{mk} should all be about the same and will tell us what n is.

In each segment of the transform, (m = 1-64 or 65-128 or 129-192 or 193-256), we calculate the weighted average A of unit vectors with argument $2\pi c_{mk}$ on the complex plane. The weighting is with respect to power.

$$A = \left(\sum_{k=1,2} \sum_{m} ||g_{mk}\ g_{m,k+1}||\ \exp\ (2\pi i c_{mk}) \right) \Big/ \left(\sum_{k=1,2} \sum_{m} ||g_{mk}\ g_{m,k+1}|| \right)$$

$$= \left(\sum_{k=1,2} \sum_{m} ||g^{*}_{mk}\ g_{m,k+1}\ \exp\ [-2\pi i\beta(m-1)/256]|| \right) \Big/ \left(\sum_{k=1,2} \sum_{m} ||g_{mk}\ g_{m,k+1}|| \right)$$

We also calculate in each segment an estimate of the scatter of the c_{mk},

$$\alpha = (1-AA^{*})^{1/2}$$

We pick the segment with the smallest scatter. The corresponding value of A yields our best estimate of n; we pick an n minimizing:

$$||A/||A|| - \exp\ (2\pi i\beta n)|| \ .$$

Since $\beta = 6/25$ and n is an integer, it suffices to consider $n = 1,2,\ldots,25$.

With n and the best segment well determined, the three interlaced transforms may be combined in a meaningful way. Let m_b be the final subscript of the best segment. $m_b = 64$, 128, 192 or 256. The new, combined transform will cover the frequency range:

$$(m_b - 128 + 256\ n)/64 \text{ Hertz}$$

to

$$(m_b + 127 + 256\ n)/64 \text{ Hertz}.$$

We arbitrarily assume that the phase shift is linear over that entire range and that the g_{mk}'s are all aliased from that range. The phase of each g_{m1} and g_{m3} is modified to align with g_{m2}, and the three are averaged. The results are plotted and the digicoder with the $(m_b - 1 + 256\ n)/64$ Hertz line is in the middle (i.e., the 128th point).

This method breaks down for cases in which the original signal contains two good frequencies which cannot without aliasing be included in a single 256 point range. Only one of the peaks will be smoothed correctly.

NOTE: The Fourier transform subroutine used by this program delivers the usual backward transform. The write-up above, however, is from the point of view of the usual forward transform, which gives a larger phase to a signal sampled later. Thus, the program's G arrays are the conjugates of the g's in the write-up, the original signal also having been conjugated.

In other words, given a time series $f_1,\ldots,f_{256}$, subroutine FORER calculates $g_1,\ldots,g_{256}$ with

$$g_{m+1} = \sum_{j=0}^{255} f_{j+1} \exp (imj\ 2\pi/256)$$

of

$$g^*_{m+1} = \sum_{j=0}^{255} f^*_{j+1} \exp (-imj\ 2\pi/256) .$$

The computer program outputs a heading including the input value of the maximum number of cases to process.

Then, for records 2-7 of each case, it prints the prefaces. For each of the two frequencies, first antenna only, these are followed by the segment number of the best segment, the best value of n in that segment, the point number in the original Fourier transform which will appear on the extreme right when re-arranged for the Digicoder plot, and the number of Hz, module 100, at the center of the Digicoder plot. Then come the βn averages and associated α estimates for each of the four segments.

Input Tape Format

Each case occupies seven physical records. Each physical record is 343-344 words, comprising 3430 to 3440 6-bit bytes. Before the input can be interpreted, it must be aligned properly. Let k be the minimum integer such that $250 < k < 323$ and such that the k^{th} byte of the record is the beginning of a 288 x 11 array of bytes with all zeros in the first 18 rows. If there is no such k, set k to 271. Slide the entire record so that the k^{th} byte will be in the 271^{st} position. If $k < 271$ fill the initial part of the buffer with zeros. Then the following format applies.

Consider the bytes to be arranged in standard Fortran order in an array dimensioned (3, 2, 3, 4, 48). (The last few positions of this array will be unoccupied). Then, for $\ell = 1, 2, 3$, the (i, j, k, ℓ, m)-th byte of the array is the i^{th} byte of the m^{th} sample from the ℓ^{th} interlaced set from the k^{th} antenna at the j^{th} carrier frequency. The three bytes ($i = 1,2,3$) in each sample are:

byte 1: $|Re(z)|$

byte 2: 1 in the 3^{rd} bit (10 octal) if and only if $Re(z) \geq 0$, plus 1 in the 4^{th} bit (4 octal) if and only if $Im(z) \geq 0$.

byte 3: $|Im(z)|$

For $\ell = 4$, $m > 3$, there is no data.

For $\ell = 4$, $m = 1,2,3$, there are 18 bytes available for each of three "prefaces".

Preface 1 -	bytes 1-3	Code digits 6, 7, 3
	bytes 4-6	Three decimal digits of day of year
	bytes 7-12	Six decimal digits of hours, minutes, and seconds.
	bytes 13-14	Code

Preface 1 - (Cont.)	bytes 15-16	Two digits containing double the record number within this case.
	bytes 17-18	Code
Preface 2 -	bytes 1-3	Three decimal digits giving frequency setting of 1st antenna, 1st frequency.
	bytes 4-6	Same as 1-3 but for 2nd frequency.
	bytes 7-12	Same as 1-6 but for 2nd antenna.
	bytes 13-18	Same as 1-6 but for 3rd antenna.
Preface 3 -	bytes 1-18	Same as Preface 2, except 3 digits give range setting instead of frequency setting.

There is an end-of-file after the last record of the last case.

If the first byte of a frequency is 0, 1, 6, 7, 10, 11, 12, or 13, the corresponding raw sample must be conjugated to compensate for a hardware difference in the way the data were collected.

Output Digicoder Tape Format

The output tape is formatted for the Digicoder, a machine which produces shaded plots.

The program writes two files, one for each frequency. Each file has a header record, repeated 3 times, then one data record for each case on the input tape. The header record contains preface information in various standard arrangements.

Each record has 245 words, or 2450 6-bit bytes. The last two bytes are zero. The other 2448 are a 408 x 6 array, plotted in six lines. The first 24 bytes of each line are a preface, the same for all six lines, as follows.

Bytes 1-12:	Same as corresponding bytes of Preface 1 of record 2 of this case from the input tape.
Byte 13:	Decimal integer 13
Byte 14:	Decimal integer 15
Bytes 15-16:	Hz modulo 100 of center line, point 129.
Bytes 17-18:	From input tape.
Bytes 19-21:	Frequency bytes of first antenna, from Preface 2 of record 2 of input tape, bytes 1-3 or 4-6.
Bytes 22-24:	Range bytes of first antenna, from Preface 3 of input tape.

The remaining 384 bytes in each line contain 256 data values packed into three bytes for each pair of values.

Byte 1:	$\lvert v_1 \rvert$
Byte 2:	50 (octal) if and only if $v_1 \geq 0$ plus 4 (octal) if and only if $v_2 \geq 0$.
Byte 3:	$\lvert v_2 \rvert$

Line 1 contains the real parts of the combined antenna 1 transform; line 2, the imaginary parts. Lines 3-6 contain the transforms from antennas 2 and 3, with the same Doppler shift.

Combined Aircraft Data Transform Tape Format

This tape contains one file consisting of two logical records for each case processed. There is one record for each carrier frequency. Each record contains 1591 words as follows.

WORDS	
1-18	LPX array of 18 digits from Preface 1 of the first record used in this case. Integers.
19-36	FREQ array of 18 digits from Preface 2 as above. Integers.
37-54	RNG array of 18 digits from Preface 3 as above. Integers.
55	Hz the number of Hertz at the 129th member of the following transform. Given module 100; -6 appears as 94.
56-1591	Complex array H in normal Fortran order, dimensioned 256 x 3. H(I,J) = the combined transform entry for the Jth antenna at Hz + (I-129)/64 Hertz.

Sky Polarization

Initiator: F. Volz

Problem No: 3034-5 Project No: 7621

A series of four programs were written to aid in the reduction of observations of neutral points of sky polarization in the clear sky during twilight. The Initiator has data gathered over a three year period, showing evidence of changes in relation to variations of stratospheric aerosol content.

The main portion of the effort was directed towards presentation of the data in a variety of printed, punched, and plotted formats. Certain corrections and interpolations were performed. In addition, it was necessary to write a subroutine calculating solar elevation as a function of date, Universal Time, and station latitude and longitude.

Damping Functions In Infrared Absorption

Initiator: Dr. Bernard Bendow

Problem No: 3055-3 Project No: 3326

This problem is one of a set of problems directed toward the prediction of the infrared absorption intensity and line shape as a function of frequency for various models of ionic crystals and semiconductors. In particular, this problem continues the work performed under Problem No. 3055-1 for Air Force contract F19628-70-C-0120.

This problem required the calculation of

$$I(\omega) = \sum_{\vec{R},\vec{R^1},\vec{R}_3} \sum_{n=1}^{\infty} \frac{1}{n!} \left[\frac{\partial F^{n+1}}{\partial D^{n+1}}\right]_{D=0} \rho_n \left(W,\vec{R},\vec{R^1},\vec{R}_3\right)$$

where, $\sum_{\vec{R},\vec{R^1},\vec{R}_3}$ refers to a sum over all the latice sites of a unitary cubic crystal, and where distances are measured from one of the latice sites.

Here:

$$\rho_{n+1}(\omega) = \int_{-\infty}^{\infty} d\omega^1 \; \rho_n(\omega-\omega^1) \; \rho_1(\omega^1)$$

$$\rho_1(\omega) = C_{11}(-\vec{R}_3,\omega) + C_{22}(\vec{R^1}-\vec{R}-\vec{R}_3,\omega) - C_{12}(\vec{R}_3-\vec{R^1},\omega) - C_{12}(\vec{R}-\vec{R}_3,\omega)$$

and,

$$F = \exp\left(-\frac{A-DB}{E^2}\right) \; (E^{-3})$$

where,

$$A = a_1(|\vec{\bar{R}}|)^2 + a_2(|\vec{\bar{R}}_1|)^2;\ B = \vec{\bar{R}}\cdot\vec{\bar{R}}^1;\ E = (4a_1a_2 - D^2)^{1/2}$$

where

$$\vec{\bar{R}} = \vec{R}+\vec{\eta}\ ;\ \vec{\bar{R}}^1 = \vec{R}^1+\vec{\eta}\ ;\ a_1 = \frac{1}{2}(C_{11}(0,0) + C_{22}(0,0) - C_{12}(0,0))$$

$$+ Ro^2;\ a_2 = \frac{1}{2}(C_{11}(0,0) + C_{22}(0,0) - C_{12}(0,0)) + Ro^2$$

where, the vector $\vec{\eta}$ is an input parameter.

An explanation of the general theory leading to equations of this form was also presented in the final report for the above mentioned contract. For this problem two forms of C_{ij} were tried. These two forms are

$$C_{ij}(\vec{R},\omega) = \frac{1}{\gamma^2} n_b \frac{3}{2} m_s^{-1} \frac{\sin\left[Ko \frac{(\omega-\omega_1\gamma)}{(1-\omega_1)\gamma} |\vec{R}|\right]}{Ko|\vec{R}|}$$

$$\sqrt{\frac{\varepsilon_j\varepsilon_k}{R_jR_k}} \frac{(\omega\ \omega_1\gamma)}{\omega(1-\omega_1)^2} \left[\frac{1}{e^{BW}-1} + 1\right] \quad \text{for } \gamma\ \omega_1 \leq \omega \leq \gamma$$

$$C_{ij}(\vec{R},\omega) = e^{\beta\omega}\ C_{ij}(\vec{R},-\omega) \quad \text{for } -\gamma \leq \omega \leq \gamma\omega_1$$

$$C_{ij}(\vec{R}_1,\omega) = 0, \quad \text{otherwise}$$

where

$$\varepsilon_1 = \sqrt{\frac{m_2}{m_1+m_2}}\ ;\ \varepsilon_2 = -\sqrt{\frac{m_1}{m_1+m_2}}\ \ R_1 = \frac{m_1+m_2}{m_2}\ \ R_2 = \frac{m_1+m_2}{m_1}$$

and γ, n_b, m_s, Ko, ω_1, m_1, m_2, β are input parameters

and

$$C_{ij}(R,\omega) = \frac{1}{\gamma} n_d^{3/2} m_s^{-1} \frac{\varepsilon_j \varepsilon_k}{\sqrt{R_j R_k}} \frac{\sin(Ko\overline{K}|\vec{R}|)}{2(1-\overline{K})\, Ko|\vec{R}|} \frac{\overline{K}}{\omega} \left(\frac{1}{e^{\beta\omega}-1} + 1\right) \quad \text{for } 0 \leq \omega \leq \gamma$$

$$C_{ij}(\vec{R},\omega) = C_{ij}(\vec{R},-\omega)\, e^{\beta\omega} \quad \text{for } -\gamma \leq \omega \leq 0$$

$$C_{ij}(\vec{R},\omega) = 0, \text{ otherwise}$$

where

$$\overline{K} = 1 - \sqrt{1 - \frac{\omega}{\gamma}} \quad \text{for } 0 \leq \omega < 1 \quad \overline{K} = 1\text{-DELTA if } \omega = 1;$$

$$\varepsilon_1 = \sqrt{\frac{m_2}{m_1+m_2}}\ ;\ \varepsilon_2 = -\sqrt{\frac{m_1}{m_1+m_2}}\ ;\ R_1 = \frac{m_1+m_2}{m_2}\ ;\ R_2 = \frac{m_1+m_2}{m_1}\ ;$$

$$Ko = (6\pi^2 n_c)^{1/3} \text{ and } \gamma,\ n_b,\ m_s,\ \beta,\ n_c,\ \text{DELTA},\ m_1,\ m_2$$

are input parameters.

To perform the calculations, a program was written which did the algebraic manipulation needed to derive the derivatives of F. This program generated card output for insertion in other programs, which do the actual calculations. Derivatives up to the twelfth order were obtained. This order of differentiation was found to be appropriate in evaluating $I(\omega)$.

The computer program used the trapezoidal rule to approximate the integration needed to generate ρ_n from ρ_1 using the recursion relationship $\rho_{n+1}(\omega) = \int_{-\infty}^{\infty} dw^1 \rho_n(\omega-\omega^1)\ \rho_i(\omega^1)$ and the knowledge that $\rho_n(t) = 0$ for $|t| > n\gamma$. The program calculated and plotted results of $I(\omega)$ versus ω for all the values

of the sum, such that, $|\vec{R}|^2 + |\vec{R}^1|^2 \leq$ IR (an input parameter) and $|\vec{R}_3| <$ M, where M equals 1,2,3,..., ISRRT (another input parameter).

Analysis of the Temperature Gradient in the Atmosphere

Initiator: Mr. A. Cole

Problem No: 3065-1 Project No: 8624

The purpose of this problem is to provide an objective method for obtaining the horizontal temperature gradient between the North Pole and the equator from observed data at levels between 30 and 90 km. In essence, this method smooths the observed temperatures and provides interpolated values for 15° intervals of latitude. The interpolated temperatures were to be used with appropriate atmospheric pressures to construct U.S. Reference Atmospheres, representing mean monthly conditions at 15, 30, 45, 60, 75 and 90° N. latitude.

For a given month, the Initiator provided 13 sets of data. Each set representing measurements of temperature versus latitude for a fixed altitude. The method of least squares is used to determine the best fit for each data set by polynomials of order 1 thru 6. The results of this processing were presented in a tabulated form that facilitates comparison between the order of polynomials fitted to a particular data set. This comparison is essential to the Initiator to ascertain his preference that for a specific altitude and month, a certain polynomial best describes the dependence of temperature on latitude. This effort utilized the least squares program of the Analysis and Simulation Branch Computer Library.

Exponential Curve Fitting for UV Absorption Data

Initiator: Mr. L. Weeks

Problem No: 3069 Project No: 6690

The purpose of this problem is to analyze ultra-violet absorption data obtained in the 110 to 220 km. region from rocket-borne photometers. The results of this analysis are in turn utilized in the determination of the molecular oxygen number density of this region.

The expected behavior of ultra-violet absorption data ($I(h_i)$ is that it undergoes an exponential variation with respect to altitude. This behavior requires the determination of the 'best' values for the parameters I_o, h_o, H_1 and H_2, such that, the measured data $I(h_i)$ can be represented by the expression

$$I(h_i) = I_o \exp - \left\{.5 \exp - (h_i - h_o)/H_1 + .5 \exp - (h_i - h_o)/H_2\right\}$$

where, h_i is the independent variable for altitude and 'best' values are in accordance with the criteria of least squares, i.e., minimize

$$\phi = \sum_i (I(h_i) - \text{Expression})^2$$

Using standard iteration techniques, convergence was not obtained for the curve fitting in the prescribed form. Also, convergence was not obtained when a logarithmic transformation was applied to both the data and the prescribed form of the curve fit.

The 'best' estimates for the parameters were successfully obtained when utilizing the Levenberg Method and simultaneously constraining the parameters H_1 and H_2. A full description of this method and its application are presented in the Final Report, AFCRL-TR-73-0433 mentioned in the introduction of this report.

The results of this processing were presented at the AGU conference in San Francisco in December, 1973.

Tracking and Analysis of Variable Low Frequency Waveform

Initiator: Capt. McLain

Problem No: 3070-1 Project No: 4603

Program PROG5 was written in support of a study of Variable Low Frequency Waveform Tracking and Analysis. The purpose of this segment of the study is to calculate and plot Ionospheric Reflection Coefficients and Group Heights from VLF ionospheric waveform reflections recorded as a function of time.

Logically, the computer program proceeds in the following manner:

Sequences of three pulses, identified as groundwave, skywave and rotated skywave, are unpacked from magnetic tape and Fast Fourier analyzed for frequency content. Each Fast Fourier spectrum is fitted, according to a third order polynomial, to a given frequency interval, and the resultant amplitude and phase values of two predetermined frequencies are selected for use in computation of reflection heights and coefficients. An amount of averaging of fitted Fourier data takes place in the time domain according to an averaging time span specified by the user.

For each given time period to be analyzed, a series of 10 pairs of pen-and-ink plots are generated, consisting of 8 pairs of families of phase heights and coefficients, and 2 pairs of group heights and coefficients, all presented as functions of time (in hours). All phase heights are plotted over 6 inches on a linear scale of 0-120 km., and reflection coefficients are plotted over 4 inches on a logarithmic scale encompassing the two decades between 0.01 and 1.0. Each plot is identified according to day, year, time, frequency of analysis, and rotated or normal skywave reference data.

The user has control over several parameters within the program via input control cards. Included among these are the number of time series to be analyzed, the spacing at which the Fast Fourier spectra are to be fitted, a 30 character plot label array, the amount of time over which fitted Fourier data averaging is to take place, the starting and ending times over which analysis is to take place, and the two frequencies selected from the fitted Fourier spectra at which analysis is to take place.

Mathematics

A quantity of interest is the phase difference between the ground and skywaves (PHSG).

The mirror height is calculated from PHSG by the following formula:

$$HTMIR = \frac{1}{2}\sqrt{[DG+(PHSGC+N*T) * .29979]^2 - DG^2}$$

where

DG = distance between transmitter and receiver (KM)

PHSGC = PHSG-PHM+PHGC (μsec)

PHSG = (skywave phase data - groundwave phase data) - (Skywave phase calibration - groundwave phase calibration).

$0 \leq PHSG < T$

PHM = Phase shift of the skywave at the ionosphere (μsec)

PHM = {0 or T/2 for the normal component
T/4 or 3T/4 for the rotated component

PHGC = Correction to groundwave phase at frequency F; due to the finite conductivity of the ground (μsec)

N = Number of cycles

$0 \leq N \leq *$ (Upper boundary, N*, is established when HTMIR exceeds 120 KM).

T = 1000./F (T in μsecs, F in kHz)

.29970 = Velocity of Light (KM/μsec)

Reflection Coefficients - The reflection coefficient is a ratio of the skywave to groundwave signal strength with certain corrections. The reflection coefficient is calculated from:

$$RCOEF = \frac{ARSG}{2RAC*AMGC* \dfrac{\cos\left(\dfrac{2\pi*F*AL*\cos\theta}{9.83571x10^2}\right) - \cos\left(\dfrac{2\pi*F*AL}{9.83571x10^2}\right)}{1. - \cos\left(\dfrac{2\pi*F*AL}{9.83571x10^2}\right)}}$$

where

$$ARSG = \frac{\text{Skywave component signal amplitude}}{\text{Groundwave signal amplitude}}$$

or

$$= 10^{\frac{(\text{Skywave amplitude (dB)} - \text{Groundwave amp (dB)})}{20}}$$

if the signal amplitudes are given in decibels

RAC = Receiver antenna response amplitude correction

$$RAC = \begin{cases} 1. \text{ For the normal component} \\ \text{Cos}\theta \text{ for the rotated component} \end{cases}$$

AMGC = Correction to the groundwave amplitude at frequency F due to the finite conductivity of the ground

AL = Antenna length (KFT)

O = Skywave angle of incidence

$$O = \text{Tan}^{-1}\left(\frac{DG}{2HIMIR}\right)$$

9.83571×10^2 = Velocity of Light in KFT/μsec

F = Frequency (kHz)

Reflection heights and coefficients are calculated for both mirror phase shifts of both skywave components at each frequency. These values are computed for each data record interval and plotted vs. time of day.

Symbolic Solution of a Linear Equation

Initiator: David Anthony

Problem No: 3074-1 Project No: 7600

This problem involved solving for the C in the following equations:

$$\sum_{J=1}^{NVA} a_{IJ}\, C_{(2J,0)} = K_I \quad \text{for } I = 1,\ldots, NVA$$

where a_{IJ} and K_I are polynomials in two variables F and M1 and the solution is to be in terms of F and M1.

The method used to solve these equations is to reset the a_{IJ} and K_I to new polynomials as follows:

Reset for I = 1 then I = 2 ..... I = NVA

a_{jK} is reset to $a_{II}\, a_{jK} - a_{jI}\, a_{IK}$
$j \neq I$
$K \neq I$

K_j is reset to $a_{II}\, K_j - a_{jI}\, K_I$
$j \neq I$

a_{jI} is reset to 0.
$j \neq I$

The resulting values of C(2I,0) are then

$$C_{(2I,0)}\ K_I = \frac{K_I}{a_{II}}$$

Here K_I and a_{II} are polynomials in F and M1.

These results were then expanded in powers of F so

$$C_{(2I,0)} - \left.\frac{K_I}{a_{II}}\right|_{F=0} + \sum_{n=1}^{NK-1} \left(\left(\left. \frac{\partial^h \left(\frac{K_I}{a_{II}}\right)}{\frac{\partial^h F}{h!}} \right|_{f=0} \right) F^h \right)$$

where each term is a polynomial in M1.

Dissociation Pressure of Silicon Corbite

Initiator: Dr. J. Smiltens

Problem No: 3077-01 Project No: 5620

The equilibrium pressure for silicon, carbite, grafite and vapor has been determined by two groups of investigators. In 1930 in Germany, Grieger determined it in the range from 760 mm. mercury to 1 mm. mercury. Grievenson and Alcook determined it at lower temperature in the micropressure range. According to classical Physical Chemistry, the logarithm of vapor pressure when plotted vs. reciprocal absolute temperature should give a straight line. Both investigators have obtained the straight line. However, Grieger's straight line has a larger negative slope than Grievenson's and Alcook's. A more careful consideration and recent experimental evidence indicate that Grieger's data should depart upward from the Grievenson's and Alcook's straight line. The special condition the parabola should be tangent to the straight line.

A functional description of the required mathematical analysis and computer programming is the following:

Calculate the least squares polynomial through the submitted Grievenson and Alcook's data.

Calculate the least square parabola through the submitted Grieger's data.

Solve a system of the submitted two equations with C and X_o unknowns.

Find the real root of the resulting 5^{th} degree polynomial which satisfies the special condition: the parabola should be tangent to the straight line.

The solution of the system of the two equations submitted with C and x_o unknowns and with n representing the summing of the data:

$$2 \Sigma [y_n - A - Bx_n - C(x_o^2-2x_ox_n+x_n^2)] (x_o^2-2x_ox_n+x_n^2) = 0$$

$$2 \Sigma [y_n - A - Bx_n - C(x_o^2-2x_ox_n+x_n^2)] (2x_o-2x_n) = 0$$

is a 5th degree polynomial $a_o + a_1x + a_2x^2 + a_3x^3 + a_4x^4 + a_5x^5 = 0$ with

$a_o = A6B5 + A7B4$

$a_1 = A4B4 - A5B5 + A6B2 - A7B3$

$a_2 = A7B1 - A5B2 - A4B3 + A3B5 + A2B4$

$a_3 = A7B0 + A4B1 + A3B2 - A2B3 - A1B5$

$a_4 = A2B1 + A4B0 + A0B5 - A0B2$

$a_5 = -A0B2$

where

$A0 = -n$

$A1 = 4\Sigma x_n$

$A2 = \Sigma y_n - nA - B\Sigma x_n$

$A3 = 6\Sigma x^2$

$A4 = 2(A\Sigma x_n - \Sigma x_n y_v + B\Sigma x_n^2)$

$A5 = 4\Sigma x_n^3$

$A6 = \Sigma x^4$

$A7 = \Sigma x_n^2 y_n - A\Sigma x_n^2 - B\Sigma x_n^3$

$B0 = A0$

$B1 = 3\Sigma x_n$

$B2 = A2$

$B3 = 3\Sigma x_n^2$

$B4 = \Sigma x_n^3$

$B5 = A4$

NOTE: AIBJ = (AI) (BJ)

Rotational Constants of Diatomic Molecules

Initiator: Dr. Daniel Katayama

Problem No: 3080-1 Project No: 8627

From the analysis of the band spectra of diatomic molecules in the vacuum ultra-violet, the rotational constants of these molecules can be determined when they are in highly excited states. These constants are determined by solving a system of simultaneous equations, using matrix and least squares techniques. Also determined are the variance σ^2, and the variance-covariance matrix (V) described below in the following equations:

$$X_i = J_i(J_i+1) - \Lambda''^2$$

$$X_i'' = J_i''(J_i''+1) - \Lambda''^2$$

where J', J'', Λ' and Λ'' are data input numbers.

The system of simultaneous equations:

$$y_1 = a_o + a_1(x_1') - a_2(x_1')^2 - a_3(x_i'') + a_4(x_1'')^2$$

$$y_2 = a_o + a_1(x_2') - a_2(x_2')^2 - a_3(x_2'') + a_4(x_2'')^2$$

$$\vdots \quad \vdots \quad \vdots \quad \vdots \quad \vdots \quad \vdots$$

$$y_n = a_o + a_1(x_n') - a_2(x_n')^2 - a_3(x_n'') + a_u(x_n'')^2$$

Or, in matrix form:

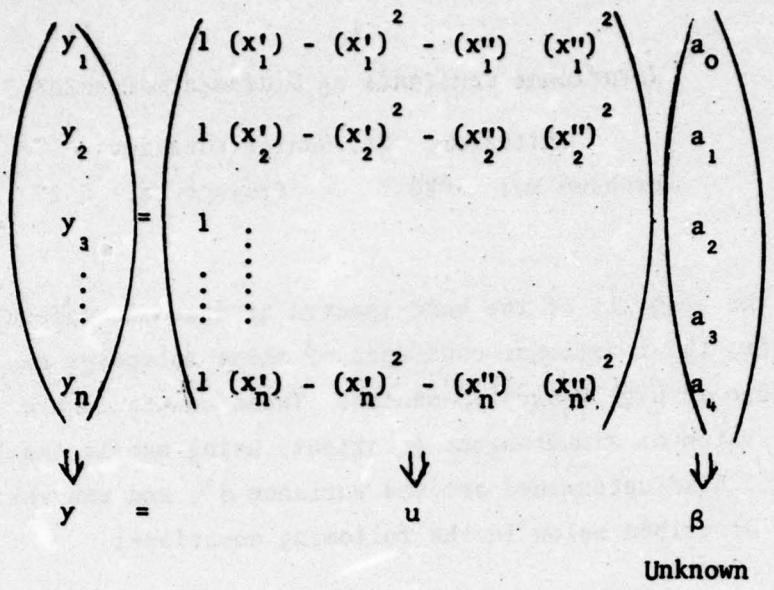

Then, in accordance with the method of least square, the required calculations are:

$$\beta = (u^t u)^{-1} u^t y$$

u^t = u transpose

$$\sigma^2 = \frac{1}{n-5}(y-u\beta)^t (y-u\beta)$$

$$V = \sigma^2 (u^t u)^{-1}$$

Construction of "Reasonable", Analytic Curves of Wind Vs. Height from Discrete Data

Initiator: Rene V. Cormier

Problem No: 4026-6 Project No: 8624

Research in support of Air Force paradrop operations, investigating the characteristics of vertically integrated boundary layer winds established a need for the construction of "reasonable" analytic functions (curves) of wind and temperature versus height from discrete data. These data were obtained at non-regularly spaced levels ranging in height from the surface to 1500 ft. and in number from 7 to 12 depending on the tower. The curves had to be capable of integration and differentiation, and because of the number involved (over 30,000) had to be generated by computer without human intervention.

A series of computer programs were written in two (2) groups and were documented under the name CORM for the SUYA Computer Center Library.

GROUP I	GROUP II
1. CORMN	5. CORMP
2. INTGRLN	6. INTGRLP
3. HERMITN	7. HERMITP
4. CORM4	

Programs CORMN, CORMP perform a polynomial interpolation using HERMITE'S interpolation formula, INTGRLN and INTGRLP integrate the area under the curve between given limits of A and B.

Programs HERMITN and HERMITP construct the polynomial using the same HERMITE'S interpolation formula, and CORM4 performs polynomial interpolation using Lagrange's interpolation formula. The difference between the programs of GROUP I and GROUP II is that:

GROUPI: Constructs a polynomial going through the points having positive or negative value.

GROUP II: If the evaluation of the constructed polynomial becomes negative (that is unreal for wind speed data) then the programs of GROUP II correct the negative values and such that the polynomial evaluation is always positive.

To accomplish the tasks outlined, the following mathematical steps have been taken:

A. Program CORMN and CORMP perform a polynomial interpolation by using HERMITE'S interpolation formula. Suppose that values of f(x) and f'(x) are known for $x_1,\ldots x_m$. A polynomial H(x) can be determined by assuming that it is expressible in the form:

$$H(x) = \sum_{k=1}^{m} h_k(x)\ f(x_k) + \sum_{k=1}^{m} \bar{h}_k(x)\ f'(x_k) \qquad (1)$$

where $h_i(x)$ and $\bar{h}_i(x)$ $(i=1,2,\ldots,m)$ are polynomials of maximum degree 2m-1:

$$h_i(x) = [1-2L_i'(x_i)(x-x_i)][L_i(x)]^2$$

$$\bar{h}_i(x) = (x-x_i)[L_i(x)]^2$$

where

$$L_i = \frac{(x-x_1)\ldots.(x-x_{i-1})(x-x_{i+1})\ldots.(x-x_n)}{(x_i-x_1)\ldots.(x_i-x_{i-1})(x_i-x_{i+1})\ldots.(x_i-x_n)}$$

For two points we have a polynomial of degree three:

$$H(x) = [f(x_1)V_1(x)+f'(x_1)W_1(x)]L_1^2(x)+[f(x_2)V_2(x)+f'(x_2)W_2(x)]L_2^2(x) \qquad (2)$$

where

$$L_1 = \frac{x-x_2}{x_1-x_2}\quad V_1 = 1 - \frac{(x-x_1)\omega''(x_1)}{\omega'(x_1)}\quad W_1 = x-x_1$$

$$L_2 = \frac{x-x_1}{x_2-x_1}\quad V_2 = 1 - \frac{(x-x_2)\omega''(x_2)}{\omega'(x_2)}\quad W_2 = x-x_2$$

and:

$$\omega(x) = (x-x_1)(x-x_2)$$

$$\omega'(x) = (x-x_1) + (x-x_2)$$

$$\omega'(x_1) = x_1-x_2$$

$$\omega'(x_2) = x_2-x_1$$

$$\omega'' = 2$$

B. Programs INTGRLN and INRGRLP integrate the function (2) for any given limits of A and B under the curve H(x). The following steps have been taken:

$$ANS = \int f(x_1)V_1(x)L_1^2(x)dx + \int f(x_2)V_2(x)L_2^2(x)dx + \int f'(x_1)W_1(x)L_1^2dx \quad (3)$$

$$+ \int f'(x_2)W_2(x)L_2^2(x)dx$$

where

$$Y1 = f(x_1) \qquad SL1 = f'(x_1) \qquad P1 = x_1-x_2$$

$$Y2 = f(x_2) \qquad SL2 = f'(x_2) \qquad P2 = x_2-x_1$$

are given.

By integrating each term of the equation (3) we get

$$\int f(x_1)V_1(x)L_1^2(x)dx = f(x_1)\int V_1(x)L_1^2(x)dx = f(x_1)$$

$$\int \left(1 - \frac{(x-x_1)^2}{P_1}\right)\left(\frac{x-x_2}{P_1}\right)^2 dx = -\frac{2f(x_1)}{P_1^3}\int (x-x_1)(x-x_2)^2 \quad (3a)$$

$$dx + \frac{f(x_1)}{P_1^2}\int (x-x_2)^2\,dx$$

$$\int f(x_2)V_2(x)L_2^2(x)dx = f(x_2)\int V_2(x)L_2^2(x)dx = f(x_2)\int\left(1 - \frac{(x-x_2)^2}{P_2}\right)$$

$$\left(\frac{x-x_1}{P_2}\right)^2 dx = -\frac{2f(x_2)}{P_2^3}\int(x-x_2)(x-x_1)^2dx + \frac{f(x_2)}{P_2^2}\int(x-x_1)^2\,dx \qquad (3b)$$

$$\int f'(x_1)W_1(x)L_1^2(x)dx = f'(x)\int(x-x_1)\frac{(x-x_2)^2}{P^2}dx = \frac{f'(x_1)}{P_1^2}\int(x-x_1)(x-x_2)^2\,dx \qquad (3c)$$

$$\int f'(x_2)W_2(x)L_1^2(x)dx = f'(x_2)\int(x-x_2)\frac{(x-x_1)^2}{P_2^2}dx = \frac{f'(x_2)}{P_2^2}\int(x-x_2)(x-x_1)^2dx \qquad (3d)$$

Since:

$$F = \int(x-a)(x-b)^2dx = \frac{1}{3}(x-b)^3(x-a) - \frac{1}{3}\int(x-b)^3\,d(x-b)dx = \frac{1}{3}(x-b)^3$$

$$(x-a) - \frac{(x-b)^4}{4} = F(a,b,x)$$

and

$$G = \int(x-a)^2\,dx = \frac{(x-a)^3}{3} = G(a,x)$$

For the given limits a and b of the integration Equation (3) becomes:

```
ANS = (C1+E1)*(F1-F2)+(C2+E2)*(F3-F4)+D1*(G1-G2)+D2*(G3-G4)
```

where

```
C1  =  -2.0*Y1/(P1**3)
C2  =  -2.0*Y2/(P2**3)
D1  =  1.0/(P1*P1)
D2  =  1.0/(P2*P2)
```

E1 = SL1*D1

E2 = SL2*D2

F1 = F(X1,X2,B)

F2 = F(X1,X2,A)

G1 = G(X2,B)

G2 = G(X2,A)

F3 = F(X2,X1,B)

F4 = F(X2,X1,A)

G3 = G(X1,B)

G4 = G(X1,A)

and

Y1 = $f(x_1)$

Y2 = $f(x_2)$

SL1 = $f'(x_1)$

SL2 = $f'(x_2)$

P1 = x_1-x_2

P2 = x_2-x_1

C. Program CORM4 performs the Lagrangian interpolation (given N points to fit exactly by a polynomial of degree n-1) using the formula:

$$Y(x) = \frac{\sum_{j=1}^{n} a_j \, y_i/(x-x_j)}{\sum_{j=1}^{n} a_j/(x-x_j)}$$

where the given data are (x_i,y_i), i=1,2,...,n and

$$a_j = \frac{1}{(x_j-x_1)(x_j-x_2)\ldots(x_j-x_{j-1})(x_{j+1})\ldots(x_j-x_n)}$$

Inverted Depth to Total Depth

Initiator: Rene V. Cormier

Problem No: 4026-7 Project No: 8624

The purpose of this problem under the title, "Inverted Depth to Total Depth", is to study the meteorology of integrated boundary layer winds in support of Air Force paradrop operations. Specifically, the effect of atmospheric stability on integrated boundary layer winds.

Conventional methods of determining atmospheric stability are inadequate to define the stability of the atmospheric layers under integration. This program develops a new stability parameter. It considers the temperature structure throughout the depth of the layer rather than just top and bottom temperatures. It finds the ratio of the depth within which the temperature is constant or increases with height to the total depth under integration.

The following steps have been taken:

Polynomial interpolation is performed on the input vertical temperature profile using Hermite's interpolation formula in order to perform the integration.

The coefficients of a defining cubic polynomial function are evaluated.

The maxima and minima of the function are then found by considering the first and second derivatives of the function.

To accomplish the tasks outlined, the following mathematical steps have been taken:

The polynomial interpolation and integration is done using the method and procedures described in problem number 4026-6, project 8624 above.

Evaluate the coefficients of the cubic polynomial $H(x) = ax^3+bx^2+cx+d$.

$$a = \frac{y'_1+y'_2}{(x_2-x_1)^2} + \frac{2(y_1-y_2)}{(x_2-x_1)^3}$$

$$b = \frac{1}{(x_2-x_1)^2}\left[y_1+y_2-(x_1+2x_2)y'_1-(x_2+2x_1)y'_2\right] - \frac{2}{(x_2-x_1)^3}$$

$$\left[(x_1+2x_2)y_1 - (x_2+2x_1)y_2\right]$$

$$c = \frac{1}{(x_2-x_1)^2}\left[2(x_1y_2+x_2y_1) - (x_1^2+2x_1x_2)y'_2 - (x_2^2+2x_1x_2)y'_1\right]$$

$$+ \frac{2}{(x_2-x_1)^3}\left[(x_2^2+2x_1x_2)y_1 - (x_1^2+2x_1x_2)y_2\right]$$

$$d = \frac{1}{(x_2-x_1)^2}\left[x_2^2y_1+x_1^2y_2 - x_1x_2^2y'_1 - x_1^2x_2y'_2\right] + \frac{2}{(x_2-x_1)^3}$$

$$\left[x_1^2x_2y_2 - x_1x_2^2y_1\right]$$

From the two point Hermite's interpolation formula:

$$H(x) = \left[y_1v_1(x) + y'_1w_1(x)\right]L_1^2(x) + \left[y_2v_2(x) + y'_2w_2(x)\right]L_2^2(x)$$

where

$$L_1 = \frac{x-x_2}{x_1-x_2} \qquad v_1 = 1 - \frac{(x-x_1)w''(x_1)}{w'(x_1)} \qquad w_1 = x-x_1$$

$$L_2 = \frac{x-x_1}{x_2-x_1} \qquad v_2 = 1 - \frac{(x-x_2)w''(x_2)}{w'(x_2)} \qquad w_2 = x-x_2$$

and

$$w(x) = (x-x_1)\ (x-x_2)$$

$$w'(x) = (x-x_1) + (x-x_2)$$

$$w'(x_1) = x_1-x_2$$

$$w'(x_2) = x_2-x_1$$

$$w' = 2$$

Expansion of GRAPPAC[2]

Initiator: Mr. R. Gosselin

Problem No: 4040-1 Project No: 0002

CALCOMP plotter simulation capability on CDC's Interactive Graphics System was made available to all computer users through expansion of the GRAPPAC system to include all CALCOMP entry points. An instruction booklet, skeleton deck, and associated permanent files were prepared. As a result, CALCOMP jobs can now be debugged quickly and easily without waiting for hard copy test plots to be prepared.

In addition, CALCOMP type programs can now be made to accept input from the graphics console through the addition of a very simple subroutine call. Selective erasure is available.

---

[1] GRAPPAC: A package of Fortran Subroutines for use with the 6000 Series 274 Interactive Graphic System of the Control Data Corporation, Frona B. Vicksell, Space Data Analysis Lab., Boston College, Chestnut Hill, Mass. 02167, AFCRL-72-0698.

Analysis of Observed Electron Density Profiles

Initiator: Mr. R. Allen

Problem No: 4041-1 Project No: 8666

Support was provided for study of a set of observed electron density profiles. The profiles were obtained from Lincoln Laboratory, Bedford, Ma. Programs were written first to present the data in graphical form for visual screening, then to perform certain calculations, producing a new data base for use in future statistical studies. The calculations for each profile involved integrating the available densities, with extrapolation if needed, over the altitude range 200 to 1000 km., to obtain total content and slab thickness. In addition, Chapman functions and parabolas were fitted to the peak density region to obtain estimates of the density scale height above the peak, below the peak, and on both sides simultaneously.

Modeling Electron Density Profiles

Initiator: Mr. R. Allen

Problem No: 4041-2 Project No: 8666

In a study related to account no. 4041-2, statistical and graphical comparisons were made between three diffeqent sets of observed electron density profiles and a model provided by the Air Weather Service and modified by the Initiator. The model has a variable scale height Chapman function on the topside of the F2-region, a fixed scale height for a distance of one scale height for a distance of one scale height below the F2 peak, then linear interpolation on the logarithms of the densities down to the E-region peak. The bottom side of the E region is another Chapman function.

Inputs to the model include the peak F2 density and its height, latitude, longitude, date, time, and 10.7 cm. solar flux or sunspot number.

Theoretical Predictions of the Electron Distribution Function in the Ionosphere

Initiator: Dr. J. Jasperse

Problem Nos: 4585, 4688, 4799 Project No: 6688

These problems involved making theoretical predictions of the electron distribution function in the ionosphere. Over a period of time, the model considered has been made more and more extensive until the following integral-differential equation was solved for H(z,E) in the latest computer program.

$$\left\{ \sum_{j=1}^{NJ} \left(\frac{2\,m_e}{m_{nj}+m_e}\right) \gamma_{mnj}(z,E)\, E^{3/2} + \sum_{s=1}^{NS} \left(\frac{2\,m_e}{m_{is}+m_e}\right) \gamma^1_{mis}(z) \right.$$

$$\left. + K_3\, I^0_0(z,E) \right\} H(z,E) = \int_E^{E_2} dE^1 \sum_{j=1}^{NJ} G_j(z,E^1)$$

$$+ \int_E^{E_2} dE^1 \sum_{j=1}^{NJ} G^1(z,E^1) - \int_E^{E_2} dE^1 \sum_{\ell=1}^{NL} (E^1)^{1/2}\, \gamma_{r\ell}(z,E^1)\, H(z,E^1)$$

$$- \int_E^{E_2} dE^1 \sum_{t=1}^{55} \sum_{k=1}^{MK(t)} (E^1)^{1/2}\, \gamma_{tk}(z,E^1)\, \theta\,(E^1-E_{tk})\, H(z,E^1)$$

$$+ \int_E^{E_2} dE^1 \sum_{t=1}^{55} \sum_{k=1}^{MK(t)} (E^1+E_{tk})^{1/2}\, \gamma_{tk}(z,E^1+E_{tk})\, H(z,E^1+E_{tk})$$

$$- \int_E^{E_2} dE^1 \sum_{t=1}^{55} \sum_{k=1}^{MK(t)} \exp\left[-\frac{E_{tk}}{K_1 T_n(z)}\right] (E^1+E_{tk})^{1/2}\, \gamma_{tk}(z,E^1+E_{tk})\, H(z,E^1)$$

$$+\int_{E}^{E_2} dE' \sum_{t=1}^{55} \sum_{k=1}^{MK(t)} \exp\left[-\frac{E_{tk}}{k_1 T_n(z)}\right] (E')^{1/2}\, \gamma_{tk}(z,E')\, \theta(E'-E_{tk})\, H(z,E'-E_{tk})$$

$$-\left\{\sum_{j=1}^{NJ} \left(\frac{2\, m_e}{m_{nj}+m_e}\right) \gamma_{mnj}(z,E)\, E^{3/2}\, K_1 T_n(z)\right.$$

$$+\sum_{s=1}^{NS} \left(\frac{2\, m_e}{m_{is}+m_e}\right) \gamma^1_{mis}(z)\, K_1 T_i(z)$$

$$\left.+\frac{2K3}{3}\left[I^0_2(z,E)+J^0_{-1}(z,E)\right]\right\} \frac{\partial}{\partial E} H(z,E)$$

Where:

$$\gamma_{mnj}(z,E) = N_{nj}(z)\, (CE)^{1/2}\, Q_{mj}(E)$$

$$\gamma^1_{mis}(z) = K_2\, N_{is}(z)$$

$$\gamma_{r\ell}(z,E) = N_{is}(z)\, (CE)^{1/2}\, Q_{r\ell}(E)$$

$$\gamma_{tk}(z,E) = N_{nt}(z)\, (CE)^{1/2}\, Q_{tk}(E)$$

$$I^0_0(z,E) = \int_{E_1}^{E} dE'(E')^{1/2}\, H(z,E')$$

$$I^0_2(z,E) = \int_{E_1}^{E} dE'(E')^{3/2}\, H(z,E')$$

$$J^0_{-1}(z,E) = E^{3/2} \int_E^{E_2} dE^1 \, H(z,E^1)$$

$$G_j(z,E) = \sum_{m=1}^{MMM(J)} N_{nj}(z) \, Q_{pijm}(E+E_{pijm}) \, I(z,E+E_{pijm})$$

$$I(z,E) = I(b,E) \exp\left\{-\sec\chi \sum_{j=1}^{NJ} Q_{paj}(E) \int_z^b dz^1 \, N_{nj}(z^1)\right\}$$

$$G^1_j(z,E^1) = K_s \, N_{nj}(z)\left\{2\sum_{k=1}^{NK}\int_{E^1+E_{ijk}}^{E_2} dE^{11}E^{11}D_{ijk}(E^{11},E^1)\,H(z,E^{11})\right.$$

$$\left. - E^1 \, H(z,E^1) \sum_k \theta(E^1-E_{ijk}) \, Q_{ijk}(E^1)\right\}$$

$$\theta(X-X^1) = \begin{cases} 0 & X < X^1 \\ 1 & X \geq X^1 \end{cases}$$

$$D_{ijk}(E^{11},E^1) = \frac{q_0 \, A_{ijk}}{2(E^{1/2}+E_{ijk})^2} \left(\frac{E_{ijk}}{E^{1/2}+E_{ijk}}\right)^{P_{ijk}}$$

$$* \left(\frac{E^{1/2}+E_{ijk}}{E^{11}}\right)^{O_{ijk}} \left[1 - \left(\frac{E^{1/2}+E_{ijk}}{E^{11}}\right)^{B_{ijk}}\right]^{N_{ijk}}$$

For $E_{ijk} \leq E^{11} \leq E_2$ and $0 \leq E^1 \leq E^{11}-E_{ijk}$

$D_{ijk}(E^{11},E^1) = 0$ for all other values of E^1 and E^{11}

$$Q_{ijk}(E^1) = \int_{E_1}^{E^1 - E_{ijk}} dE^{11}\, D_{ijk}(E^1, E^{11})$$

For t=1, k=1,7 MK(1)=7

$$Q_{tk}(E) = \begin{cases} 0 \text{ for } E_1 \leq E < E_{tk} \\ \left(\frac{q_o A_{tk}}{E^2_{tk}}\right) \left(\frac{E_{tk}}{E}\right) O_{tk} \left[1 - \left(\frac{E_{tk}}{E}\right)^{B_{tk}}\right]^{N_{tk}} \end{cases}$$

$$\text{For } E_{tk} \leq E \leq E_2$$

For t=2 MK(2)=23

For t=2, K=1, 8 $Q_2K(E)$ is linearly interpolated from a set of $Q_{2K}(e)$ versus E values

For t=2, K=9-23

$$Q_{tk} = \begin{cases} 0 \text{ for } E_1 \leq E < E_{tk} \\ \left(\frac{q_o A_{tk}}{E_{tk}^2}\right) \left(\frac{E_{tk}}{E}\right)^{O_{tk}} \left[1 - \left(\frac{E_{tk}}{E}\right)^{B_{tk}}\right]^{N_{tk}} \end{cases}$$

$$\text{For } E_{tk} \leq E \leq E_2$$

For t=3 MK(3)=14

For t=3 K=1-4 $Q_{3k}(E)$ is linearly interpolated from a set of $Q_{3k}(E)$ versus E values

For t=2 K=5-14

$$Q_{tk} = \begin{cases} 0 \quad \text{For} \quad E_1 \leq E < E_{tk} \\ \left(\frac{q_o A_{tk}}{E_{tk}^2}\right) \left(\frac{E_{tk}}{E}\right)^{O_{tk}} \left[1 - \left(\frac{E_{tk}}{E}\right)^{B_{tk}}\right]^{N_{tk}} \quad \text{For} \quad E_{tk} \leq E \leq E_2 \end{cases}$$

For t=4 MK(4)=2

For t=4, K=1,2 $Q_{4k}(E)$ is linearly interpolated from a set of $Q_{4k}(E)$ versus E values.

For t=5,55 MK(t)=1

For t=5,K=1 $Q_{51}(E)$ is linearly interpolated from a set of $Q_{51}(E)$ versus E values

For t=6-35 K=1

$$E_{t_1} = B_1[(t-4)\ (t-3) - (t-6)\ (t-5)]$$

and

$$Q_{t1} = \begin{cases} 0 \quad \text{For} \quad E_1 \leq E < E_{t1} \\ 4.7 * 10^{-17}(q_1)^2 \frac{(t-5)\ (t-4)}{(2t-11)\ (2t-9)} \left[\frac{E-E_{t1}}{E}\right]^{1/2} \\ \text{For} \quad E_{t1} \leq E \leq E_{c1} \\ 0 \quad \text{For} \quad E_{c1} < E \leq E_2 \end{cases}$$

For t=36-55

$$E_{t1} = B_2[(t-34)\ (t-33) - (t-36)\ (t-35)]$$

and

$$Q_{t_1} = \begin{cases} 0 \quad \text{For} \quad E_1 \leq E \leq E_{t1} \\ 4.7 * 10^{-17}(q_2)^2 \dfrac{(t-35)\ (t-34)}{(2t-71)\ (2t-69)} \left[\dfrac{E-E_{t1}}{E}\right]^{1/2} \quad \text{For} \quad E_{t_1} \leq E \leq E_{c2} \\ 0 \quad \text{For} \quad E_{c_2} < E \leq E_2 \end{cases}$$

$$N_{n_4}(z) = N_{n_1}(z) \left\{ \frac{5}{5 + 3\exp[-\frac{E_{41}}{K_1 T_n(z)}] + \exp[-\frac{E_{42}}{K_1 T_n(z)}]} \right\}$$

$$N_{n_5}(z) = N_{n_1}(z) \left\{ \frac{3\exp[-\frac{E_{41}}{K_1 T_n(z)}]}{5 + 3\exp[-\frac{E_{41}}{K_1 T_n(z)}] + \exp[-\frac{E_{42}}{K_1 T_n(z)}]} \right\}$$

For t = 6-35

$$X_t = B_1(t-6)\ (t-5)$$

and

$$N_{nt}(z) = N_{n_2}(z) \left\{ \frac{(2t-11)\exp[-\frac{X_t}{K_1 T_n(z)}]}{\sum_{u=6}^{35}(2u-11)\exp[-\frac{X_u}{K_1 T_n(z)}]} \right\}$$

For t = 36-55

$$Y_t = B_2(t-36)\ (t-35)$$

and

$$N_{nt}(z) = N_{n_3}(z) \left\{ \frac{(2t-71)\ \exp[-\frac{Y_t}{K_1 T_n(z)}]}{\sum_{U=36}^{55} (2U-71)\ \exp[-\frac{Y_u}{K_1 T_n(z)}]} \right\}$$

$$N_{i_2} = q_2 \left\{ C^{1/2} \int_{E_1}^{E_2} dE\ E\ Q_{r_2}(E)\ H(z,E) + (K_{211}+K_{214})\ N_{n_1} + (K_{233}+K_{234})\ N_{n_3} + K_{244}\ \gamma\ N_{n_3} \right\}^{-1}$$

$$N_{i_1} = [q_1 + K_{211}\ N_{n_1}\ N_{i_2}] \left\{ C^{1/2} \int_{E_1}^{E_2} dEE\ Q_{r_1}(E)\ H(z,E) + K_{124}\ N_{n_2} + K_{133}\ N_{n_3} + K_{144}\ \gamma\ N_{n_3} \right\}^{-1}$$

$$N_{i_3} = [q_3 + K_{233}\ N_{n_3}\ N_{i_2} + K_{133}\ N_{n_3}\ N_{i_1}] \left\{ C^{1/2} \int_{E_1}^{E_2} dE\ E\ Q_{r_3}(E)\ H(z,E) + K_{324}\ N_{n_2} + K_{344}\ \gamma\ N_{n_3} \right\}^{-1}$$

$$N_{i_4} = \left\{ [K_{214}\ N_{n_1} + K_{234}\ N_{n_3} + K_{244}\ \gamma\ N_{n_3}]\ N_{i_2} + [K_{124}\ N_{n_2} + K_{144}\ \gamma\ N_{n_3}]\ N_{i_1} + [K_{324}\ N_{n_2} + K_{344}\ \gamma\ N_{n_3}]\ N_{i_3} \right\} \left\{ C^{1/2} \int_{E_1}^{E_2} dE\ E\ Q_{r_4}(E)\ H(z,E) \right\}^{-1}$$

$$q_2 = \int_{E_1}^{E_2} dE(G_2 + G_2^1) + \int_{E_1}^{E_2} dE\ G_{1,m=2}$$

where

$$G_{1,m=2} = N_{n_1}(z)\ Q_{pi_{12}}(E+E_{pi_{12}})\ I(z,E+E_{pi_{12}})$$

$$q_1 = \int_{E_1}^{E_2} dE(G_1 + G_1^1) - \int_{E_1}^{E_2} dE\ G_{1,m=2}$$

$$q_3 = \int_{E_1}^{E_2} dE(G_3 + G_3^1)$$

$$Ne(z) = \sum_{\ell=1}^{4} N_{i\ell}$$

The program considers the integrals of the form $\int_{E_{low}}^{E_{high}} dE\ E\ Q_{r\ell}(E)\ H(z,E)$ to be broken up into a sum of sub-intervals $[E_{low} = EMID^{(L)}, EMID^{(L+1)}]$, $[EMID^{(L+1)}, EMID^{(L+2)}]$ ..., $[EMID^{(L+V)}, E^{(L+V+1)} = E_{high}]$ and the program has a set of E value $E_1 = EP_1, EP_2 \ldots EP_{NE} = E_2$ where one and only one of these EP_i values occur within each sub-interval. Then

$$\int_{EMID^{(j)}}^{EMID^{(j+1)}} dE\ E\ Q_{re}(E)\ H(z,E)$$

is approximated as

$$\text{For } \ell = 1 = H(z,EP_{(v)}) * 2.248.10^{-20}((EMID^{(j+1)})^{3/2} - (EMID^{(j)})^{3/2})$$

$$\text{For } \ell = 2 = H(z,EP_{(v)}) * 6.426727273.10^{-16}((EMID^{(j+1)})^{1.1} - (EMID^{(j)})^{1.1})$$

$$\text{For } \ell = 3 = H(z,EP_{(v)}) * 3.033666666710^{-16}((EMID^{(j+1)})^{.9} - (EMID^{(j)})^{.9})$$

$$\text{For } \ell = 4 = H(z,EP_{(v)}) * 4.39163636364.10^{-16}((EMID^{(j+1)})^{1.1} - (EMID^{(j)})^{1.1})$$

where $EP_{(v)}$ is the EP value such that

$$EMID^{(j)} \leq EP_{(v)} \leq EMID^{(j+1)}$$

$$K221 = K211S \left(\frac{1000}{T_n(z)}\right)^{.2}$$

$$K214 = K214S \left(\frac{1000}{T_n(z)}\right)^{.4} + K214SS \left(\frac{1000}{T_n(z)}\right)^{.2}$$

$$K233 = K233S \left(\frac{1000}{T_n(z)}\right)^{.8}$$

$$K133 = K133S \left(\frac{1000}{T_n(z)}\right)^{.4}$$

$$K144 = K144S \left(\frac{T_n(z)}{1000}\right)^{1.6}$$

$$K124 = \begin{cases} K124S \left(\frac{750}{T_n(z)}\right) & \text{for } T_n \leq 750 \\ K124S \left(\frac{T_n(z)}{750}\right)^2 & \text{for } T_n \geq 750 \end{cases}$$

For these calculations we have the following input data

K211S, K214S, K214SS, K233S, k234, K244, K124S, K133S, K144S, K324, K344, GAMMA, M_e, K_1, K_2, K_3, K_4, K_5, χ, C, a set of $EP_{(i)}$ values, a set of Z values ($Z_{(i)}$), NJ, M_{nj}, q_o, NK(J), E_{ijk}, A_{ijk}, P_{ijk}, ϕ_{ijk}, B_{ijk}, N_{ijk}, NS, M_{is}, $N_{n_1}(z)$, $N_{n_2}(z)$, $N_{n_3}(z)$, NL (NL = NS is implicitly assumed), MM(J), E_{pijm}, E_{1k}, A_{1k}, ϕ_{1k}, B_{1k}, E_{2k}, A_{2k}, ϕ_{2k}, B_{2k}, N_{2k}, E_{3k}, A_{3k}, ϕ_{3k}, B_{3k}, N_{3k}, E_{41}, E_{42}, E_{51}, q_1, E_{C1}, B_1, q_2, E_{C_2}, B_2

In addition the program reads the following bar graphs:

Bar graphs

NI_b values of I_b versus E

$NQPAJ_J$ values of Q_{paj} versus E

$NQPIJK_{JM}$ values of Q_{pijm} versus E

And finally the program reads the following graphs which are linearly interpolated

NTN values of T_n versus z

NT values of T_i versus z

NQM_J values of P_{mj} versus z

Given the preceding data the differential-integral equation for H(z,E) is approximated by a difference equation for a particular value of z. To do this, the equation is evaluated at the points EP_i.

The integral part of the equation is usually approximated by assuming $H(z,E)$ is a bar graph with values $H(z,E_v)$ covering intervals $[EMID^{(L)}, EMID^{(L+1)}]$. Exceptions to this rule are for $\int dEEQ_{re}\, H(z,E)$ and $\int dE^1 \sum_{j=1}^{NJ} G_j(z,E^1)$ which are handled as previously described (for $\int dE\, E\, Q_{re}\, H(z,E)$). Another exception is that above a read-in value for E the terms

$$- \int_E^{E_2} dE^1 \sum_{t=1}^{55} \sum_{k=1}^{MK(t)} (E^1)^{1/2}\, \gamma_{tk}(z,E^1)\, \theta(E^1-E_{tk})\, H(z,E^1)$$

$$+ \int_E^{E_2} dE^1 \sum_{t=1}^{55} \sum_{k=1}^{NK(t)} (E^1+E_{tk})^{1/2}\, \gamma_{tk}(z,E^1+E_{tk})\, H(z,E^1+E_{tk})$$

and

$$- \int_E^{E_2} dE^1 \sum_{t=1}^{55} \sum_{k=1}^{MK(t)} \exp\left[-\frac{E_{tk}}{K_1 T_n(z)}\right] (E^1+E_{tk})^{1/2}\, \gamma_{tk}(z,E^1+E_{tk})\, H(z,E^1)$$

$$+ \int_E^{E_2} dE^1 \sum_{t=1}^{55} \sum_{k=1}^{MK(t)} \exp\left[-\frac{E_{tk}}{K_1 T_n(z)}\right] (E^1)^{1/2}\, \gamma_{tk}(z,E^1)\, \theta(E^1-E_{tk})\, H(z,E^1-E_{tk})$$

are approximated by

$$\sum_{t=1}^{55} \sum_{k=1}^{MK(t)} E_{tk} \left[(E_2)^{1/2}\, \gamma_{tk}(z,E_2)\, H(z,E_2) - (E)^{1/2}\, \gamma_{tk}(z,E)\, H(z,E)\right]$$

and by

$$- \sum_{t=1}^{55} \sum_{k=1}^{MK(t)} E_{tk} \exp\left[- \frac{E_{tk}}{K_1 T_n(z)}\right] \left[(E_2+E_{tk})^{1/2} \gamma_{tk}(z,E_2+E_{tk})\, H(z,E_2)\right.$$

$$\left. - (E+E_{tk})^{1/2} \gamma_{tk}(z,E+E_{tk})\, H(z,E)\right]$$

Respectively where we have used the approximation $\frac{f(E) - f(E-E_{tk})}{E_{tk}} \sim \frac{d\, f(E)}{dE}$.

The derivative part of the equation is found at the values $EP_{(v)}$ in terms of central differences generally a seven point rule is used (a smaller odd point rule can be read in as this input parameter) except near $EP_{(1)}$ and $EP_{(NE)}$. Thus, $EP_{(3)}$ and $EP_{(NE-2)}$ use five point rules, $EP_{(2)}$ and $EP_{(NE-1)}$ use three point rules and

$$\left.\frac{\partial\, H(z,E)}{\partial\, E}\right|_{E = EP_{(NE)}} \sim \frac{H(z,EP_{(NE)} - H(z,EP_{(NE-1)})}{EP_{(NE} - EP_{(NE-1)}} \quad .$$

The equation at $EP_{(1)}$ is replaced by the equation

$$1 = \int_{E_1}^{E_2} dE(E)^{1/2}\, H(z,E)/Ne(z) \qquad \text{so}$$

$\left.\frac{\partial\, H(z,E)}{\partial\, E}\right|_{E = EP_{(1)}}$ is never approximated.

Using the logic specified above, the problem was reduced to the solution of NE non-linear equations, one for each $EP_{(v)}$ value for the values of

$H(z,EP_{(v)})$ for a specified z value. This set of equations was solved for $H(z,EP_{(v)})$ using a modified Newton-Raphson method. Thus, if $\Delta H(z,EP_{(v)})$ is the correction calculated by applying the Newton-Raphson method to the NE equations. Then the corrected $H(z,EP_{(v)})$ = the old $H(z,EP_{(v)})$ + $2^{-L}\ \Delta H(z,EP_{v})$ where L is the smallest integer which reduces the value of ETϕT. Where $ET\phi T = SCA(*EREEQ(1))^2 + \sum_{i=2}^{NE} (EREEQ(i))^2$. Where EREEQ(j) is the amount by which the j^{th} equation is not satisfied when the guessed values of $H(z,EP_{(v)})$ are tried. The program continues to correct $H(z,EP_{(v)})$ until a "solution" is found.

In addition to the above solution the program calculates and plots the following quantities when asked by the input data.

Oxygen Excitation Cross-section (versus Energy)

$$= \sum_{k=1}^{7} Q_1 K(E) + Q_{41}(E) + Q_{42}(E) + Q_{51}(E)$$

Oxygen Ionization Cross-section (versus Energy)

$$= \sum_{k=1}^{3} Q_{i1K}(E)$$

N_2 Rotational Cross-section (versus Energy)

$$= \sum_{t=6}^{35} Q_{t_1}(E)$$

N_2 Excitation Cross-section (versus Energy)

$$= \sum_{k=1}^{23} Q_{2K}(E)$$

N_2 Ionization Cross-section (versus Energy)

$$= \sum_{k=1}^{6} Q_{i_2k}(E)$$

O_2 Rotational Cross-section (versus Energy)

$$= \sum_{t=36}^{55} Q_{t_1}(E)$$

O_2 Excitation Cross-section (versus Energy)

$$= \sum_{k=1}^{14} Q_{3K}(E)$$

O_2 Ionization Cross-section (versus Energy)

$$= \sum_{k=1}^{7} Q_{i_3k}(E)$$

After each iteration of $H(z,EP_{(v)})$ the program calculates and points the following quantities:

$$I = \frac{\int_{E_1}^{E_2} dE\ F(z,E))}{N_e(z)} \quad \text{where } F(z,E) = \sqrt{E}\ H(z,E)$$

$$T_e = 7736.666667\ \left(\int_{E_1}^{E_2} E*F(z,E)\ dE\right)/N_e(z)$$

$$N_e(z) = \sum_{i=1}^{4} N_{ie}$$

$$\text{Integral of } G^1 = \int_{E_1}^{E_2} dE \sum_{j=1}^{NJ} G_j^1(z,E)$$

$$\text{and each integral of } G_j^1 = \int_{E_1}^{E_2} dE\ G_j^1(z,E) \text{ for } J = 1,2,3$$

When the program finds a solution for $H(z,EP_{(v)})$, the program also calculates and prints (plots)

$$F^1(z,E) = \left\{ \sum_{t=1}^{55} \sum_{k=1}^{MK(t)} \left[1 - \exp\left(-\frac{E_{tk}}{K_1 T_n(z)}\right)\right] E_{tk}\ \gamma_{tk}(z,E)\ \theta(E-E_{tk}) \right.$$

$$+ \sum_{j=1}^{NJ} E\left(\frac{2\ m_e}{m_{nj}+m_e}\right) \gamma_{mnj}(z,E) + \sum_{s=1}^{NS} \frac{1}{\sqrt{E}} \left(\frac{2\ m_e}{m_{ij}+m_e}\right) \gamma_{mis}^1(z)$$

$$\left. + \frac{1}{\sqrt{E}}\ V_{ee}{}^1(z) + K_5\ E^{1/2} \sum_{j=1}^{NJ} \sum_{k=1}^{NK(J)} E_{ijk}\ N_{nj}(z)\ \theta(E-E_{ijk})\ Q_{ijk}(E) \right\}^{-1}$$

$$\times \int_{E}^{E_2} dE^1 \sum_{j=1}^{NJ} G_j(z,E^1)$$

Check for $G^1 = K_5 \sum_{j=1}^{NJ} \sum_{k=1}^{NK(J)} N_{nj}(z) \int_{E_{ijk}}^{E_2} dE^1 \, E^1 \, Q_{ijk}(E^1) \, H(z,E^1)$

conductivity =

$$\sigma_{33} = \frac{2}{3} K_4 \int_{E_1}^{E_2} dE \, E^{3/2} \frac{\partial}{\partial E} (H(z,E))/(\sum_{j=1}^{NJ} \gamma_{mnj}(z,E) + E^{-3/2} \sum_{s=1}^{NS} \gamma^1{}_{mis}(z))$$

approximate conductivity = $\sigma_{33}(z)_{approx.}$

$$= K_4 \int_{E_1}^{E_2} dE \left(\frac{F(z,E)}{\sum_{j=1}^{NJ} \gamma_{mnj}(E,z) + E^{-3/2} \sum_{j=1}^{NJ} \gamma^1_{mij}(z)} \right)$$

Average Ionization Collision Frequency = $\overline{\nu}_i(z)$

$$= \left(\frac{K_5}{N_e(z)}\right) \sum_{j=1}^{NJ} N_{nj}(z) \sum_{k=1}^{NK(J)} \int_{E_{ij}}^{E_2} dE^1 (E^1)^{1/2} \, Q_{ijk}(E^1) \, F(z,E^1)$$

Alternate calculation for Electron Concentration =

$$N_e^1 = \left(\frac{1}{2 \sum_{L=1}^{NL} f_{iL}(z)\ \bar{\alpha}_{rL}(z)} \right)$$

$$\left\{ [4 \sum_{L=1}^{NL} f_{iL}(z)\ \bar{\alpha}_{rL}(z) \int_{E_1}^{E_2} dE^1 \sum_{j=1}^{NJ} G_j(z,E^1) + \bar{V}_i^2(z)] + \bar{V}_i(z) \right\}$$

$\bar{\alpha}_{rL}(z)$ for L = 1,2,3 and 4

$$= \frac{C^{1/2}}{N_e(z)} \int_{E_1}^{E_2} dE\ E\ Q_{rL}(E)\ H(z,E)$$

Approximate Average Ion Collision Frequency =

$$V_p(z) = \frac{K_5}{N_e(z)} \sum_{j=1}^{NJ} N_{nj}(z) \sum_{K=1}^{NK(J)} \int_{E_{ij}}^{E_2} dE^1 (E^1)^{1/2}\ Q_{ijk}(E^1)\ F^1(z,E^1)$$

Approximation for the Electron Concentration Using $V_p(z)$ =

$$N_e^p = [\frac{1}{2 \sum_{L=1} f_{iL}(z)\ \bar{\alpha}_{rL}(z)}] \left\{ 4 \sum_{L=1}^{NL} f_{iL}(z)\ \bar{\alpha}_{rL}(z) \right.$$

$$\left. \int_{E_1}^{E_2} dE^1 \sum_{j=1}^{NJ} G_j(z,E^1) + V_p^2(z)] + V_p(z) \right\}$$

Maxwellian Approximation to F = $F_m(z,E)$ =

$$4\pi\ N_e(z)\ (\frac{E^{1/2}}{2})\ [\frac{1}{\pi K_1 T_e(z)}]^{3/2}\ \exp(-\frac{E}{K_1 T_e(z)})$$

Early in the program the program can read in guesses for $N_e(z)$, N_{i_1}, N_{i_2}, N_{i_3}, N_{i_4} and $T_e(z)$ and use $(F_M(z,EP_{(v)}) + F^1(z,EP_{(v)})/(EP_{Iv})^{1/2}$ as the initial guess for $H(z,EP_{(v)})$ to start the iteration procedure.

Finally, for a given z value the program calculates

$$E_x = \frac{1}{(CE)^{1/2}} \left\{ \sum_{t=1}^{55} \sum_{k=1}^{MK(t)} [1 - \exp(-\frac{E_{tk}}{K_1 T_n(z)}) E_{tk} \gamma_{tk}(z,E) \theta(E-E_{tk}) \right.$$

$$+ \sum_{j=1}^{NJ} E \left(\frac{2 m_e}{m_{nj}+m_e}\right) \gamma_{mnj}(z,E) + \sum_{s=1}^{NS} \frac{1}{(E)^{1/2}} \left(\frac{2 m_e}{m_{ij}+m_e}\right) \gamma^1_{mis}(z)$$

$$\left. + \frac{1}{(E)^{1/2}} \gamma^1_{ee}(z) + K_5 E^{1/2} \sum_{j=1}^{NJ} \sum_{k=1}^{NK(J)} E_{ij} N_{nj}(z) \theta(E-E_{ijk}) Q_{ijk}(E) \right\}$$

This program will be submitted to the SUYA computer program library upon completion of problem 4799. The Initiator intends to further refine the equations for H(z,E). In any case, a separate program has been written which uses the calculated H(z,E) functions to calculate

$$SF(z,E) = 4.72 \cdot 10^6 \; E \; H(z,E)$$

$$SF^1(z,E) = 4.72 \cdot 10^6 \; E \; H^1(z,E)$$

$$q_{ex}(z) = 5.93 \cdot 10^7 \; N_o(z) \int_{E_{ex_1}}^{E_{ex2}} dE \; Q_o(E) \; E \; H(z,E)$$

$$q^1_{ex}(z) = 5.93.10^7\ N_o(z) \int_{E_{ex_1}}^{E_{ex_2}} dE\ Q_o(E)\ (E)^{1/2}\ F^1(z,E)$$

and

$$q_{ro}(z) = f_{io}(z)\ 4\cdot10^{-12}\ \left(\frac{300}{T(z)}\right)^{.7}\ [N_e(z)]^2$$

where $N_o(z)$, $f_{io}(z)$, $T(z)$, $N_e(z)$, E_{ex_2}, E_{ex_1} are input parameters and $Q_o(E)$ is an input function.

The results of the program seem to agree with experiments for low values of altitude, up to about 200 kilometers. In fact, they predict fine structure which the instruments which have been used to measure electrons in the ionosphere were too coarse to find. Above about 200 kilometers the model needs improvement. The initiator hopes to refine the model even further and explain the electron distribution above 200 kilometers.

Study of Source Location by Computer Simulation

Initiator: Dr. K. Toman

Problem No: 4620 Project No: 5631

Locating sources of radiation, finding radar targets, and determining one's own position are requirements in radio surveillance, detection, and navigation respectively. There also exists in the environmental sciences the need for determining, for example, the location of the origin of natural or man-made atmospheric or seismological disturbances.

In the following treatise we have restricted ourselves to study, on a computer, the problem of locating sources from time-of-arrival measurements made at four locations. We developed and tested an error analysis to determine how errors in time differences reveal themselves as errors in source location and signal velocity. Furthermore, we ascertained how these errors change with range, azimuth, signal velocity, and network configuration. The results, subject to certain assumptions, can be used for existing or planned time-of-arrival measurement networks. These assumptions are: (a) source and synchronized receiving stations are located at the surface of a spherical earth along which the signal propagates, (b) the velocity of the signal is uniform along the great-circle paths from source to receiving stations, (c) the signal is not bandwidth limited nor is it dispersed in frequency, and (d) individual errors are normally distributed and uncorrelated[1]. Assumption (a) can be broadened to include, in an idealized form, the case of remote sensing of atmospheric waves by ionospheric sounding techniques. Assumption (b) can be broadened to include rectilinear propagation and reflection of a radio signal from a mirror-like ionosphere of known height.

The locations of the source S and of the receiving stations A, B, C, and D on the surface of the earth of radius R = 6378 km are expressed in geographical coordinates θ (longitude) and ϕ (latitude). Using differences Δt of the arrival times for the propagating signal at the synchronized stations, the location of the source (θ_S, ϕ_S) and the signal velocity (v) can be determined from the following equations:

---

[1] Cooper, D.C. and Laite, P.J. (1969) Statistical Analysis of Position Fixing in Three Dimensions, Proc. IEE 116 (No. 9):1505-1508.

$$\frac{v\Delta t_{A-B}}{R} = \cos^{-1}\left[\sin\phi_A \sin\phi_S + \cos\phi_A \cos\phi_S \cos(\theta_S-\theta_A)\right]$$

$$- \cos^{-1}\left[\sin\phi_B \sin\phi_S + \cos\phi_B \cos\phi_S \cos(\theta_S-\theta_B)\right] .$$

$$\frac{v\Delta t_{C-B}}{R} = \cos^{-1}\left[\sin\phi_C \sin\phi_S + \cos\phi_C \cos\phi_S \cos(\theta_S-\theta_C)\right]$$

$$- \cos^{-1}\left[\sin\phi_B \sin\phi_S + \cos\phi_B \cos\phi_S \cos(\theta_S-\theta_B)\right] .$$

$$\frac{v\Delta t_{D-B}}{R} = \cos^{-1}\left[\sin\phi_D \sin\phi_S + \cos\phi_D \cos\phi_S \cos(\theta_S-\theta_D)\right]$$

$$- \cos^{-1}\left[\sin\phi_B \sin\phi_S + \cos\phi_B \cos\phi_S \cos(\theta_S-\theta_B)\right] . \qquad (1)$$

In the method used for obtaining the solutions θ_S, ϕ_S, and v from the time differences Δt_{A-B}, Δt_{C-B}, and Δt_{D-B} of known arrival times t_A, t_B, t_C, and t_D of the signal relative to a common time reference, two of the equations in Eq.(1) were combined, a speed v_i was assumed, and θ_{S_i}, ϕ_{S_i} were determined. These "initial" source coordinates were entered into the third equation to determine a speed v_c which was compared with v_i. If $v_i < v_c$ then v_i was increased and vice versa. This iteration, which employed the False Position Method[2], was continued until the difference between v_i and v_c was negligibly small (for example, $\left|v_i\, v_c^{-1} - 1\right| < 10^{-6}$). The initial assumption for v_i was thereby only limited by considerations of minimizing computer search time. The iteration procedure was used in the neighborhood of v=18000 m/min. For a given source location, arrival times at the four stations and their time differences were computed using this speed. For performing the inverse task, these time differences were used to redetermine the source location and velocity prior to assuming that the former are subject to errors. In order to determine the effect of these time-difference errors on errors in source location and signal velocity an error analysis was developed. Errors were imposed upon time differences Δt by assuming that they represent standard deviations of a normal distribution. The resulting errors in source location and signal velocity were viewed in terms of probability bounds.

---

[2] Scarborough, J.B. (1966) Numerical Mathematical Analysis, John Hopkins Press, Baltimore, 6th ed., p. 197.

In this error analysis it was assumed that the errors of the independent variables Δt_{A-B}, Δt_{C-B}, and Δt_{D-B} of Eq.(1) are small and uncorrelated. Based on these assumptions the formula for the propagation of the mean-square error[3] could be used to estimate the mean-square errors $\sigma^2_{\theta_S}$, $\sigma^2_{\phi_S}$, and σ^2_v of the dependent variables θ_S, ϕ_S, and v as follows:

$$\sigma^2_{\theta_S} = \left(\frac{\partial\theta_S}{\partial\Delta t_{A-B}}\sigma_{\Delta t_{A-B}}\right)^2 + \left(\frac{\partial\theta_S}{\partial\Delta t_{C-B}}\sigma_{\Delta t_{C-B}}\right)^2 + \left(\frac{\partial\theta_S}{\partial\Delta t_{D-B}}\sigma_{\Delta t_{D-B}}\right)^2 . \qquad (2)$$

$$\sigma^2_{\phi_S} = \text{(Replace } \theta_S \text{ in the above with } \phi_S) ,$$

$$\sigma^2_v = \text{(Replace } \theta_S \text{ in the above with v) ,}$$

where $\sigma_{\Delta t_{A-B}}$,... etc., represent the standard deviations from the mean assumed for the time-of-arrival differences between selected station pairs. As seen from Eq.(1), explicit expressions for θ_S, ϕ_S, and v were not available. The evaluation of their partial derivatives $\partial\theta_S/\partial\Delta t_{A-B}$,... etc. [Eq.(2)] required the use of a special property of the Jacobian matrix and its inverse[4].

$$\begin{bmatrix} \frac{\partial\Delta t_{A-B}}{\partial\theta_S} & \frac{\partial\Delta t_{A-B}}{\partial\phi_S} & \frac{\partial\Delta t_{A-B}}{\partial v} \\ \frac{\partial\Delta t_{C-B}}{\partial\theta_S} & \frac{\partial\Delta t_{C-B}}{\partial\phi_S} & \frac{\partial\Delta t_{C-B}}{\partial v} \\ \frac{\partial\Delta t_{D-B}}{\partial\theta_S} & \frac{\partial\Delta t_{D-B}}{\partial\phi_S} & \frac{\partial\Delta t_{D-B}}{\partial v} \end{bmatrix}^{-1} = \begin{bmatrix} \frac{\partial\theta_S}{\partial\Delta t_{A-B}} & \frac{\partial\theta_S}{\partial\Delta t_{C-B}} & \frac{\partial\theta_S}{\partial\Delta t_{D-B}} \\ \frac{\partial\phi_S}{\partial\Delta t_{A-B}} & \frac{\partial\phi_S}{\partial\Delta t_{C-B}} & \frac{\partial\phi_S}{\partial\Delta t_{D-B}} \\ \frac{\partial v}{\partial\Delta t_{A-B}} & \frac{\partial v}{\partial\Delta t_{C-B}} & \frac{\partial v}{\partial\Delta t_{D-B}} \end{bmatrix} \qquad (3)$$

whereby the partial derivatives $\partial\Delta t_{A-B}/\partial\theta_S$,... etc., were obtained from Eq.(1). Using this approach, the mean-square errors in θ_s, ϕ_S, and v were computed

---

[3] Deming, W.E. (1964), Statistical Adjustment of Data, Dover Publications, New York, p. 39.

[4] Irving, J., and Mullineaux, N. (1959), Mathematics in Physics and Engineering, Academic Press, New York, p. 800.

by means of Eq.(2) from the errors assumed for the time differences. The results of these computations were used as error bounds (error boxes) centered on true source locations. These error bounds were tested by generating a sequence of independent errors in time-of-arrival differences, using distributions for means and variances that were derived from available random number routines. Although these bounds were found to contain the appropriate number of "false" source locations, it was noted that their distribution seemed to fill these error boxes only partially, due to an elongated scatter of points in a direction toward the network with relatively little scatter in azimuth. It was also noted that the inherent nonuniformity of the geographic coordinate system would give the appearance of large errors in terms of σ_{θ_S}, when the source is near a geographic pole, and the appearance of small errors when it is near the equator. For these reasons it was decided to describe the "probable location of the source" not only in terms of longitude and latitude, but also with respect to distance and azimuth. This made it necessary to choose a reference point relative to which distance and azimuth are defined. Although any point on the surface of the earth could be chosen, one of the stations, B, of a network was usually designated the reference point.

Equations were obtained that relate the coordinates of a source in latitude (ϕ_S) and longitude (θ_S) to range (Dist) and azimuth (Az) for a reference station B (ϕ_B, θ_B).

$$\phi_S = \sin^{-1}\left\{\sin\phi_B \cdot \cos(\mathrm{Dist}/R) + \cos\phi_B \cdot \sin(\mathrm{Dist}/R) \cdot \cos \mathrm{Az}\right\}$$

$$\theta_S = \theta_B - \sin^{-1}\left\{\sin(\mathrm{Dist}/R) \cdot \sin \mathrm{Az}/\cos\phi_S\right\}. \qquad (4)$$

From these equations the partial derivatives $\partial\phi_S/\partial\mathrm{Az}$, $\partial\phi_S/\partial\mathrm{Dist}$, $\partial\theta_S/\partial\mathrm{Az}$, $\partial\theta_S/\partial$ Dist were determined and related to the partials of the time differences Δt with respect to azimuth and distance by

$$\frac{\partial \Delta t}{\partial Az} = \frac{\partial \Delta t}{\partial \theta_S} \cdot \frac{\partial \theta_S}{\partial Az} + \frac{\partial \Delta t}{\partial \phi_S} \cdot \frac{\partial \phi_S}{\partial Az}$$

$$\frac{\partial \Delta t}{\partial\ Dist} = \frac{\partial \Delta t}{\partial \theta_S} \cdot \frac{\partial \theta_S}{\partial\ Dist} + \frac{\partial \Delta t}{\partial \phi_S} \cdot \frac{\partial \phi_S}{\partial\ Dist}, \tag{5}$$

where $\partial\Delta t/\partial\theta_S$ and $\partial\Delta t/\partial\phi_S$, as well as $\partial\Delta t/\partial v$ were obtained from Eq.(1). The partial derivatives of azimuth, distance, and velocity with respect to the time differences that were to provide distance and azimuth error boxes analogous to Eq.(2) were obtained from the partial derivatives of the time differences with respect to azimuth and distance [obtained from Eqs.(4) and (5)] as well as velocity [obtained from Eq.(1)] by utilizing, as before, the Jacobian inverse property.

$$\begin{bmatrix} \frac{\partial \Delta t_{A-B}}{\partial Az} & \frac{\partial \Delta t_{A-B}}{\partial Dist} & \frac{\partial \Delta t_{A-B}}{\partial v} \\ \frac{\partial \Delta t_{C-B}}{\partial Az} & \frac{\partial \Delta t_{C-B}}{\partial Dist} & \frac{\partial \Delta t_{C-B}}{\partial v} \\ \frac{\partial \Delta t_{D-B}}{\partial Az} & \frac{\partial \Delta t_{D-B}}{\partial Dist} & \frac{\partial \Delta t_{D-B}}{\partial v} \end{bmatrix}^{-1} = \begin{bmatrix} \frac{\partial Az}{\partial \Delta t_{A-B}} & \frac{\partial Az}{\partial \Delta t_{C-B}} & \frac{\partial Az}{\partial \Delta t_{D-B}} \\ \frac{\partial Dist}{\partial \Delta t_{A-B}} & \frac{\partial Dist}{\partial \Delta t_{C-B}} & \frac{\partial Dist}{\partial \Delta t_{D-B}} \\ \frac{\partial v}{\partial \Delta t_{A-B}} & \frac{\partial v}{\partial \Delta t_{C-B}} & \frac{\partial v}{\partial \Delta t_{D-B}} \end{bmatrix} \tag{6}$$

The above equations were used to evaluate the errors of source location (ϕ_S, θ_S, or Dist, Az) and signal velocity v from given errors in the time differences and to appraise the effects of different network configurations on estimates of the errors involved in locating a radiating source.

The results of the error analysis were tested by using statistical distributions of time-differences $(\Delta t_{A-B})_i, \ldots$, etc., that in turn yielded a distribution of source location coordinates and signal velocity $(\phi_S, \theta_S, v)_i$. For given means and variances of the time differences their normal (Gaussian) distributions were obtained by taking finite-sample means from random numbers for which routines were available at AFGL's CDC 6600 digital computer. For certain purposes, rectangular distributions were also used.

In order to illustrate the results of the error analysis and the above tests, coordinate-transformation and plotting programs were developed, furthering the purpose of providing a clear visualization of network performance and testing procedure. The initial source location S (ϕ_S, θ_S) was placed at the center of a grid system whose elements were made to represent latitude and longitude error boxes expressed by σ_{ϕ_S}, σ_{θ_S}. These displays, which comprise 10 × 10 standard deviations and thus exaggerate the smaller error, were obtained by rectilinear projection from their positions on the curved surface of the earth onto a plane tangent to S, such that great-circle paths through S would appear as straight lines.

The results of this study were presented to Commission VI of V.R.S.I. during the 1973 International IEEE/G-AP Symposium and V.S.N.C./V.R.S.I. Meeting in Boulder, Colorado.

BIBLIOGRAPHY

Martine, Joseph E. and Power, Leo F. Jr., Numerical and Data Analysis Techniques Applied to Scientific Research, Final Report, AFCRL-TR-73-0433.

Toman, Kurt and Martine, Joseph E., Study of Source Location Error by Computer Simulation, Physical Sciences Research Paper, No. 574, AFCRL-TR-73-0684.

Eigenvalue-Eigenvector Determination

Initiator: Mr. G. Borgiotti

Problem No: 4721 Project No: 4600

This problem involved finding the eigenvalues and eigenvectors of the problem:

$$\lambda_j \psi_j(x) = \frac{1}{2\pi} \int_{-1}^{1} \frac{\sin c(x-\xi)}{x-\xi} \psi_j(\xi)\, d\xi$$

The Initiator wanted accurate values for the largest eigenvalues and their associated eigenfunctions. Towards this end the function $\psi_i(x)$ was represented by a large number (N up to 2001) of equally spaced points and the largest eigenvalues, eigenfunctions were determined as follows:

1. Set up an equally spaced grid of X values X_i
2. For the 1^{st}, 3^{rd},... $(2n+1)^{th}$ eigenfunctions (j) make an initial guess of a constant for the values of $\psi_j(X_i)$. For the 2^{nd}, 4^{th},... $(2n)^{th}$ (j) eigenfunction make an initial guess $\psi_j(X_i)=X_i$
3. For every eigenfunction except the first, reset

$$\psi_j(X_i) = \psi_j(X_i) - \sum_{L=1}^{j-1} \psi_L(X_i) \left(\frac{\int_{-1}^{1} \psi_j(\xi)\, \psi_L(\xi)\, d\xi}{\lambda_L} \right)$$

where $\int_{-1}^{1} \psi_j(\xi)\, \psi_L(\xi)\, d\xi$ is approximated using a trapazoidal rule

4. Store $\psi_j(X_i)$ in $\psi_s(X_i)$
5. Calculate and reset $\psi_j(X_i)$ through

$$\psi_j(X_i) = \frac{1}{2\pi} \int_{-1}^{1} \frac{\sin c(X_i-\xi)}{X_i-\xi} \psi_j(\xi)\, d\xi$$

again using a trapazoidal rule approximation

6. Repeat step 3.

7. Using the trapazoidal rule approximation calculate

$$FKK1 = \frac{N-1}{4} \int_{-1}^{1} \psi_j(X)\, \psi_s(X)\, dx$$

and

$$FK2 = \frac{N-1}{4} \int_{-1}^{1} (\psi_j(X))^2\, dx$$

and

$$FK21 = \frac{N-1}{4} \int_{-1}^{1} (\psi_s(X))^2\, dx$$

8. Check if $\left|1 - \frac{(FKK1)^2}{FK2*FK21}\right| <$ ERR where ERR is an input parameter when this condition is satisfied $\lambda_j = \frac{FKK1}{FK21 \cdot \pi}$ and $\psi_j(X)$ is finally reset to

$$\psi_j(X) \sqrt{\frac{\lambda_j (N-1)}{FK2*4}}$$

If condition 8 is satisfied increment j and go to step 2.
If condition 8 is not satisfied go to step 4.

The results of this analysis were reasonably accurate, since the eigenvalues checked with eigenvalues found by an independent method. The program did have problems when c=8 since as c gets larger λ_2 and λ_4 have eigenvalues which are nearly equal. This prevents the procedure used from separating the 2nd and the 4th eigenfunction. Consider the following:

Let $F_n(X)$ be the n^{th} guess of $\psi_j(X)$. Then $F_n(X) = \sum_{\ell=1}^{\infty} a_\ell\, \psi_j(X)$ where if j is odd $a_2=a_4=\ldots=a_{2n}=\ldots=0$ since $F_n(X)$ is even and if j is even $a_1=a_3=\ldots=a_{2n+1}=\ldots=0$ since $F_n(x)$ is odd. Further the procedure reset $F_n(X)$ so that $a_1=a_2=\ldots a_{j-1}=0$. With this knowledge the function $F_{n+1}(X)$, to the accuracy of the integration satisfies the formula.

$$F_{n+1}(X) = K \sum_{\ell=j}^{\infty} a_e \lambda_e \psi_e(X)$$

where K is a constant. If $\lambda_j >> \lambda_{j+2}$ the iterations quickly lead to

$$F_N(X) \sim K_1 \psi_j(X)$$

where K_1 is a constant but if $\lambda_j \sim \lambda_{j+2}$ then the iteration leads to

$$F_N(X) \sim K_2(a_j\psi_j(x) + a_{j+2} \psi_{j+2}(x))$$

where K_2 is a constant.

The initial guess for $F_1(x)$ was good enough so that $a_2 > 100\ a_4$ so the problem was not as serious as might otherwise have been the case.

This program has been run with c=4 and c=8 for the first 5 and 8 eigenvalues, eigenfunctions, respectively.

Coupled Mode Propagation of Hydromagnetic Waves

Initiator: Dr. H. Radoski

Problem No: 4729 Project No: 7601

There are two fundamental hydromagnetic modes called the poloidal or isotropic and toroidal or guided modes. In an inhomogeneous medium, such as the earth's magnetosphere, these modes must always be coupled. Simple geometric models of the magnetosphere have been developed to study such coupled mode propagation. The case to be treated is the cylindrical model. No analytic solutions to the wave equations have been discovered. It is felt that numerical solutions should afford valuable insight into the development in time and space of the electric and magnetic fields.

The purpose of this problem is to perform the required numerical analysis and computer programming necessary to calculate and plot $P(x,t)$, $T(x,t)$ as functions of x between $x = 0$ and $x = x_o$ for a set of values of t between $t = 0$ and $t = t_{MAX}$, $P(x,t)$, $T(x,t)$ as functions of t between $t = 0$ and $t = t_{MAX}$ for a set of values of x between $x = 0$ and $x = x_o$, such that the following partial differential equations are satisfied:

$$(\partial^2/\partial t^2 + n^2x^{-2} + m^2)\ T(x,t) = m(\partial/\partial x)\ P(x,t)$$

$$[\partial^2/\partial t^2 + n^2x^{-2} - x^{-1}(\partial/\partial x)\ x(\partial/\partial x)]\ P(x,t) = -mx^{-1}(\partial/\partial x)\ xT(x,t)$$

A sample case with the values used as input parameters and the boundary conditions that were satisfied is presented below:

$$m = 1,\ n = 1,\ x_o = 1,\ t_{MAX} = 20$$

$$T(x,t = 0) = (\partial/\partial t)\ P(x,t = 0) = (\partial/\partial t)\ T(x,t = 0) = 0$$

$$P(x,t = o) = J_1(\omega x),\ \text{where } J_1(\omega) = 0$$

$$T(x = o,t) = P(x = o,t) = P(x = x_o,t) = o$$

The resulting calculations are then to be checked by the following associated conservation theorem:

$$\int_o^{x_o} \phi x dx = \text{constant}$$

$$\phi = G + I$$

$$G = T(x,t)^2 + (BZ)^2$$

$$I = P(x,t)^2 + (BR)^2 + (BF)^2$$

$$(BZ) = (m/x) \int_o^t T(x,t)\ dt$$

$$(BR) = (m/x) \int_o^t P(x,t)\ dt$$

$$(BF) = \int_0^t [\partial/\partial x\ P(x,t) - mT(x,t)]dt$$

$$EG = \int_0^{x_o} Gx\ dx$$

$$EI = \int_0^{x_o} Ix\ dx$$

Difference methods[@] were applied to the coupled partial differential equations such that the error term was of the order δ^4, where δ represents the difference in the independent variable between two adjacent grid points. This approach was unstable in that the calculated solutions became divergent at the boundary $x=0$. Analysis of the coupled equations and intermediate calculations seem to attribute this divergence to the term $(1/x)\ (\partial/\partial x)\ P(x,t)$. This approach was then modified by re-evaluating the solutions (P,T) at a particular time (t) for distances $x=\delta,2\delta,\ldots,i\delta$ from a polynomial, with no linear term, fitted to the above solutions at distances $x=0$, $(i+1)\delta$, $(i+2)\delta$,... this modification was successful in preventing the divergence and yielding possibly acceptable results. However, this later procedure was discontinued in preference to finding a method for calculating the solutions at all points and without such smoothing, nevertheless, it was encouraging to find such simplification so helpful.

It was next decided to utilize a predictor/corrector method (1) based on the following correction formula:

$$P(x,t_i) = (P(x,t_{i+1}) + 6P(x,t_{i-1}) - 4P(x,t_{i-2}) + P(x,t_{i-3}))/4$$

$$T(x,t_i) = (T(x,t_{i+1}) + 6T(x,t_{i-1}) - 4T(x,t_{i-2}) + T(x,t_{i-3}))/4$$

This formula was derived by equating difference approximations for the second order partial with respect to time at the t_{i-1} increment in time. It has an associated error term of the order δ^4. The procedure followed was to calculate values for P and T at t_{i+1}, use the above formulas to correct the values at t_i, recalculate the values at t_{i+1}, compare the later two predicted

---

[1] Numerical Methods for Scientists and Engineers, R.W. Hamming, McGraw-Hill, 1962, p. 186-210.

values at t_{i+1}, and should the comparison be adequate, proceed to the t_{i+2} evaluation, else perform the iteration of correcting the values at t_i, etc. The choice of correcting the t_i points rather than the t_{i+1} points was made in view of having two successive points for adjustment. In addition, it was preferred to provide the iteration option than resort to a variable time step.

The validity of resulting calculations of P and T were supported by both their satisfying the conservation theorem and their repeatability with a change in the grid size (δ). During the processing for various combinations of the parameters and initial conditions, it was noted that as the parameter related to faster damping of the P wave amplitude approaches 10, the solutions diverged at the boundary x=1, for the grid size $\delta = .001$ in both space and time dimensions as time (t) approached 10.

The computer core and/or time requirements seem to preclude any further significant reduction in δ or extended use of the iteration method. And so, in order to meaningfully extend the range of processing, it seems a variable grid size should be used in the spacial dimension, especially near the boundaries and a re-analysis of these coupled partial differential equations is required in order to find a more suitable correction formula.

As can be readily appreciated, a significant computer programming effort was required to develop a structure which could efficiently store and retrieve data for both calculation and presentation purposes. In particular, to provide the options for selecting when (time t_o) and where (distance x_o) the solutions P and T are to be outputted in plotted form.

@VIZ., letting i (upper) and j be indices respectively referring to time and space incrementing in the difference grid; then, excluding points near a boundary the predicting formula used for P(x,t) is the following:

$$P_j^{i+1} = 2P_j^i - P_j^{i-1} - \delta t^2 \Big\{ (n^2/x_j^2)\, P_j^i - (-P_{j+2}^i + 8P_{j+1}^i - 8P_{j-1}^i + P_{j-2}^i)/$$

$$(12\delta x\, x_j) - (P_{j+1}^i - 2P_j^i + P_{j-1}^i)/\delta x^2$$

$$+ m[(-T_{j+2}^i + 8T_{j+1}^i - 8T_{j-1}^i + T_{j-2}^i)/12\delta x + T_j^i/x_j] \Big\}$$

Power Spectral Analysis of Tide Data

Initiator: Mr. David Anthony

Problem No: 4754 Project No: 8607

This problem involved the Power Spectral Analysis (P.S.D.) of tide data presented as a function of time. The data was initially presented to us on paper tape but was first copied onto magnetic tape before beginning any analysis. The Maximum Entropy Method was used to determine the P.S.D.'s and the following is the procedure used:

Initially, the data was read from the magnetic tape and edited. This involved determining "bad" or missing data points and linearly interpolting to supply "corrected" points. Occasionally, the editing detected large gaps in the data, in which case the data was processed as if each group of data came from a separate paper tape. The edited data was then placed on what was called the "first master" data tape. It should be noted that the tide data was edited and stored on this "first master" in increasing time order.

The edited data was then re-read and an interpolation performed between the sets of data. The interpolation was performed by modifying a theoretical tide subroutine supplied by the problem initiator. Letting T(t) represent the tide value associated with time t, then, this program determines values for A, B and Δt such that $A+B*T(t+\Delta t)$ is a "best fit" in a least squares sense of the data on either side of the gap in the data. The program then finds values of A^1 and B^1 such that $A^1+B^1*T(t+\Delta t)$ touches the data point immediately preceding the data gap and touches the data point immediately following the data gap. The values of the function $A^1+B^1*T(t+\Delta t)$ at the times at which data points are missing are the interpolated data values.

This data set is now stored on the "second master" tape, from which a low-pass numerical filter[1] is applied to the data. The pass-band was set less than $\frac{Ny}{NDEC}$ where, Ny is the original Nyquist Frequency of the data and NDEC is a decimation factor, which is an input parameter to this program.

---

[1] K.W. Behannon and N.F. Ness, "The Design of Numerical Filters for Geomagnetic Data Analysis", NASA Technical Note, NSDS-TND-33411.

The data is then decimated by NDEC, and MM coefficients (MM is predetermined prior to execution) determined from the maximum entropy method (MEM) are applied to the decimated data. (A similar approach is used in the solution of Problem No. 4810, described later). A Fast Fourier Transform is now used to determine 16385 P.S.D. values at equally spaced frequencies, spaced between zero and the new Nyquist Frequency.

The maximums found above are then analyzed by finding the "exact" frequency of the maximum (i.e., the peak power point). This is accomplished by a search in the region of the maximum until $P_{M-1} \geq .99 * P_m \leq P_{m+1}$ where, P_m is the power at the peak power point, and P_{m-1} (P_{m+1}) is the power at the next lower (higher) frequency studied. In addition, the area (energy) in the vicinity of the peak is calculated. This area is between points at half the peak power or a minimum of a power versus frequency curve, whichever definition defines a smaller integral.

The results showed that the high frequencies agreed with theoretical values to within .1% but the low frequencies were inaccurate. The energy under the peak also followed the expected pattern. We expect to improve the accuracy of results with an improved MEM.

A Laser Beam Slewing Through a Turbulent Medium

Initiator: Dr. R. Fante

Problem No: 4756 Project No: 2153

When a laser beam is slewed through a turbulent medium the spectrum of the intensity and phase fluctuations are affected. The purpose of this problem is to evaluate the integral equations which describe the frequency spectra of the log-amplitude and phase fluctuations. For a beam slewing at an angular rate ω_s the frequency spectra of the log-amplitude Q_x and phase fluctuation Q_s is known to be

$$Q_x(\Omega) = \int_0^1 d\xi \int_{\frac{\Omega^2}{(1+\gamma\xi)^2}}^{\infty} dt \; \frac{e^{-t(1-\xi)^2 \left(\frac{a}{1+a^2}\right)}}{(t+F)^{11/16}(t(1+\gamma\xi)^2-\Omega^2)^{1/2}} \sin^2\left(\frac{t(1-\xi)}{2}\left(\frac{1+a^2\xi}{1+a^2}\right)\right)$$

$$Q_s(\Omega) \qquad\qquad \cos^2\left(\frac{t(1-\xi)}{2}\left(\frac{1+a^2\xi}{1+a^2}\right)\right)$$

where $\Omega = \frac{\omega}{\sqrt{o}}\sqrt{\frac{L}{k}}$, ω = radian fluctuation frequency, $\sqrt{o}$ = ambient atmospheric wind speed, L = path length in turbulence, k = signal wavenumber, $\gamma = \omega_s L/r_o$, $F = L/(kL_0^2)$, L_o = outer scale size of the turbulent eddies.

It is readily noted that there is a singularity at the lower limit of the t integral. That is, at

$$t = \Omega^2/(1+\gamma\xi)^2$$

Analysis of the integrand reveals it is of the form $1/\sqrt{x}$. Hence, it was found acceptable to increment this limit by adding

$$\frac{(1+\gamma\xi)^2}{2}\left(\frac{\Omega^2}{1+\gamma\xi)^2} + F\right)^{11/16} (RF)$$

with RF representing an assumed insignificant fraction of the integration.

The infinity at the upper limit of the t integration was replaced by

$$\frac{-(1+a^2)}{a(1-\xi)^2} \log\left(\frac{a(1-\xi)^2}{(1+a^2)}(RF)\right)$$

This was determined by noting that the exponential term of the integrand eventually becomes dominant.

These double integrations were satisfactorily evaluated using the Adaptive Simpson Rule[1] technique developed by this laboratory.

---

[1] A New Adaptive Simpson Integration Routine, Neil Grossbard, Space Data Analysis Laboratory, Boston College, Chestnut Hill, Mass. 02167; AFCRL-70-0504, Scientific Report No. 1, September 1970.

A Functional Determination for Fitting Roentgen Measurements

Initiator: Mr. R. Frederickson

Problem No: 4766 Project No: 5621

The purpose of this problem is to determine a functional curve fit to data which represents the dependence to exposure readings in Roentgens/minute (Ro) on the radial distance from the collimator center line to the ion probe center.

The given raw data, Ro, is first corrected by the factor R/R^1 which is defined as follows:

$$R = \int_{.1}^{1.25} E\, N(E)\, \mu(E)\, dE$$

$$R^1 = \int_{.1}^{1.25} S(E)\, E\, N(E)\, \mu(E)\, dE$$

$$N(E) = nIe^{-n} \qquad (.1 \leq E < 1.25)$$

$$N(E) = e^{-n} \qquad (E = 1.25)$$

(n is an input parameter)

$$I = 1.25\, [\sin(1.37(E-.1))]^{1/3}$$

$$\mu(E) = 4.505 \times 10^{-2} - 2.325 \times 10^{-2}E + 1.344*10^{-2}E^2$$

$$-3.728*10^{-3}E^3 - 3.64*10^{-3}E^{-1} + 1.66*10^{-4}E^{-2}$$

$$S(E) = 8.733*10^{-1} + 4.999*10^{-2}E + 8.234*10^{-2}E^2$$

$$-3.178*10^{-2}E^3 + 3.053*10^{-2}E^{-1} - 9.856*10^{-4}E^{-2}$$

Notice that N(E) has a "delta function" contribution at E=1.25. Analysis of the above integrals reveal that it is satisfactory to utilize Simpson's Rule for their numerical evaluation using the continuous form for N(E) and adding

(i) $1.25\ \mu(1.25)\ \exp(-N)$ to R.

(ii) $1.25\ S(1.25)\ \mu(1.25)\ \exp(-N)$ to R^1.

The procedure chosen to determine the functional curve fit to the data is to minimize the least square expression

$$\phi = \sum_{m=1}^{M} \left(R_o(t_m) - F(t_m, a_j)\right)^2$$

where, M equals the number of data points, t_m is the independent variable (radial distance), F the mathematical model function, and a_j the parameters in that function. A rather remarkable curve-fit to this data is obtained upon using the following mathematical model

$$F(t,a_j) = a_0 + a_1 \exp(a_2 \exp(a_3 t a^4))$$

A computer program incorporating the Space Data Analysis Laboratory version of applying the Method of Levenberg to certain nonlinear problems readily determines appropriate values for the parameters a_j. Included in the output of this program are the description of the fitting expression, the estimated values for the parameters, the input data, the fitted evaluations, the corresponding differences, the associated variances, the standard deviation and plotting.

Evaluation and Plotting of Sets of Double Integrals

Initiator: Dr. G. Borgiotti

Problem No: 4773 Project No: 4600

This problem involves the evaluation and plotting of sets of double integrals. The plots are generally of $g(US_1|\sin\theta o)$ versus US_1 where

$$g(US_1|\sin\theta o) = \int_{-1}^{1} f(X_1|\sin\theta o)\, e^{j(US_1)X_1}\, dx_1$$

with

$$f(x_1|\sin\theta o) = \int_{-1}^{1} \exp\left\{ \frac{-jS_1 K_a}{\sin\theta_a}\left[\sqrt{1 + \frac{\sin^2\theta_a}{\mu^2}(\xi_1^2 - 2\mu X_1 \xi_1)} - \sqrt{1 + \frac{\xi_1^2}{\mu^2}\sin^2\theta_a}^{-1}\right]\right\} \sum_{P=-4}^{3} dp + 1/2 \exp\left(j\left(p+\frac{1}{2}\right)\pi\left(\xi_1 - \frac{\sin\theta o}{\sin\varepsilon}\right)\right) d\xi_1$$

given $j = \sqrt{-1}$, μ=6.25, $\sin\theta a$=1/2, Ka=314.16 and $\sin\varepsilon$=.08 and the values of S_1, dp+1/2 are input parameters.

In order to calculate $f(x_1|\sin\theta o)$ the value of the real and imaginary parts of $f(x_1|\sin\theta o)$, $f_r(x_1|\sin\theta o)$, $f_I(x_1|\sin\theta o)$ are calculated separately. Thus, let

$$ARG1 = \frac{S_1 Ka}{\sin\theta a}\left[\sqrt{1 + \frac{\sin^2\theta a}{\mu^2}(\xi_1^2 - 2\mu\, x_1\xi_1)} - \sqrt{1 + \frac{\xi_1^2}{\mu^2}\sin^2\theta a}\right] \text{ and}$$

Let $ARG_P = \left(p+\frac{1}{2}\right)\pi\left(\xi_1 - \frac{\sin\theta o}{\sin\varepsilon}\right)$

Then

$$f_R(X_1|\sin\theta o) = \sin(ARG1) \sum_{p=-4}^{3} dp+\frac{1}{2} \sin(ARG_p)$$

$$+ \cos(ARG1) \sum_{p=-4}^{3} dp+\frac{1}{2} \cos(ARG_p)$$

and

$$f_I(X_1|\sin\theta o) = \cos(ARG1) \sum_{p=-4}^{3} dp+\frac{1}{2} \sin(ARG_p)$$

$$- \sin(ARG1) \sum_{p=-4}^{3} dp+\frac{1}{2} \cos(ARG_p)$$

The integrals for $f_R(X_1|\sin\theta o)$ and $f_I(X_1|\sin\theta o)$ are approximated by an adaptive Simpson Rule[1] technique developed by this Laboratory.

Values of $f(X_1|\sin\theta o)$ are calculated for a given value of $\sin\theta o$ $X_1 = -1$, $-1+\Delta X$; $-1+2\Delta X$,... 0, ΔX,... 1 where $\Delta X = \frac{1}{N}$, N set through an input parameter. These values of $f(X_1|\sin\theta o)$ are then multiplied by weights, as if, to approximate

$$\int_{-1}^{1} f(X_1|\sin\theta o)\, dX_1$$

by Simpson's Rule. The first N+1 of these weighted $f(X_1|\sin\theta o)$ (X_1 varies from -1 to 0) are placed in the first N+1 locations of a complex array f*. The last N values of the weighted $f(X_1|\sin\theta o)$ (X_1 varies from ΔX to 1) are placed in location 4097-N through 4096 of f*. Locations N+2 through 4096-N of f* are set to zero and a 4096 point Fast Fourier Transform (F.F.T.) is applied to f*. The resultant answers contain $g(US_1|\sin\theta 0)$ for values of $US_1 = \frac{L}{4096*\Delta t}$, where L varies between -2048 and 2048.

---

[1] A New Adaptive Simpson Integration Routine, Neil Grossbard, Space Data Analysis Laboratory, Boston College, Chestnut Hill, Mass. 02167; AFCRL-70-0504, Scientific Report No. 1, September 1970.

The method used to calculate $g(US_1|\sin\theta o)$ is a general method which can be used to get sets of integrals of the general form

$$X(s) = \int_a^b y(t)\, e^{jts}\, dt\ .$$

The results of this problem were accurate plots of $g(US_1|\sin\theta o)$. One plot for each of a set of values of S_1 and θo.

Analysis of Multi-Exponential Luminescent Decay Rates

Initiator: Mr. R. O'Neil

Problem No: 4789 Project No: 8658/CDNA

When optical radiation at a given wavelength may be the result of one or more specific atomic or molecular transitions, the magnitude of the various contributing emitters may be established by analysis of the time dependent optical radiation. The analysis is simplified if the number of contributing radiating states is known and/or if the transition probabilities are appreciably different. Recovery of the number and magnitude of the luminescent decays as well as the exponential term coefficients will then be further analyzed as a function of molecular collision frequency to provide reaction rate coefficients for various processes.

The purpose of this problem is to determine the number and magnitude of luminescent decay rates in oxygen and oxygen-nitrogen gas mixtures for the case where the decay may be described by either one, two or three exponential rates. This requires developing or applying existing programs to various experimental data to solve an expression of the form:

$$I = I_1 e^{-x_1 t} + I_2 e^{-x_2 t} + I_3 e^{-x_3 t} + I_4$$

where I is given for various values of t, and the I_i, X_j and their standard deviations are to be determined.

The data was presented in two forms: (i) tabulated, (ii) a data tape representing an analog/digital conversion. The first form could be readily processed; whereas, the second, which was output by the AFGL ac/dc facility, required both unpacking and sorting. The unpacking was done by programs obtained from the Boston College SDAL Satellite Group. The resulting data tape was processed such that the data representing the magnitude of the luminescent decay is sorted in terms of time identifying the beam status on/off and then placed onto another tape.

Data sets selected from this later tape were then curve fitted by the exponential programs developed by the Boston College SDAL Numerical Analysis Section. For each data set, the curve fitting was for all the data, some of the data as "averaged data" and including or excluding constraints on the parameter, in particular, the parameter representing the background level.

The output of this rather substantial processing was provided in both printed and plotted form. In addition to plotting on a linear or regular scale, an option was also included for displaying the results using logarithmic scaling. This was accomplished by taking the logarithm of the difference between the data and the background level and selecting proper intercepts, such that the decay rates could be interpreted as the slopes of straight lines which correspond to the so-called best fittings. A composite plot was also generated which showed the dependency of the slow decay rate on the omission of data pertaining to a fast decay rate as a function of time.

The results of this effort were presented at the meeting of the American Geophysical Union in December, 1975, at San Francisco, California. It is also intended that these results be published in an AFGL, Scientific Report.

Electron-Ion Mathematical Modelling in the Ionosphere

Initiator: Dr. John Jasperse

Problem No: 4799 Project No: 8627

The purpose of this problem is to find a mathematical model to explain the behavior of electrons and ions in the ionosphere. Towards this end many models were investigated.

The first model tried assumes the ionosphere contains monoenergetic photo-electrons. This model calculates the normalized electron velocity distribution function (F_{norm} (X)) and the electron temperature compared to the photo-electron temperature ((T_e/T_{pe}) (y)). The equations used are the following:

$$F_{norm}(X) = \frac{2}{\sqrt{X_1}} \quad \frac{\sqrt{X}}{1 + (V_l/V_r)\sqrt{X}\ \theta\ (\sqrt{X}-1)}$$

$$\{\ \delta\ (X-X_0) + \sum_{m=1}^{M} B_m\ \delta\ (X-(X_0-m))\ \}$$

$$(T_e/T_{pe})(y) = \frac{1}{1 + y\sqrt{X_0}} + \sum_{m=1}^{M-1} C_m(y)\ \frac{[1-mX_0^{-1}]}{1 + y\ (X_0-m)^{\frac{1}{2}}} + C_M(y)\ [1-M\ X_0^{-1}]$$

where $B_m = \prod_{\ell=1}^{m} \left[\frac{[X_0 - (\ell-1)]^{\frac{1}{2}}}{V_r/V_1 + [X_0 - (\ell-1)]^{\frac{1}{2}}}\right]$ and

$$C_m(y) = \prod_{\ell=1}^{m} \left(\frac{X_0 - (\ell-1)]^{\frac{1}{2}}}{y^{-1} + [X_0 - (\ell-1)]^{\frac{1}{2}}}\right)$$

Here $V_r = \alpha\ n_e$ with α the recombination coefficient and n_e the recombination frequency.

$V_1 = \sqrt{X_1}/L_1$ with X_1 the threshhold velocity squared and L_1 the mean free path.

X_0 is the photo-electron velocity squared

M is an arbitrary input parameter.

In addition to the above,

$$I = \frac{1}{1 + (V_1/V_r)\sqrt{X_0}} + \sum_{m=1}^{M-1} B_m \frac{1}{1 + (V_1/V_r)(X_0-m)^{\frac{1}{2}}} + B_m$$

is calculated. I should equal one, if the equality stands up.

The second model tried assumes the ionosphere contains exponentially distributed energies of photo-electrons.

The solution of this model is approached as n goes to infinity of the velocity distribution function.

$$F_{norm}^{(N)}(X) = \left(\frac{2}{\sqrt{X_1}\ X_0}\right)\left[\frac{\sqrt{X}}{1 + (V_1/V_r)\sqrt{X}\ \theta\ (\sqrt{X} - 1)}\right]$$

$$(1 - \exp(-X_0^{-1}))^{-1} \exp(-X/X_0)\ B^{(N)}(X)$$

and the electron temperature compared to the photo-electron temperature

$$T_e^{(N)}/T_{pe} = \frac{\sqrt{X_1}}{X_0} \int_0^b dx \frac{\sqrt{X}}{2} F_{norm}^{(N)}$$

Where $\theta(X) = 1$ if $X \geq 0$; $= 0$ otherwise

$$B^{(N)}(X) = [1 - \exp(-X_0^{-1})] + \exp(-NX_0^{-1})\ C_N(X)$$

$$+ [1 - \exp(-X_0^{-1})] \sum_{n=1}^{N-1} \exp(-nX_0^{-1})\ C_n(X)$$

$$C_n(X) = \prod_{m=1}^{n} \left[\frac{(x+m)^{\frac{1}{2}}}{V_r/V_1 + (X+m)^{\frac{1}{2}}}\right]$$

the input data is the same as the first model, with b the upper limit of the ratio of V_1/V_r.

The integral is calculated as the sum of

$$\frac{\sqrt{X_1}}{X_0} \int_0^1 dx \frac{\sqrt{X}}{2} F_{norm}^{(N)} + \frac{\sqrt{X_1}}{X_0} \int_1^b dx \frac{\sqrt{X}}{2} F_{norm}^{(N)}$$

with each integral evaluated using a trapazoidal rule.

In addition the following quantities are calculated:

$$I^{(N)} = \int_0^b dx \; \frac{\sqrt{X_1}}{2\sqrt{X}} \; F^{(N)}_{norm} \; (X)$$ where this check should approach one as N approaches infinity

$$F^{(0)}_{norm} \; (X) = \left(\frac{2}{\sqrt{X_1}\; X_0}\right) \left[\frac{\sqrt{X}}{1 + (V_1/V_r)\sqrt{X}\;\theta\;(\sqrt{X}-1)}\right] [1 - \exp(-X_0^{-1})]^{-1}$$

$$\exp(-X/X_0)$$

$$I^{(0)} = \int_0^b dx \; \frac{\sqrt{X_1}}{2\sqrt{X}} \; F^{(0)}_{norm} \; (X)$$

$$\frac{T_e^{(0)}}{T_{pe}} = \frac{\sqrt{X_1}}{X_0} \int_0^b dx \; \frac{\sqrt{X}}{2} \; F^{(o)}_{norm} \; (X)$$

and the electron source function

$$(V^2 \; G_{norm}) \; (X) = (2\alpha n_e/(X_0\sqrt{X_1})) \; \sqrt{X} \; \exp(-X/X_0)$$

The third model calculates the photo-electron source function

$$S_0 \; (z) = Q_{pL1} \; n_1(z) \; I_{b1} \exp[A_1(z)] \text{ where } n_1 \; (z) = n_{a1} \exp[(a-z)/h_1]$$

and $A_1 \; (z) = h_1 \; Q_{pa1} \left|\sec \chi\right| \; [n_1(b) - n_1(z)]$.

We also calculate the spherical electron flux

$$\rho_e \; (z) = \left[\frac{4}{\pi\alpha_r \; F_{ion} \; (z)}\right]^{\frac{1}{2}} \left[\frac{1}{y(z)}\right] [S_0(z) - \frac{5}{2} \; S_2 \; (z)] \text{ and}$$

calculate the electron density $n_e(z) = (\frac{\pi}{4})^{\frac{1}{2}} \; y(z) \; \rho_e(z)$ and calculate the

the electron temperature $T_e(z) = 3.2991 \; (10^{-12}) \left[\frac{1}{y(z)}\right]^2$

Here a is the base height of the ionosphere

b is the base height of the exosphere

Q_{pL1} is the photo-electron ionization cross-section

Q_{pa1} is the photo-electron absorption cross-section

n_{a1} is the neutral particle density at a

h_1 is the scale height

I_{b1} is the photo-electron flux at b

χ is the zenith angle

α_r is the recombination coefficient

$F_{ion}(z)$ is the value of the fractional ion concentration at the height z.

$S_2(z) = 0$

y(z) is the electron velocity at the height z.

y(z) is either a set of input parameters or if the temperature is calculated then:

$$\frac{1}{y(z)} = \frac{1}{y_0} \left\{ \frac{1}{1 + X(z)\sqrt{X_0}} + \sum_{m=1}^{M-1} C_m(X(z)) \frac{[1-m X_0^{-1}]}{1 + X(z)(X_0-m)^{\frac{1}{2}}} \right.$$

$$\left. + C_M(X(z))[1-MX_0^{-1}] \right\}^{\frac{1}{2}}$$

where $X(z) = V' L'^{-1}(z)/\alpha_r \; F_{ion}(z) \; n_e(z)$ and

$$L^{-1}(z) = Q' n'(a) \exp((a-z)/h_1)$$

and $$C_m(X(z)) = \prod_{\ell=1}^{m} \left(\frac{[X_0 - (\ell-1)]^{\frac{1}{2}}}{X(z)^{-1} + [X_0 - (\ell-1)]^{\frac{1}{2}}} \right)$$

here Y_0 is the photo-electron temperature

Q' is the inelastic scattering cross-section

n'(a) is the neutral particle density at a

V' is the threshhold velocity

X_0 is the square of the photo-electron velocity

M is an input parameter $(M \to \infty)$

The fourth model solves the following integral equation

$$\rho_e(z) = I_1 + K_{11}\,(I_{11} + F_{11}\,\rho_e(z) + F_{12}\,(\rho_e(z)^2))$$

where $K_{11} = \frac{1}{2}\int_a^b dz'\, E_1\left(\frac{fh}{L_{e\ell}}\,\middle|\, e^{-z/h} - e^{-z'/h}\right|)$

E_1 is the exponential integral of the first kind

$$I_1 = I^{(in)} \exp\left[-\frac{fh}{\mu_0 L_{e\ell}}\left(\exp\left(-\frac{z}{h}\right) - \exp\left(-\frac{b}{n}\right)\right)\right]$$

$$I_{11} = S_0(z') - \frac{5}{2}\,S_2(z')$$

$$F_{11} = fL_{e\ell}^{-1}(z') + (S-1)\,L_i^{-1}(z')\,e^{-V_i^2 y^2(z')}\,(1 + V_i^2\,y(z)^2)$$

$$F_{12} = -\left(\frac{\pi\alpha_r}{4}\right) y^2(z')\,F_{ion}(z')$$

further $L_{e\ell}^{-1}(z') = L_{e\ell}^{-1} \exp\left(-\frac{z'}{h}\right)$

$$L_i^{-1}(z') = L_i^{-1} \exp\left(-\frac{z'}{h}\right)$$

with $L_{e\ell}^{-1} = Q_{e\ell}\, n(a) \exp\left(\frac{a}{h}\right)$

$$L_i^{-1} = Q_i\, n(a) \exp\left(\frac{a}{h}\right)$$

Here $I^{(in)}$ is the incident flux at b

μ_0 is the cosine of the angle of the incident flux

f is an additive fraction in the equation

h is a scale height

n(a) is the neutral particle density at a

Q_{el} is the elastic cross-section

V_I is the ionization threshhold velocity

S is the mean number of electrons per ionizing collision

To solve this integral equation we consider a monotonically increasing set of NVAL z_k values starting at a and ending at b. K_{11} is then approximated, except at $z = z'$, by

$$K_{11} = \sum_{K=1}^{NVAL} \frac{1}{2} \left(E_1 \frac{fh}{L_{el}} \left| e^{-e/h} - e^{-zk/h} \right|\right) \Delta (z_k)$$

with $z_0 = z_1 = a$ and $z_{NVAL} = z_{NVALTI} = b$

$$\Delta (z_k) = \frac{1}{2} (z_{k+1} - z_{k-1}) \quad \text{at } z = z_k$$

the term in the sum is approximated, using a taylor series expansion, by

$$\frac{1}{2} E_1 \left(\frac{fh}{L_{el}} \left| e^{-z/h} - e^{-zk/h} \right|\right) \Delta (z_k) \text{ as } z \to z_k$$

$$+ \frac{1}{2} E_1 \left(\frac{fh}{L_{el}} \left| e^{-z/h} - e^{-zk/h} \right|\right) \Delta_f (z_k)$$

$$+ \frac{1}{2} E_1 \left(\frac{fh}{L_{el}} \left| e^{-z/h} - e^{-zk/h} \right|\right) \Delta_h (z_k)$$

where $E_1 \left(\frac{fh}{L_{el}} \left| e^{-z/h} - e^{-zk/h} \right|\right) \Delta_i (z_k)$ (i=f or h)

$$= h \left(-\varepsilon_{ij} - \varepsilon_i \ln \left(\frac{fh}{L_{el}}\right) - \frac{1}{2} \left(\frac{\varepsilon_i^2}{2}\right) + e^{-z/h} \left(2 - e^{\varepsilon_i/2} - e^{-\varepsilon_i/2}\right)\right.$$

$$\left. - \sum_{n=1}^{\infty} \left(\frac{\exp(-2nz/h)}{2n\,(2n)!}\right)\left(\varepsilon_i - (1-e^{-\varepsilon_i/2})\left(1 + \frac{1-e^{-\varepsilon_i/2}}{2}\right)\right.\right.$$

$$+ (1 - e^{\varepsilon_{i/2}}) \left(1 + \frac{1 - e^{\varepsilon_{i/2}}}{2}\right))$$

$$- \sum_{n=2}^{\infty} \frac{\exp\left(\frac{-(2n-1)z/h}{(2n-1)\,(2n-1)!}\right)}{} \left((1 - e^{-\varepsilon_{i/2}}) \left(1 + \frac{1-e^{-\varepsilon_{i/2}}}{2}\right)\right.$$

$$\left. + (1 - e^{\varepsilon_{i/2}}) \left(1 + \frac{1-e^{\varepsilon_{i/2}}}{2}\right)\right) + 2 \sum_{n=1}^{\infty} \frac{1}{n^2} (1 - e^{-M\varepsilon i/2})$$

here $\Delta_f (z_k) = \frac{1}{2} (z_{k+1} - z_k)$

$$\Delta_b (z_k) = \frac{1}{2} (z_k - z_{k-1})$$

$$\varepsilon_i = \frac{\Delta_i}{h}$$

Error bounds were found for truncating the above infinite sums and the above term was evaluated to a fractional accuracy of .0001.

With this approximation for K_{11} NVAL equations were formed, one for each value of z_k. This set up NVAL equations in NVAL unknowns. We solved this equation as follows:

After setting up the equation NVAL initial guesses for the values of $\rho_e(z_k)$ are made. These initial guesses are either input data or

$\rho_e(z_k) = \sqrt{\frac{4\,(S_0\,(z_k) - 5/2\,S_2\,(z_k))}{\alpha\,\pi\,F_{ion}\,(z_k)}}$. A "better" guess is then calculated as described below.

For each equation find the amount (E(z)) for which the equation is not satisfied. Then calculate all the possible derivatives $\frac{\partial E(z)}{\partial \rho(z_k)}$. Then form NVAL equations; one for each z value considered.

$$\sum_{k=1}^{NVAL} \Delta z_k \frac{\partial E(z)}{\partial \rho(z_k)} = -E(z)$$

and solve the NVAL linear equation in NVAL Δz_k unkowns for the $\Delta z'_k$ s. Then form new $\rho(z_k)$ values

$\rho_{NEW}(z_k) = \rho_e(z_k) + \alpha \Delta z$ and calculate the new $E(z_k)$'s

($E_{NEW}(z_k)$). Here α is initially one but is halved until

$\sum_{k=1}^{NVAL} (E_{NEW}(z_k))^2 < \sum_{k=1}^{NVAL} (E(z_k))^2$. This is the "beter" guess for $\rho(z)$. This process is repeated until, judging by the amount of error and the changes in $\rho(z)$ the process appears to have converged. As in the third model y(z) is either an input parameter or is calculated as indicated in equation (1). In addition to $\rho_e(z)$ and y(z) the program also calculates the electron concentration $n_e(z) = (\frac{\pi}{4})^{\frac{1}{2}} y(z) \rho_e(z)$, and the electron temperature $T_e(z) = 3.2991\ 10^{-12}/(y(z))^2$. If y(z) is changed the program does each correction of $\rho_e(z_k)$ after changing y(z).

The fifth model solves the following integral equations

$$\rho_e(z) = I_1 + K_{11}(I_{11} + F_{11}\rho_e(z))^{-2}) + K_{12}(I_{21} + F_{21}\rho_e(z) J(z) + F_{22} J(z))$$

$$\text{and } J(z) = I_2 + K_{21}(I_{11} + F_{11}\rho(z) + F_{12}(\rho(z))^2) + K_{22}(I_{21} + F_{21}\rho(z) + F_{22} J(z)) \quad (2)$$

where $K_{12} = \frac{3}{2} \int_a^b dz'\ E_2\left(\frac{fh}{Le\ell} \left| e^{-z/h} - e^{-z'/h} \right|\right) \text{sign}(z-z')$;

$K_{21} = \frac{1}{2} \int_a^b dz'\ E_2\left(\frac{fh}{L_{e\ell}} \left|e^{-z/h} - e^{-z'/h}\right|\right) \text{sign}(z-z')$;

$K_{22} = \frac{3}{2} \int_a^b dz'\ E_3\left(\frac{fh}{L_{e\ell}} \left|e^{-z/h} - e^{-z'/h}\right|\right)$

where sign (X) = 1 for $X \geq 0$ and -1 for $X < 0$ and where E_n is the exponential integral of the nth kind

$$\text{Further } I_2 = -I^{(in)} \mu_0 \exp\left[-\frac{fh}{\mu_0 L_{e\ell}} \left(\exp\left(-\frac{z}{h}\right) - \exp\left(-\frac{b}{h}\right)\right)\right];$$

$$F_{21} = -\left(\frac{2\alpha_r}{3}\right) y^2(z') F_{ion}(z');$$

$$F_{22} = -(1-f) L_{e\ell}^{-1}(z') - \sum_{k=1}^{N} L_k^{-1}(z') f_4(V_k y(z')$$

$$-L_i^{-1}(z') f_4(V_i y(z'));$$

$$\text{where } f_4(x) = \frac{4}{3\sqrt{\pi}} \left[X^3 e^{-X^2} + \frac{3}{2} X e^{-X^2} + \frac{3\sqrt{\pi}}{4} (1-\text{erf}(X))\right]$$

$$L_k^{-1}(z') = L_k^{-1} \exp\left(-\frac{z'}{h}\right)$$

$$L_k^{-1} = Q_k n(a) \exp\left(\frac{a}{h}\right) \quad \text{for } K = 1, 2, \ldots, N$$

Here N is the number of inelastic cross-sections used in the analysis
Q_k is the Kth inelastic cross-section
V_k is the Kth threshhold velocity

This set of integral equations is solved exactly analogous to the fourth method but 2NVAL equations in 2NVAL unknowns are formed. The additional unknowns are the $J(z_k)$'s and the additional equations come from solving (2). If $J(z_k)$ is to be initialized it is calculated from the initialized $\rho_e(z_k)$ values as the approximation of

$$J(z_k) = I_2 + K_{21}(I_{11} + F_{11} \rho_e(z) + F_{12}(\rho_e(z))^2) + K_{22} I_{21}$$

AD-A034 047 BOSTON COLL CHESTNUT HILL MASS SPACE DATA ANALYSIS LAB F/G 9/2
NUMERICAL AND DATA ANALYSIS TECHNIQUES APPLIED TO SCIENTIFIC RE--ETC(U)
MAR 76 J E MARTINE, L F POWER F19628-73-C-0136

UNCLASSIFIED BC-SDAL-76-2 AFGL-TR-76-0091 NL

2 OF 2
AD
A034047

END

DATE
FILMED
2-77

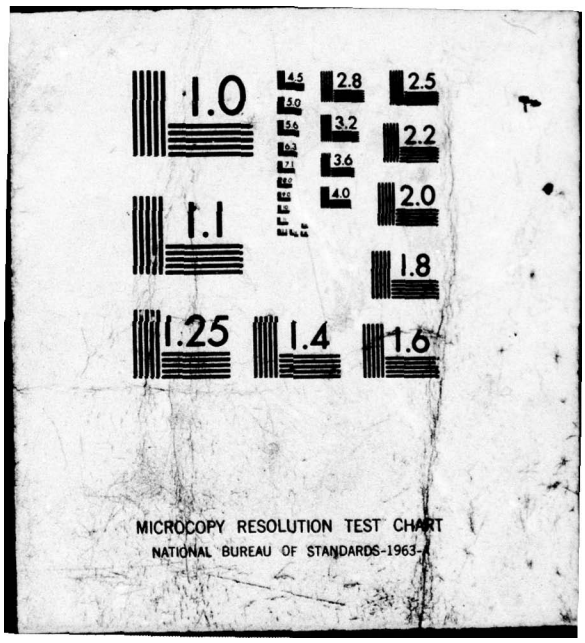
1.0
1.1
1.25
1.4
1.6
1.8
2.0
2.2
2.5
2.8
3.2
3.6
4.0
4.5
5.0
5.6
6.3
MICROCOPY RESOLUTION TEST CHART
NATIONAL BUREAU OF STANDARDS-1963-A

After "solving" for $\rho_e(z_k)$ and the particle current density $J(z_k)$ we calculate

$n_e(z_k) = (\frac{\pi}{4})^{\frac{1}{2}} y(z_k)\ \rho(z_k)$ the electron drift velocity $U(z_k) = \dfrac{J(z_k)}{n_e(z_k)}$

and $T_e(z_k) = 3.2991\ 10^{-12}/(y(z_k)^2$

From the mathematics supplied by the Initiator, the following equation serves as a check:

$$J(b) - J(a) = \int_a^b dz' \{S_0(z') - (\frac{\pi\alpha_r}{4}) F_{ion}(z') y^2(z') \rho^2(z')$$

$$+ (S-1) L_i^{-1}(z') e^{-V_i^2 y(z')^2} (1 + V_i^2 y^2(z')) \rho(z') \}$$

This equation has been checked with the integrals calculated using a trapazoidal rule.

Another set of equations derived from the supplied mathematics should also check:

$$\frac{\partial}{\partial z} J(z) = S_0(z) - (\frac{\pi\alpha_r}{4}) F_{ion}(z) y^2(z) \rho^2(z) \qquad (3)$$

$$+ (S-1) L_i^{-1}(z) (1 + V_i^2 y^2(z)) e^{-V_i^2 y^2(z)} \rho(z)$$

for all z values. This equation is checked for the NVAL z_k values considered. For the purpose

$\frac{\partial}{\partial z} J(z_k)$ for K ≠ or NVAL is approximated by fitting a parabola through the points z_{k-1}, z_k and z_{k+1} and then finding the derivative of the parabola at the point z_k. The derivative at z_1 and z_{NVAL} is approximated as

$$\frac{\partial}{\partial z} J(z_1) \simeq \frac{J(z_2) - J(z_1)}{z_2 - z_1} \qquad \text{and}$$

$$\frac{\partial}{\partial z} J(z_{NVAL}) \simeq \frac{J(z_{NVAL}) - J(z_{NVAL-1})}{z_{NVAL} - z_{NVAL-1}}$$

The program may reset y(z) as in the third model or by finding y(z) values which satisfy (3). When equation (3) is used, equation (3) is not used for checking. In any case the program now solves for the electron temperature $T_e(z_k) = 3.2991 \cdot 10^{-12}/(y(z_k))^2$.

The sixth model solves the following integral equations in a manner exactly comparable to that used in the fourth and fifth models.

$$\rho_e(z) = -\frac{4}{3\pi} J^2(z)/\rho_e(z) + I_1 + K_{11} I_{11} + K_{12} I_{21} + K_{13} I_{31}$$

$$+ K_{11} F_{11} \rho_e(z') + K_{11} F_{12} \rho_e^2(z') + K_{12} F_{21} \rho_e(z') J(z')$$

$$+ K_{12} F_{22} J(z') + (K_{11} F_{13} + K_{13} F_{31}) J^2(z')$$

$$+ (K_{11} F_{14} + K_{13} F_{32}) J^2(z')/\rho_e(z')$$

$$J(z) = I_2 + K_{21} I_{11} + K_{22} I_{21} + K_{23} I_{31}$$

$$+ K_{21} F_{11} \rho_e(z') + K_{21} F_{12} \rho_e^2(z') + K_{22} F_{21} \rho_e(z') J(z')$$

$$+ K_{22} F_{22} J(z') + (K_{21} F_{13} + K_{23} F_{31}) J^2(z')$$

$$+ (K_{21} F_{14} + K_{23} F_{32}) J^2(z')/\rho_e(z')$$

where $K_{13} = \frac{15}{4} \int_a^b dz' E_3 \left(\frac{fh}{L_{e\ell}} \left| e^{-z/h} - e^{-z'/h} \right|\right)$;

$$K_{23} \frac{15}{4} \int_a^b dz' E_4 \left(\frac{fh}{L_{e\ell}} \left| e^{-z/h} - e^{-z'/h} \right|\right);$$

Further $I_{21} = S_1(z') = 0$

$I_{31} = S_2(z') = 0$

$$F_{13} = \alpha_r \, y^2(z') \, F_{ion}(z') \, F_{ion}(z')$$

$$F_{14} = \left(\frac{4}{3\pi}\right) \{ (4-3f) \, L_{e\ell}^{-1}(z') + \sum_{k=1}^{N} \alpha \, L_k^{-1}(z') \, e^{-V_k^2 y^2(z')}$$

$$[2 + 2V_k^2 y^2(z') + V_k^4 y^4(z')] + L_i^{-1}(z') \, e^{-V_i^2 y^2(z')}$$

$$[S + 3 + (S + 3) V_i^2 y^2(z') + 2S V_i^4 y^4(z')] \}$$

$$F_{31} = -\frac{2\alpha_r}{5} \, y^2(z') \, F_{ion}(z');$$

$$F_{32} = -\left(\frac{32}{15\pi}\right) \{1-f) \, L_{e\ell}^{-1}(z') + \sum_{k=1}^{N} L_k^{-1}(z') \, e^{-V_k^2 y^2(z')}$$

$$(1 + V_k^2 y^2(z') + \frac{1}{2} V_k^4 y^4(z')) + L_i^{-1}(z') \, e^{-V_i^2 y^2(z')}$$

$$(1 + V_i^2 y^2(z') + \frac{1}{2} V_i^4 y^4(z')) \}$$

After "solving" for $\rho_e(z_k)$ and the particle current density $J(z_k)$ we calculate

$$N_e(z_k) = \left(\frac{\pi}{4}\right)^{\frac{1}{2}} y(z_k) \, \rho(z_k);$$

$$U(z_k) = J(z_k)/N_e(z_k);$$

$$T_e(z_k) = 3.2991 \cdot 10^{-12}/(y(z_k))^2$$

and the spherical electron flux

$$\rho_e(z_k) = \rho(z_k) \{ 1 + \left(\frac{4}{3\pi}\right) J^2(z_k)/\rho^2(z_k)$$

The integral and derivative checks explained in model five also are used in model six as may be the change in $y(z_k)$ from equations (1) or (3).

When $y(z_k)$ is incremented from (3) then the derivative check is not used. Further when $y(z_k)$ is increment then $T_e(z_k)$, $N_e(z_k)$ and $U(z_k)$ are recalculated after the changes before a new iteration on $\rho_e(z_k)$ and $J(z_k)$ is begun.

The final model tried is the same as model six except $\rho_e(z_k)$ is not calculated and the change in $y(z_k)$ which occurs is the implementation of the following equation. This equation is approximated using methods previously discussed.

$$\left(\frac{32}{15\pi}\right)\frac{J^2(z)}{\rho(z)} = I_3 + K_{31}N_{11} + K_{32}N_{21} + K_{33}N_{31}$$

$$+ K_{31}\left\{H_{11}\,y^2(z') + \sum_{k=1}^{N}\left[H_{11}^k V_k^4\, y^4(z') + H_{12}^k V_k^2\, y^2(z') + H_{13}^k\right]\right.$$

$$e^{-V_k^2 y^2(z')} + \left[H_{11}^L V_i^4\, y^4(z') + H_{12}^i V_i^2\, y^2(z') + H_{13}^L\right]e^{-V_i^2 y^2(z')}\Big\}$$

$$+ K_{32}\left\{H_{21}\,y^2(z') + \sum_{k=1}^{N}\left[H_{21}^k V_k^3\, y^3(z') + H_{22}^k V_k\, y(z')\right)e^{-V_k^2 y^2(z')}\right.$$

$$+ H_{23}^k\left(1 - \mathrm{erf}\left(V_k\, y((z'))\right)\right] + \left(H_{21}^i V_i^3\, y^3(z') + H_{22}^i V_i\, y(z')\right)$$

$$\exp\left(-V_i^2\, y^2(z')\right) + H_{23}^i\left(1 - \mathrm{erf}\left(V_i\, y(z')\right)\right)\Big\}$$

$$+ K_{33}\left\{H_{31}\,y^2(z') + \sum_{k=1}^{N}\left[H_{31}^k V_k^4\, y^4(z') + H_{32}^k V_k^2\, y^2(z')\right.\right.$$

$$\left.+ H_{33}^k\right]e^{-V_k^{-2} y^2(z')} + \left[H_{31}^i V_i^4\, y^4(z') + H_{32}^i V_i^2\, y^2(z') + H_{33}^i\right]$$

$$e^{-V_i^2 y^2(z')}\Big\}$$

where $K_{31} = \frac{1}{2}\int_a^b dz' \left[\frac{3}{2} E_3 \left(\frac{fh}{L_{e\ell}} \mid e^{-z/h} - e^{-z'/h}\mid\right)\right.$

$\left. - \frac{1}{2} E_1 \left(\frac{fh}{L_{e\ell}} \mid e^{-z/h} - e^{-z'/h}\mid\right)\right];$

$K_{32} = \frac{3}{2}\int_a^b dz \left[\frac{3}{2} E_4 \left(\frac{fh}{L_{e\ell}} \mid e^{-z/h} - e^{-z'/h}\mid\right) - \frac{1}{2} E_2 \left(\frac{fh}{L_{e\ell}} \mid e^{-z/h} - e^{-z'/h}\mid\right)\right]$

sign $(z-z')$

$K_{33} = \frac{15}{4}\int_a^b dz' \left[\frac{3}{2} E_5 \left(\frac{fh}{L_{e\ell}} \mid e^{-z/h} - e^{-z'/h}\mid\right)\right.$

$\left. - \frac{1}{2} E_3 \left(\frac{fh}{L_{e\ell}} \mid e^{-z/h} - e^{-z'/h}\mid\right)\right]$

and $I_3 = I^{(in)} \left(\frac{3}{2}\mu_0^2 - \frac{1}{2}\right) \exp\left[-\frac{fh}{L_{e\ell}} \left(\exp\left(-\frac{z}{h}\right) - \exp\left(\frac{-b}{h}\right)\right)\right]$

$N_{11} = S_0 (z') - \frac{5}{2} S_2 (z') + fL_{e\ell}^{-1} (z') \rho(z') + \frac{4}{3\pi} L_{e\ell}^{-1} (z')(4-3f)$

$J^2 (z')/\rho (z')$

$N_{21} = S_1 (z') - (1 - f) L_{e\ell}^{-1} (z') J (z')$

$N_{31} = S_2 (z') - \left(\frac{32}{15\pi}\right) (1 - f) L_{e\ell}^{-1}(z') J^2 (z')/\rho (z')$

$H_{11} = -\left(\frac{\pi\alpha_r}{4}\right) F_{ion} (z') \rho^2 (z') + \alpha_r F_{ion} (z') J^2 (z')$

$H_{21} = -\left(\frac{2\alpha_r}{3}\right) F_{ion} (z') \rho (z') J(z')$

$H_{31} = -\left(\frac{2\alpha_r}{5}\right) F_{ion} (z') J^2 (z')$

$H_{11}^k = \left(\frac{8}{3\pi}\right) L_k^{-1} (z')/\rho (z')$

$$H_{12}^{k} = \left(\frac{16}{3\pi}\right) L_k^{-1}(z') J^2(z')/\rho(z')$$

$$H_{13}^{k} = \left(\frac{16}{3\pi}\right) L_k^{-1}(z') J^2(z')/\rho(z')$$

$$H_{11}^{i} = \left(\frac{8S}{3\pi}\right) L_i^{-1}(z') J^2(z')/\rho(z')$$

$$H_{12}^{i} = \frac{4(S+3)}{3\pi} L_i^{-1}(z') J^2(z')/\rho(z') + (S-1) L_i^{-1}(z') \rho(z')$$

$$H_{13}^{i} = \frac{4(S+3)}{3\pi} L_i^{-1}(z') J^2(z')/\rho(z') + (S-1) L_i^{-1}(z') \rho(z')$$

$$H_{21}^{k} = -\left(\frac{4}{3\sqrt{\pi}}\right) L_k^{-1}(z') J(z')$$

$$H_{22}^{k} = -\left(\frac{2}{\sqrt{\pi}}\right) L_k^{-1}(z') J(z')$$

$$H_{23}^{k} = -L_k^{-1}(z') J(z')$$

$$H_{21}^{i} = -\left(\frac{4}{3\sqrt{\pi}}\right) L_i^{-1}(z') J(z')$$

$$H_{22}^{i} = -\left(\frac{2}{\sqrt{\pi}}\right) L_i^{-1}(z') J(z')$$

$$H_{23}^{i} = -L_i^{-1}(z') J(z')$$

$$H_{31}^{k} = -\left(\frac{16}{15\pi}\right) L_k^{-1}(z') J^2(z')/\rho(z')$$

$$H_{32}^{k} = -\left(\frac{32}{15\pi}\right) L_k^{-1}(z') J^2(z')/\rho(z')$$

$$H_{33}^{k} = -\left(\frac{32}{15\pi}\right) L_{k}^{-1}(z') J^{2}(z')/\rho(z')$$

$$H_{31}^{i} = -\left(\frac{16}{15\pi}\right) L_{i}^{-1}(z') J^{2}(z')/\rho(z')$$

$$H_{32}^{i} = -\left(\frac{32}{15\pi}\right) L_{i}^{-1}(z') J^{2}(z')/\rho(z')$$

$$H_{33}^{i} = -\left(\frac{32}{15\pi}\right) L_{i}^{-1}(z') J^{2}(z')/\rho(z')$$

The results of the methods discussed varied from case to case. The two methods, model 5 and model 6, judged to be the closest approximations to the actual ionosphere were close approximations of each other. For this reason the investigator judged that the particular approach which was programmed, has been pushed as far as reasonable at the present time. The final result, model 6, did not conform to the experimental results in the ionosphere. The investigator thinks this is because the magnetic field was not incorporated in his model. The investigator intends to add the magnetic field and return for programing services for the improved model.

Exact Evaluation of Derivatives in the Calculation of the Atomic Coulomb Integrals

Initiator: Dr. J. Jasperse

Problem No: 4800 Project No: 8627

OUTLINE

1. BACKGROUND

This request for numerical analysis and scientific computer programming support involves the derivation and application of certain product, reciprocal and natural logarithm algorithms to the exact evaluations of derivatives of given functions.

The primary function, $J^{\gamma\delta\alpha\beta}$ (see mathematics, J function), is defined and used by Jasperse[1] in the calculation of Atomic Coulomb Integrals (ACI), $L^{\gamma\delta\alpha\beta}_{n'''on''on'ono}$. These integrals arise in studying the physical properties of ozone, an important constituent of the earth's atmosphere.

In the original analysis/programming support request, the J function was specified by the Initiator as a function of 4 variables, (α, β, γ, δ), where the computational requirement was to calculate "high order" derivatives of a function of four variables. Certain derivatives of the J function subsequently would be applied to computations of L integrals. However, preliminary inspection of the J function showed that it was necessary to treat four dummy constants, (a,b,c,d), as variables when taking partial derivatives. Therefore, the problem was immediately expanded to a requirement for evaluations of high order derivatives of a function of eight variables, a considerably more complex undertaking.

It should be noted that the J function contains logarithmic terms, an additional problem to be dealt with.

It should further be noted that previous attempts by the Initiator to compute ACI (to which the J function is applied) by direct integration techniques had met with limited success; low order computations had been generated on a computer, but the higher order calculations were beyond the scope of the techniques and equipment available at that time. These low order calculations were presented to be used in a study of accuracy at the time when the evaluated J function would be applied to ACI calculations.

2. PROCEDURE

The synoptic approach taken to the problem is outlined below. Some of the steps included were not known at the onset of the effort, but were made necessary by difficulties encountered as the analytical investigation proceeded. Obviously, most of the effort outlined below progressed in a parallel fashion rather than in specifically sequential steps.

Evaluations of J Function Derivatives and Application to Calculations of L Integrals.

1. Define a basic method of evaluation of J function derivatives by applying product and reciprocal forms of algorithms.
2. Expand existing algorithms[2] (Product, reciprocal) from functions of 1 variable to functions of 8 variables.
3. Prove the validity of the above.
4. Determine suitable approximations for terms such as $LN\left[\frac{\text{Polynomial 1(8 Variables)}}{\text{Polynomial 2(8 Variables)}}\right]$ which can reasonably be evaluated on the computer by the methods product and reciprocal algorithms.
5. Apply evaluated J function to computations of certain low order ACI. It is necessary to have prepared compatible programs or subroutines to evaluate Coulomb integrals, Sturmian functions and Gegenbauer Polynomials. Generate study of accuracy of results compared to previous calculations by direct integration technique.
6. Determine an efficient computer index storage scheme to allow evaluation of large numbers of partial derivatives of high order J functions.
7. Derive algorithm for exact evaluation of derivatives of terms such as; $LN\left[\frac{\text{Polynomial 1(8 Variables)}}{\text{Polynomial 2(8 Variables)}}\right]$.
8. Prove validity of the above.
9. Apply logarithmic derivative algorithm to appropriate portion of J function; compare accuracy of results to approxiamtion techniques.

10. Apply logarithmic derivative algorithm to low order ACI calculations; compare accuracy of results to previous study.

11. Compute high order ACI.

3. MATHEMATICS

3.1 The following function (J Function) is given by the Initiator[1] [p. 17, Eq. 19]:

$$J^{\gamma\delta\alpha\beta} = \frac{\pi^2}{2(fga^2b^2c^2\delta^2 - ega^2b^2d^2\gamma^2 - fb^2c^2d^2\alpha^2 + ea^2c^2d^2\beta^2)}$$

$$X \ \ell n \frac{(fabc\delta + abd\gamma + acd\beta)(gabc\delta + bcd\alpha + eacd\beta)}{(eabd\gamma + abc\delta + bcd\alpha)(gabd\gamma + acd\beta + fbcd\alpha)}$$

where α, β, γ, δ are expansion parameters; e,f are particle mass ratios; a, b, c, d are dummy variables introduced in a derivative substitution technique.

3.2 The Atomic Coulomb Integral (L integral) is given[1] [p. 17, Eq. 20]:

$$L^{\gamma\ \ \delta\ \ \alpha\ \ \beta}_{n'''on''on'ono} = N^{\gamma}_{n'''o} N^{\delta}_{n''o} N^{\alpha}_{n'o} N^{\beta}_{no} X\left\{D^{\gamma\ \ \delta\ \alpha\ \beta}_{n'''n''n'n} J^{\gamma\delta\alpha\beta}\right\}_{a,b,c,d = 1}$$

where N are normalization factors of the Sturmian function.

3.3 The differential operator, D, is defined[1] [p. 17, Eq. 21]:

$$D^{\gamma\ \ \delta\ \ \alpha\ \ \beta}_{n'''\ n''\ n'\ n} \equiv - \sum_{P_1=0}^{n'''-1} S^{\gamma P_1}_{n'''o} \left(\frac{\partial}{\partial\gamma^2}\right)^{n'''-P_1} \left(\frac{\partial}{\partial c^2}\right)^{P_1}$$

$$X \sum_{P_2=0}^{n''-1} S^{\delta P_2}_{n''o} \left(\frac{\partial}{\partial\delta^2}\right)^{n''-P_2} \left(\frac{\partial}{\partial d^2}\right)^{P_2} \sum_{P_3=o}^{n'-1} S^{\alpha P_3}_{n'o} \left(\frac{\partial}{\partial\alpha^2}\right)^{n'-P_3-1} \left(\frac{\partial}{\partial a^2}\right)^{P_3} n'$$

$$\times \sum_{P_4=o}^{n-1} S_{no}^{\beta P_4} \left(\frac{\partial}{\partial \beta^2}\right)^{n-P_4} \left(\frac{\partial}{\partial b^2}\right)^{P_4}$$

3.4 Derivative Algorithms for Numerical Evaluation

The method taken to evaluate partial derivatives of the J function with respect to $(\alpha,\beta,\gamma,\delta,a,b,c,d)$ consists of being able to define evaluations of partial derivatives (to as high an order as required by the full evaluation) of each component term of the overall expression, and then being able to algebraically combine the partial derivatives of those terms in a manner which forms the evaluation of the partial derivatives of the sum, product, reciprocal or natural logarithm of the given component terms. By defining all partial derivatives of all component terms of the J function, and by using a high speed computer to evaluate the expressions and manipulate the combining of the expressions, the evaluations of the partial derivatives of the full J function can eventually be obtained.

Obviously, algorithms are required, based principally upon Leibniz's Rule, to form the evaluations of partial derivatives of Products of terms of polynomial functions of eight variables, reciprocal of such a term and the natural logarithm of such a term.

The algorithms used to perform these operations are given below.

3.4.1 Derivatives of a Product of Functions of More Than 1 Variable

$$D_{X_1,X_2\ \ldots}^{I_1,I_2\ \ldots}(f(x)g(x)) = \sum_{i_1=o}^{I_1}\sum_{i_2=o}^{I_2}\cdots\binom{I_1}{i_1}\binom{I_2}{i_2}\cdots D_{X_1,X_2\ \ldots}^{i_1,i_2\ \ldots}(f(x)) \cdot D_{X_1,X_2\ \ldots}^{I_1-i_1,I_2-i_2\ \ldots}(g(x))$$

where $D_{X_1}^{N}(f(x))$ represents the N^{th} derivative of $f(x)$ with respect to variable X_i.

3.4.2 Derivatives of a Reciprocal of a Function of More than 1 Variable

$$D_{X_1,X_2\ldots}^{I_1,I_2\ldots}(1/f(x)) = -\sum_{i_1=o}^{I_1-1}\sum_{i_2=o}^{I_2-1}\cdots\binom{I_1}{i_1}\binom{I_2}{i_2}\cdots$$

$$(1/f(x))\, D_{X_1,X_2\ldots}^{I_1-1,I_2-1\ldots}(f(x))/f(x)$$

3.4.3 Derivatives of the Natural Logarithm of a Function of More Than 1 Variable

$$D_{X_1,X_2,X_3\ldots X_N}^{I_1,I_2,I_3\ldots I_N}\{\ln(f(x))\} = \sum_{i_1=o}^{I_1}\sum_{i_2=o}^{I_2}\sum_{i_3=o}^{I_3}\cdots\sum_{i_n=o}^{I_n-1}\binom{I_1}{i_1}\binom{I_2}{i_2}\binom{I_3}{i_3}$$

$$\cdots\binom{I_N-1}{i_N} D_{X_1,X_2,X_3\ldots X_N}^{i_1,i_2,i_3\ldots i_N}\{1/f(x)\}$$

$$D_{X_1,X_2,X_3\ldots X_N}^{I_1-i_1\,I_2-i_2\,I_3-i_3\ldots I_N-i_N}\{f(x)\}$$

3.5 The expression selected to approximate $\ln(x)$ terms in the initial evaluations of the J function consisted of:[3]

$$\ln x = 2\left[\frac{x-1}{x+1} + \frac{1}{3}\left(\frac{x-1}{x+1}\right)^3 + \frac{1}{5}\left(\frac{x-1}{x+1}\right)^5 + \ldots\right] \quad (x>o)$$

Derivatives of this expression were initially obtained using the product and reciprocal algorithms defined above.

3.6 An example of introducing substitute derivative expressions with dummy variables to evaluate an integral expression is given below.

Given

$$\int_0^\infty e^{-x^2}\,dx = \frac{\sqrt{\pi}}{2}$$

Find

$$\int_0^\infty x^2 e^{-x^2}\,dx =$$

Introduce dummy variable α

$$\int_0^\infty e^{-\alpha x^2}\,dx = \frac{1}{2}\sqrt{\frac{\pi}{\alpha}}$$

Take $\frac{\partial}{\partial\alpha}$ of each side

$$\frac{\partial}{\partial\alpha}\int_0^\infty e^{-\alpha x^2}\,dx = \frac{\partial}{\partial\alpha}\frac{1}{2}\sqrt{\frac{\pi}{\alpha}}$$

Rewrite

$$\int_0^\infty \frac{\partial}{\partial\alpha} e^{-\alpha x^2}\,dx = -\frac{1}{4}\frac{\sqrt{\pi}}{\alpha^{3/2}}$$

Take $\frac{\partial}{\partial\alpha}$

$$-\int_0^\infty x^2 e^{-\alpha x^2}\,dx = -\frac{1}{4}\frac{\sqrt{\pi}}{\alpha^{3/2}}$$

Evaluating at $\alpha=1$

$$\int_0^\infty x^2 e^{-(1)x^2} = \frac{1}{4}\frac{\sqrt{\pi}}{\alpha^{3/2}}\Bigg|_{\alpha=1} = \frac{\sqrt{\pi}}{4}$$

3.7 Derivative Variable Transformations

Derivatives were evaluated with respect to first order variables but were required in the differential operator, D, with respect to second order variables. Therefore, the following relations were applied to each term of the Differential operator:

$$1.\quad \left(\frac{\partial}{\partial X^2}\right)^1 = \frac{1}{\partial X}\ \frac{\partial}{\partial X^1}$$

$$2.\quad \left(\frac{\partial}{\partial X^2}\right)^2 = \frac{1}{4X^2}\left(\frac{\partial^2}{\partial X^2}\right) - \frac{1}{X}\ \frac{\partial}{\partial X^1}$$

3.8 First Order Derivative Expressions

Expressions for certain first-order derivatives of the J function were derived and are presented below:

Given:

$$J^{\gamma\delta\alpha\beta} = \left(\frac{\pi^2}{2}\right) \frac{1}{fg\delta^2 - eg\gamma^2 + e\beta^2 - f\alpha^2}\ \ln\left[\frac{(f\delta+\gamma+\beta)(g\delta+\alpha+e\beta)}{(e\gamma+\delta+\alpha)(g\gamma+\beta+f\alpha)}\right]$$

Rewrite:

$$\frac{2}{\pi^2} J^{\gamma\delta\alpha\beta} = (fg\delta^2 - eg\gamma^2 + e\beta^2 - f\alpha^2)^{-1}\ [\ln(f\delta+\gamma+\beta) + \ln(g\delta+\alpha+e\beta) - \ln(e\gamma+\delta+\alpha) + \ln(g\gamma+\beta+f\alpha)]$$

3.8.1

$$\frac{2}{\pi^2}\ \frac{\partial J}{\partial \delta} = [(-1)(fg\delta^2 - eg\gamma^2 + e\beta^2 - f\alpha^2)^{-2}\ (2fg\delta)][\ln(\ ) + \ln(\ ) - \ln(\ ) - \ln(\ )]$$

$$+ (fg\delta^2 - eg\gamma^2 + e\beta^1 - f\alpha^2)^{-1}\ \left[\frac{f}{f\delta+\gamma+\beta} + \frac{g}{g\delta+\alpha+e\beta} - \frac{1}{(e\gamma+\delta+\alpha)}\right]$$

3.8.2

$$\frac{2}{\pi^2}\frac{\partial}{\partial\gamma}\frac{\partial J}{\partial\delta} = [(-1)(-2)(2fg\delta)(fg\delta^2-eg\gamma^2+e\beta^2-f\alpha^2)^{-3}(-2eg\gamma)][\ell n + \ell n - \ell n - \ell n]$$

$$+ [(-1)(2fg\delta)(fg\delta^2-eg\gamma^2+e\beta^2-f\alpha^2)^{-2}][\frac{1}{f\delta+\gamma+\beta} - \frac{e}{e\gamma+\delta+\alpha} - \frac{g}{g\gamma+\beta+f\alpha}]$$

$$+ [(-1)(fg\delta^2-eg\gamma^2+e\beta^2-f\alpha^2)^{-2}(-2eg\gamma)][\frac{f}{f\delta+\gamma+\beta} + \frac{g}{g\delta+\alpha+e\beta} - \frac{1}{e\gamma+\delta+\alpha}]$$

$$+ [(fg\delta^2-eg\gamma^2+e\beta^2-f\alpha^2)^{-1}][\frac{(-1)f}{(f\delta+\gamma+\beta)^2} - \frac{(-1)e}{(e\gamma+\delta+\alpha)^2}]$$

3.8.3

$$\frac{2}{\pi^2}\frac{\partial}{\partial\alpha}\frac{\partial}{\partial\beta}\frac{\partial}{\partial\gamma}\frac{\partial J}{\partial\delta} = [\frac{(24\cdot16)e^2f^2g^2\alpha\beta\gamma\delta}{D^5}][\ell n\ \frac{(f\delta+\gamma+\beta)(g\delta+\alpha+e\beta)}{(e\gamma+\delta+\alpha)(g\gamma+\beta+f\alpha)}]$$

$$+ [\frac{48e^2fg^2\beta\gamma\delta}{D^4}][\frac{1}{g\delta+\alpha+e\beta} - \frac{1}{e\gamma+\delta+\alpha} - \frac{f}{g\gamma+\beta+f\alpha}]$$

$$- [\frac{48ef^2g^2\alpha\delta\gamma}{D^4}][\frac{1}{f\delta+\gamma+\beta} + \frac{e}{g\delta+\alpha+e\beta} - \frac{1}{g\gamma+\beta+f\alpha}]$$

$$+ [\frac{48ef^2g\alpha\beta\delta}{D^4}][\frac{1}{f\delta+\gamma+\beta} - \frac{e}{e\gamma+\delta+\alpha} - \frac{g}{g\gamma+\beta+f\alpha}]$$

$$- [\frac{48e^2fg\alpha\beta\gamma}{D^4}][\frac{f}{f\delta+\gamma+\beta} + \frac{g}{g\delta+\alpha+e\beta} - \frac{1}{e\gamma+\delta+\alpha}]$$

$$+ [\frac{8efg^2\gamma\delta}{D^3}][\frac{e}{(g\delta+\alpha+e\beta)^2} - \frac{f}{(g\gamma+\beta+f\alpha)^2}]$$

$$+ [\frac{8efg\beta\gamma}{D^3}][\frac{e}{(e\gamma+\delta+\alpha)^2} + \frac{fg}{(g\gamma+\beta+f\alpha)^2}]$$

$$+ [\frac{8e^2g\beta\gamma}{D^3}][\frac{g}{(g\delta+\alpha+e\beta)^2} - \frac{1}{(e\gamma+\delta+\alpha)^2}]$$

$$- \left[\frac{8f^2g\alpha\delta}{D^3}\right]\left[\frac{g}{(g\gamma+\beta+f\alpha)^2} - \frac{1}{(f\delta+\gamma+\beta)^2}\right]$$

$$- \left[\frac{8efg\alpha\gamma}{D^3}\right]\left[\frac{eg}{(g\delta+\alpha+e\beta)^2} + \frac{f}{(f\delta+\gamma+\beta)^2}\right]$$

$$- \left[\frac{8ef\alpha\beta}{D^3}\right]\left[\frac{e}{(e\gamma+\delta+\alpha)^2} - \frac{f}{(f\delta+\gamma+\beta)^2}\right]$$

$$+ \left[\frac{2fg\delta}{D^2}\right]\left[\frac{2fg}{(g\gamma+\beta+f\alpha)^3}\right] + \left[\frac{2eg\gamma}{D^2}\right]\left[\frac{2eg}{(g\delta+\alpha+e\beta)^3}\right]$$

$$+ \left[\frac{2e\beta}{D^2}\right]\left[\frac{2e}{(e\gamma+\delta+\alpha)^3}\right] + \left[\frac{2f\alpha}{D^2}\right]\left[\frac{2f}{(f\delta+\gamma+\beta)^3}\right]$$

where $D = fg\delta^2 - eg\gamma^2 + e\beta^2 - f\alpha^2$

4. VERIFICATION OF SUBROUTINES PRODUCT, RECIPROCAL

Suitable polynomial functions were selected which allowed evaluation of derivatives of their products and reciprocals by analytical methods. As it is unrealistic to analytically evaluate derivatives of products or reciprocals of expressions of functions of eight variables, functions of three variables were used. This was felt to be sufficient to show that some method for dealing with more than one variable is either valid or not valid. The algorithm derived should later be able to be expanded by symmetry to include any number of subsequent variables. In addition, the particular computer software, CDC 6600 FTN 3.4.3, was found to be bounded in subscripting capability to three indices. As a minimum of time was desired to be spent on the programming of supportive test functions for numerical evaluations, this factor was taken into account when initially deciding to limit the testing effort to functions of three variables.

Computational results showed that the derived product and reciprocal algorithms for functions of three variables were valid when compared to analytic

evaluations involving the same processes. As an additional test, use was made of the property that $\frac{\partial(K)}{\partial X} \rightarrow 0$ where K is any constant. Considering that any indexing scheme for control of storage of large multidimensional arrays can readily become complex, it was felt that a proof based upon this property would lend considerable confidence to the validity of the computer programming of the algorithms into general storage subroutine form. As a guide to the Scientific Programmer, it should be noted that, with respect to all of the derived algorithms, the value of the differential is stored in an array whose indices can lead to the order of differentiation.

Therefore, the following test was devised:

Given: $f = f(x,y,z)$, $g = g(x,y,z)$ and all derivatives of f and g through

$$\frac{\partial^n}{\partial x^n \partial y^n \partial z^n}$$

1. Evaluate all f and g at some (x_o, y_o, z_o), and store in multidimensional arrays F,G

2. Form array P = F•G using product algorithm subroutine

3. Form array $R = \frac{1}{P}$ using reciprocal algorithm subroutine

4. Form array Z = R•P using product algorithm subroutine

The contents of array Z will then be

$$Z(1,1,1) = 1.$$

all other $Z(i,j,k) = 0$.

This test not only indicates validity of the algorithm and computer subroutines, but also indicates any level of roundoff which can be attributed to the methods (in conjunction with the specific functions and data values selected) for the steps outlined.

5. PROGRAM

Functional Description

The logical computational procedure for the action taken by the computer program can be broken into a series of sequential steps. Consider that the function to be evaluated, J, can be simplified to the following expression:

$$A = Q(\frac{1}{X})\ \ell n(Y) = Q(\frac{1}{X})\ \ell n(\frac{M \cdot N}{O \cdot P})$$

where A,X,Y,M,N,O,P are polynomial functions of eight variables,

and Q is a real constant.

Then the program logical procedure for numerical evaluations of the J function and application to ACI can consist of the following:

1. Calculate and load into arrays : $d^n(O)$, $d^n(P)$
2. Calculate derivatives of product : $d^n(O \cdot P)$
3. Calculate derivatives of reciprocal : $d^n(\frac{1}{O \cdot P})$
4. Calculate and load into array : $d^n(M)$
5. Calculate derivatives of product : $d^n[(\frac{1}{O \cdot P})\ (M)]$
6. Calculate and load into array : $d^n(N)$
7. Calculate derivatives of product : $d^n\{[(\frac{1}{O \cdot P})\ (M)] \cdot N$
8. Calculate and load into array : $d^n(X)$
9. Calculate derivatives of recirprocal : $d^n(\frac{1}{X})$
10. Define constant Q

11. Calculate derivatives of reciprocal : $d^n(\frac{1}{Y})$

12. Calculate derivatives of ℓn term : $d^n[\ell n(Y)]$

13. Multiply derivative array by constant Q

14. Calculate derivatives of product : $d^n\ [(Q)\ \ell n(Y) \cdot (\frac{1}{X})\ ] = d^n(A)$

15. Select derivative terms to apply to ACI calculations, and generate family of integrals.

In addition to several test sequences of certain variables which demonstrated characteristic properties of the J function, two specific data sets were applied to the finished program, and are given below as a matter of reference.

VAR	SET1	SET2
α	2.31	2.31
β	2.31	1.14
γ	2.54555	2.54555
δ	.7093	2.54555
a	1.	1.
b	1.	1.
c	1.	1.
d	1.	1.
e	.000136	.999864
f	.000136	.5

Computational Results printed by the program include a list of the input data parameters, a list of all partial derivatives of the numerically evaluated differential operator, and a list of values of the associated family of Atomic Coulomb Integrals.

6. VERIFICATION OF J DERIVATIVE EVALUATIONS

To test the evaluations of the J function, certain low order terms were determined analytically and hand evaluated at selective data points. These included:

$$\frac{\partial}{\partial\alpha}\ \frac{\partial}{\partial\beta}\ J^{oo\alpha\beta}$$

$$\left(\frac{\partial}{\partial\alpha}\right)^2\ \frac{\partial}{\partial\beta}\ J^{oo\alpha\beta}$$

$$\frac{\partial}{\partial\alpha}\left(\frac{\partial}{\partial\beta}\right)^2\ J^{oo\alpha\beta}$$

$$\left(\frac{\partial}{\partial x}\right)^2\ \left(\frac{\partial}{\partial\beta}\right)^2\ J^{oo\alpha\beta}$$

evaluated at the points $a=b=c=d=1$

$e=f=1$

$\gamma=\delta=0$

$\alpha=1.0$

$\beta=1.01$

In addition, the analytical expressions for the first order derivatives of the J function up to $\frac{\partial}{\partial\alpha}\ \frac{\partial}{\partial\beta}\ \frac{\partial}{\partial\gamma}\ \frac{\partial}{\partial\delta}\ J^{\gamma\delta\alpha\beta}$ were determined and coded as a supplementary computer program. This was extremely useful in debugging the initial stages of the principal program to evaluate the general J expression, in that computations were compared for validity and degree of accuracy. Also, insight as to the behavior of the component terms of the derivatives of the J function was gained at this time, which was to prove valuable at a later time, during the study of computational accuracy of higher order ACI.

Other analytical studies focused upon the probable cancellation of terms in the denominator of the J function, under certain conditions of equality of pairs of terms, as suggested by the initiator on the basis of known physical relationships of the parameters. These include (at $a=b=c=d=1$) $\alpha=\beta$ and $\gamma=\delta$. While certain terms dropped out, no obviously significant pattern of cancelation was observed. This study became more significant during the study of the accuracy of the ACI evaluations.

7. COMPUTER CORE STORAGE

In programming the initial studies of the J function it became obvious that of the two standard principal computer difficulties to be overcome (central

processing time/core storage) one, C.P. time, would be of considerably less impedance. This was due primarily to the ease and speed of computation that the product and (most particularly) the reciprocal algorithms allowed. Even when extrapolated from functions of 3 variables to functions of 8 variables, it was obvious that although still large compared to other major efforts typically submitted to the machine, the C.P. time would still be within some realistically manageable range.

The core storage problem, however, when dealing with the derivatives of a function of eight variables, immediately attracts one's attention. The following chart may help to explain why. Consider that one has only a function of two variables. Then, letting $F = f(x,y)$ the storage required to hold all of the evaluations of partial derivatives to a given order, N, can be graphically presented as:

$\frac{\partial}{\partial y}$ \ $\frac{\partial}{\partial x}$	0	1	2	...	N
0	F	$\frac{\partial F}{\partial X}$	$\frac{\partial^2 F}{\partial X^2}$	...	$\frac{\partial^n F}{\partial x^n}$
1	$\frac{\partial F}{\partial Y}$	$\frac{\partial}{\partial y}\ \frac{\partial F}{\partial x}$	$\frac{\partial}{\partial y}\ \frac{\partial^2 F}{\partial x^2}$	...	
2	$\frac{\partial^2 F}{\partial y^2}$	$\frac{\partial^2 F}{\partial y^2}\ \frac{\partial F}{\partial x}$	$\frac{\partial^2 F}{\partial y^2}\ \frac{\partial^2 F}{\partial x^2}$	...	
⋮	⋮	⋮	⋮	...	⋮
N	$\frac{\partial^n F}{\partial y^n}$				$\frac{\partial^n}{\partial y^n}\ \frac{\partial^n F}{\partial x^n}$

Figure 1 - Partial Derivative Storage Format

Notice that the location containing any $\frac{\partial^m}{\partial y^m} \frac{\partial^n f}{\partial x^n}$ holds the value of the derivative evaluated at some given (x,y). One sees readily that the space required for a complete order of partial derivatives can be determined by:

$$\text{Storage} = (\text{order of derivative} + 1)^{(\text{No. of variables})}$$

A storage requirement chart can quickly show the limitations imposed upon an array size in terms of number of variables and order of derivative.

NO. OF VAR. \ ORDER	2	3	4	5	6
1	3	4	5	6	7
2	9	16	25	36	49
3	27	64	125	216	343
4	81	256	625	1296	2401
5	243	1024	3125	7776	16807
6	729	4096	15625	46656	117649
7	2187	16284	78125	279936	823543
8	6561	65536	390625	1679616	5764801

Figure 2 - Core Storage Requirements -
No. of Variables Vs. Order of Derivative

When dealing with a function of eight derivatives, one sees immediately that direct core is no longer available certainly by the 3rd order derivative, even on larger machines. One should also bear in mind that the storage requirements given above refer only to one array. Analysis of various means of evaluating the given J function showed that a minimum of 4 such arrays would be necessary. This meant that the analysis of L integrals would be limited to approximately (n'''=n''=n'=n=2) if the entire J function would be calculated with the contents kept in core.

Otherwise, several options are open to the programmer/analyst:

1. Investigate and apply external core storage capability, such as magnetic tape or disk. (Virtual Memory)

2. Break analysis into smaller steps keeping only results required by further analysis.

3. Determine those specific parts of the J function required for evaluating the L integral (not all partial derivative components of the J function are used by the differential operator, D), and find a means to limit the calculations to those levels.

4. Continue to solve the J function analytically, such that when eventually applying the product and reciprocal subroutines the numerical analysis starts at a higher level.

5. Transform the J function to allow derivatives with respect to α^2, β^2, γ^2, δ^2, rather than α, β, γ, δ.

6. Solve the J function (or the L integral, since that is the function to which the J function is eventually to be applied) analytically, either in terms of some variable or, preferably, variables, thereby significantly reducing the overall number of variables to be kept in storage when evaluating derivative expressions.

8. ATOMIC COULOMB INTEGRAL CALCULATIONS

As shown in the mathematics section of this report, an Atomic Coulomb Integral (L integral) can be calculated by applying the differential operator, D, to the derivatives of the J function, in conjunction with the appropriate normalization factors of the Sturmian functions, N.

Those ACI which could be calculated without requiring extensive external computer memory subroutines were programmed to allow evaluation of the overall procedure and to test those routines required for storage of derivatives of functions of eight variables.

Under these conditions, all ACI from order L_{1111} to order L_{2222} were successfully calculated. Comparison of some of the lower order integrals to results previously calculated by other techniques indicated that the accuracy of the newer calculations was improved. To show this effect more clearly,

and to indicate the overall degree of accuracy of the derivative technique, an additional version of the program was generated using double precision computation, thereby allowing the accuracy of each term of the L integral to be defined when compared to the single precision computations.

In this study of accuracy, a pattern of decreasing precision was observed which eventually limits the evaluation of the L ingegral. To ensure that such loss of precision was not a result of programming errors, a roundoff error analysis was applied to both the single and double precision versions of the program. The minimum detectable delta was applied to each input parameter to allow observation of the effect of a small change in input with respect to computational output over the full range of evaluations. The results of this test supported the conclusions that the overall precision of higher order ACI computation is eventually limited. Whether this is an inherent characteristic of the expression being evaluated or a function of the applied derivative technique was not determine at this time.

9. CONCLUSIONS

In reviewing the results of the application of derivative algorithms to a high speed computer to allow evaluations of partial derivatives of the J function and the numerical computations of certain ACI, it is seen that eventually other techniques are required to evaluate higher order ACI. As noted in the study of computer core storage requirements, the applications of several other methods of combinations of numerical analysis/scientific programming techniques could be investigated. In addition, the specific reason for the eventual loss of precision in this analysis should be determined.

Of the options available from the above methods, that most likely to yield accurate results in the evaluations of significantly higher ACI would appear to be of some form involving item 6; that is, an analysis which reduces the number of variables involved in the evaluation of the J function or the L integral, yet which retains a format whereby the power of the derivative algorithms derived herein can still be realistically applied to the computer to allow numerical solutions to the problem.

Under this consideration, a method outlined by Calabi[4] has been briefly reviewed, where an outline is formulated which shows that ACI can be solved in closed form according to evaluations of sums of derivatives of functions from which selective poles are removed, as typically resulting from Cauchy's Residue Theorem as applied to closed loop integration. It would be necessary to investigate whether such residues could be evaluated by use of the derivative algorithms already derived and applied to the J function of this problem. In addition, it would probably be necessary to derive a new algorithm, compatible with those already applied, which would allow evaluation of derivatives of certain functions of the form:

$$\frac{\partial^i}{\partial x^i}\left[\frac{\partial^j}{\partial y^j}\left\{f(x,y)\right\}\ y = \phi(x)\right]\ x = x_o$$

One advantage of being able to apply these derivative techniques to the Residue Theorem lies in the fact that the number of variables over which differentiation takes place can be reduced from eight to possibly two, thereby exponentially reducing the amount of core required and immediately allowing evaluations of much higher ACI.

An additional advantage would appear to be that the ACI analysis can be carried out in its general form, that is, not subjected to certain constraints (subscripts $\ell, \ell^1 = 0$) imposed by application of the J function.

On the surface, it appears that these results could be accomplished, thereby allowing the initiator to calculate full families of ACI which could then be applied to the solutions of higher order problems, such as the application of a matrix of ACI in the determination of the bound energy states of certain molecules.

BIBLIOGRAPHY

1. Jasperse, J.R., Physical Sciences Research Papers, No. 321. Air Force Cambridge Research Laboratories, AFCRL-67-0222, 1967.

2. Martine, J.E. & Power, L.F., Numerical and Data Analysis Techniques Applied to Scientific Research, Space Data Analysis Laboratory, Department of University Research, Boston College, 1973.

3. C.R.C. Standard Mathematical Tables, 11th ed., Chemical Rubber Publishing Company, Cleveland, 1957, p. 351.

4. Calabi, L., Scientific Report No. 1, The Integration of Certain Volume Integrals, Parke Mathematical Laboratories, Carlisle, Mass., 1968.

Fourier Analysis of Wind Sensor Data

Initiator: Dr. E. Dewan

Problem No: 4806 Project No: 6687

This problem involved Fourier Analyses of wind sensor data. The process used in this analysis is to find the average Power Spectral Densities (P.S.D.) of many consecutive (8192 points) sets of input data. The averaging procedure should improve the stability of the results.

In order to improve the results of the analysis, the data is pre-whitened before finding its P.S.D. and then post-darkened after the P.S.D. is calculated. Pre-whitening is useful in order to minimize leakage of Fourier power from the very large low frequency power to the smaller high frequency power. The pre-whitening used is to analyze first differences of the data. The effect of using the first differences is to multiply the original P.S.D. by $2-2\cos\left(\frac{F\pi}{Ny}\right)$ where F is the frequency in cycles per time unit and Ny is the nyquist frequency. Post-darkening is accomplished by dividing the resultant P.S.D. by $2-2\cos\left(\frac{F\pi}{Ny}\right)$ to remove the effects of pre-whitening.

The results of this problem is a P.S.D. which decreases rapidly with increasing frequency until about 2/3 the nyquist frequency and then begins to level off with frequency. These results were not unexplainable and have been used by the investigator.

Fourier Analysis of Doppler Data

Initiator: Dr. Kurt Toman

Problem No: 4810 Project No: 5631

This problem involved Fourier analyzing Doppler and various control data. The Initiator wished to study how the Power Spectral Density (P.S.D.) of his data varied with time. Towards this end short segments of the data were analyzed for their (P.S.D.). The data segments analyzed were for a particular time duration (T). Generally, all data segments for which the time duration (T) of the data was available were analyzed and the resultant P.S.D. versus frequency was plotted for each possible starting time. This set of plots will be referred to as the isometric plots.

Originally, linear methods of Fourier analysis were used to analyze the data; but in this most recent problem, a method known as the "maximum entropy method" (M.E.M.) has been used. M.E.M. was originally suggested by Burg (1967). In the analysis for this problem the method used is that described by N. Andersen[1]. Recently, it has been suggested that the algorithm used by Andersen is inaccurate (Dr. Paul F. Fougere of AFCRL private communication) and a "new" algorithm is to be tried. However, under our existing contract (F19628-73-C-0136) the Andersen algorithm has already been explored. The Andersen algorithm was independently derived and programmed by Dr. Rajan Varad[2] of this laboratory and his subroutine was modified and used in the studies. The flow chart derived by Andersen follows:

---

[1] On the Calculation of Filter Coefficients for Maximum Spectral Analyses by N. Andersen in Geophysics Vol. 39, No. 1 (February 1972) p. 69-72.

[2] Data Processing With Different Techniques for Cross-Power Spectra by W. Pfister, G.S. Sales and R. Varad. Environmental Research Papers 506 AFCRL Report PR 75-0194.

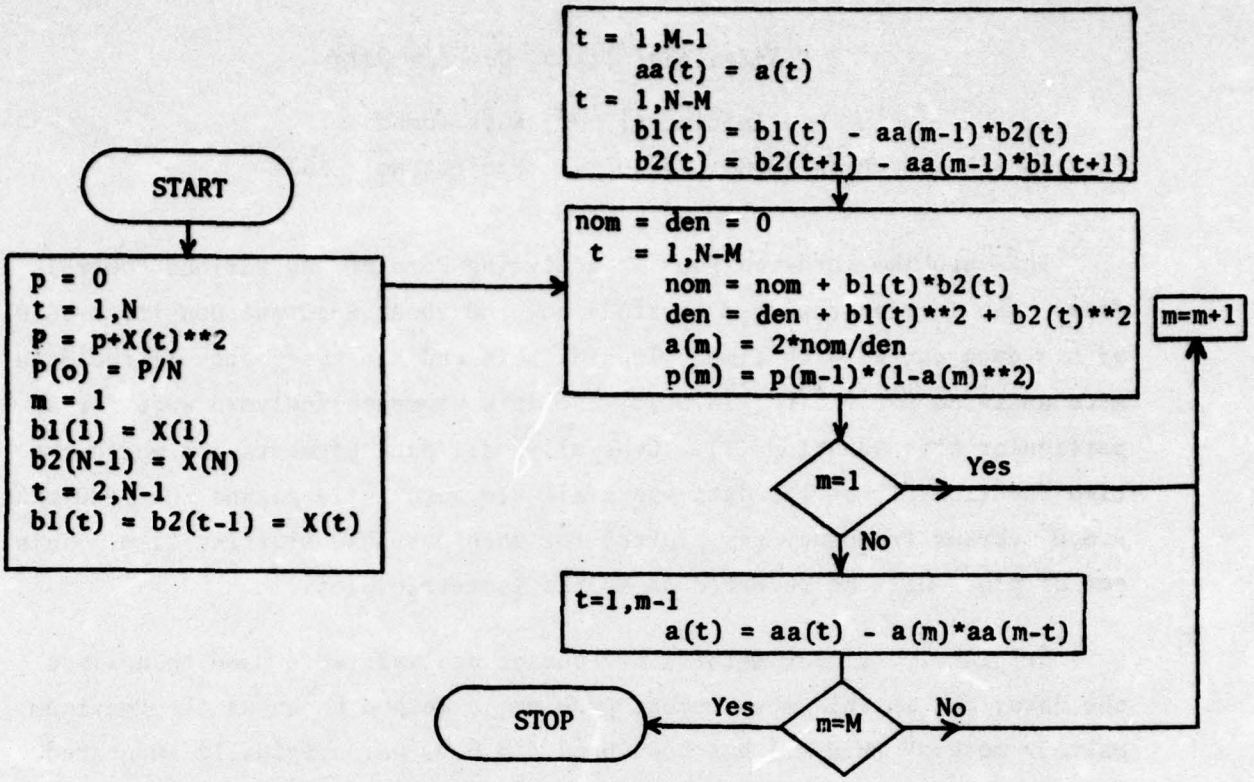

From a set of N equally spaced values (x(t)), this algorithm finds M coefficients (a_m) and the square residuals of the linear filter (P_M) such that for a time spacing Δt the P.S.D. for any frequency P(f) between 0 and the nyquist frequency is.

$$P(f) = \frac{P_M * \Delta t}{\left| 1 - \sum_{m=1}^{M} a_m e^{-2\pi i * f * m * \Delta t} \right|^2}$$

In the program, written for this problem, P(f) is initially calculated for a grid of f values (f_i). This grid is usually made up of equally spaced f values. The equal spacing is modified, however, to assure plotting at frequencies specified by the Initiator. The results are modified whenever a maximum is found in the $P(f_i)$ values and the maximum $P(f_j)$ occurs where $3 \leq j \leq N-2$. In this case, the values of $P(f_{j-2})$, $P(f_{j-1})$, $P(f_j)$, $P(f_{j+1})$ $P(f_{j+2})$ are modified by using the average values found by applying a trapezoidal rule to the P(f) between $f_{j-2} \leq f \leq f_{j+2}$. Thus, let

$$\overline{P(f_{j-2})} = \overline{P(f)} \; ; \; f_{j-2} \leq f \leq \frac{f_{(j-2)} + f_{(j-1)}}{2}$$

$$\overline{P(f_{j-1})} = \overline{P(f)} \; ; \; \frac{f_{j-2} + f_{j-1}}{2} \leq \frac{f_{j-1} + f_j}{2}$$

$$\overline{P(f_j)} = \overline{P(f)} \; ; \; \frac{f_{j-1} + f_j}{2} \leq f \leq \frac{f_j + f_{j+1}}{2}$$

$$\overline{P(f_{j+1})} = \overline{P(f)} \; ; \; \frac{f_j + f_{j+1}}{2} \leq f \leq \frac{f_{j+1} + f_{j+2}}{2}$$

$$\overline{P(f_{j+2})} = \overline{P(f)} \; ; \; \frac{f_{j+1} + f_{j+2}}{2} \leq f \leq f_{j+2}$$

and then $P(f_i)$ is reset to

$$P(f_{j-2}) = \frac{P(f_{j-2})\,(f_{j-2} - f_{j-3}) + \overline{P(f_{j-2})}\,(f_{j-1} - f_{j-2})}{f_{j-1} - f_{j-3}}$$

$$P(f_{j-1}) = \overline{P(f_{j-1})}$$

$$P(f_j) = \overline{P(f_j)}$$

$$P(f_{j+1}) = \overline{P(f_{j+1})}$$

$$P(f_{j+2}) = \frac{P(f_{j+2})\,(f_{j+3} - f_{j-2}) + \overline{P(f_{j+2})}\,(f_{j+2} - f_{j+1})}{f_{j+3} - f_{j+1}}$$

where $f_0 = f_1$ and $f_{N+1} = f_N$

This correction is necessary because the maximum entropy method makes the P.S.D. very peaked, such that the amplitude of the peak is not a "good" measure and that is what the correction attempts to simulate. This idea was gleamed from reference (3) below.

---

[3] A Comparison of Power Spectral Estimates and Applications of the Maximum Entropy Method by Henry R. Radoski, Paul F. Fougere and Edward J. Zawalick in Journal of Geophysics Research Vol. 80, No. 4, February 1, 1975, p. 619-625.

The actual program, which will be submitted to the SUYA computer program library upon completion of this problem proceeds as follows:

a. Linearly interpolate the input data to assure equally spaced data.

b. Take a first difference of the input data. The program processes these first differences. This procedure has been found, empirically, to filter out a red-noise behavior of the initial data.

c. Find a set of coefficients from the M.E.M. for the entire data set. Calculate the P.S.D. and bar-graph the logarithm of the P.S.D. at a set of frequencies g_i. The g_i's are usually equally spaced with a spacing equal to a fraction (input data) of the resolution frequency found for a linear Fourier Analysis of the data. The spacing of the g_i's are varied to have the plotting frequencies specified by the Initiator.

d. Calculate and plot the "isometric" plots $P(f_i)$ described above.

e. Repeat c.

f. Calculate and plot the results of a Kolmogoroff-Smirnov Test on the results of c. This shows whether the data could be explained as due to random noise.

From the results of parts c. and f. above, it has been assumed that the procedure using the entire data set gives very stable, and probably accurate P.S.D.'s. The results of d. are more suspect but do seem to allow identification of the presence of power at particular frequencies and how the P.S.D.'s behave as a function of time.

To test the results of the program, several test runs were made. These runs were made on data consisting of one or more frequencies plus some random noise. The random noise was necessary because the M.E.M. breaks down when the noise level is zero. The test results show that the M.E.M. is

better than a linear Fourier Analysis in predicting the frequency of an input signal. The M.E.M., however, did show some error in the frequency found and some double peaks where single peaks should exist. It is hoped that the "correction" suggested by Dr. Paul Fougere will provide more accurate answers. Towards this end, a program is being written to test Dr. Fougere's "correction".

Analysis of Vapour Trail Data From Photographs

Initiator: Gordon Best

Problem No: 4818 Project No: 7635

This problem involved the analysis of photographic data representing a vapour trail released by a rocket. The task was to determine how the vapour trail behaved with time and thereby infer the velocity versus altitude profile. The difficulty arose from the fact that the altitude of the portions of the vapour trail seen in the photographs were unknown.

Attempts were made to fit the data to velocity versus altitude models with unknown parameters. These attempts were unsuccessful as the results indicated that a very "good" guess to the solution was necessary before the parameters could be determined. A more successful procedure eventually was instituted.

The method tried, under an earlier problem, involved finding a wind velocity versus altitude curve for each azimuth and elevation reading determined from the photographs. These wind velocity versus altitude curves are the locus of points which would lead to the particular azimuth and elevation reading.

Thus let $V_{I,J}(A)$ be the wind velocity of the I^{th} photograph, taken at the J^{th} site (assuming altitude A) [There are three sites (J values)]; then, for a particular azimuth and elevation reading say $V_{L,M}(A)$ the program searches for the minimum of min $|V_{L,M}(A) - V_{I,J}(A)|$ where $M \neq J$ and with this restriction, we search over all possible values of I, J and A. The program indicates the values of I, J, A and $V_{L,N}(A)$ determined by this procedure. The point $V_{L,M}(A)$, A may be one point of the desired velocity versus altitude profile. The results of this analysis gave a rough indication of the actual wind velocity as a function of altitude.

The procedure here was refined as follows:

To find a minimum of min $((V_{L,M}(A) - V_{I,J}(A))^2 + (V_{L,M}(A) - V_{s,t}(A))^2 + (V_{I,J}(A) - V_{s,t}(A))^2)$. Where $M \neq J$, $M \neq t$ and $J \neq t$, thus we consider one point from each site. Again, with these restrictions we search over all possible values of I, J, s, t and A. After finding I, J, s, t and A by this procedure the value of

$$\frac{V_{L,M}(A) + V_{I,J}(A) + V_{s,t}(A)}{3}$$

is considered to be a possible value of the wind velocity at altitude A. This procedure leads to a more refined estimate of the wind velocity as a function of altitude.

At the present time, the preceding method is being refined to interpolate between azimuth and elevation points. We hope to further refine the wind velocity profile.

In order to implement the following procedure, we need to find $V_{L,M}(A)$. Thus, let $\vec{X}_r$ be the position of the rocket at time t_R. Also let AZ, EL, t be the azimuth, elevation and time of the reading L,M. Further, let A be the altitude of the rocket at time t_R. Then if L,M is due to a vapour trail at altitude A, its coordinates (in rectangular coordinates) are calculated as follows:

Let ϕ be the geodetic latitude of the site

λ be the longitude of the site.

Then from (page),[1] a rectangular coordinate system of this site can be expressed as

[1] Application of Vector and Matrix Methods to Triangulation of Chemical Releases in the Upper Atmosphere by Antonio F. Quesada, AFCRL Environmental Research Paper No.: 351.

$$\vec{\rho} = \hat{X}\left[\frac{a}{\sqrt{1 - \varepsilon^2 \sin^2\phi}} + h\right]\cos\phi\cos\lambda$$

$$+ \hat{y}\left[\frac{a}{\sqrt{1 - \varepsilon^2 \sin^2\phi}} + h\right]\cos\phi\sin\lambda$$

$$+ \hat{z}\left[\frac{a(1-\varepsilon^2)}{\sqrt{1 - \varepsilon^2 \sin\phi}} + h\right]\sin\phi$$

where if the shape of the earth is assumed to be an ellipse

a is the semi-major axis (equatorial radius)

b is the polar radius

ε is the eccentricity

h is the altitude of the site

and therefore

$$\frac{dx}{d\phi} = -\left[\frac{a}{\sqrt{1-\varepsilon^2\sin^2\phi}} + h\right]\sin\phi\cos\lambda + \frac{a\varepsilon^2}{(1-\varepsilon^2\sin^2\phi)^{1.5}}\sin\phi\cos^2\phi\cos\lambda$$

$$\frac{dx}{d\lambda} = -\left[\frac{a}{\sqrt{1-\varepsilon^2\sin^2\phi}}\right]\cos\phi\sin\lambda$$

$$\frac{\partial x}{\partial h} = \sin\phi\cos\lambda$$

$$\frac{dy}{d\phi} = -\left[\frac{a}{\sqrt{1-\varepsilon^2\sin^2\phi}} + h\right]\sin\phi\sin\lambda + \frac{a\varepsilon^2}{(1-\varepsilon^2\sin^2\phi)^{1.5}}\cos^2\phi\sin\phi\sin\lambda$$

$$\frac{dy}{d\lambda} = \left[\frac{a}{\sqrt{1-\varepsilon^2\sin^2\phi}} + h\right]\cos\phi\cos\lambda$$

$$\frac{dy}{dh} = \cos\phi\sin\lambda$$

$$\frac{dz}{d\phi} = -\left[\frac{a(1-e^2)}{\sqrt{1-e^2\sin\phi}} + h\right]\cos\phi + \frac{ae^2(1-e^2)}{1-e^2\sin\phi}\sin^2\phi\cos\phi$$

$$\frac{dz}{d\lambda} = 0$$

$$\frac{dz}{dh} = \sin\phi$$

A reading of AZ,EL defines a vector in the direction ($\rho_{A,E}$)

$$\rho_{A,E} = \hat{h}\,(\sin(EL)) + \hat{\phi}\,(\cos(AZ)\cos(EL)) + \hat{\lambda}\,(-\sin(AZ)\cos(EL))$$

where $\hat{h}$, $\hat{\phi}$, and $\hat{\lambda}$ are vectors of unit length.

Now transformations of $\hat{h}$, $\hat{\phi}$, $\hat{\lambda}$ into $\hat{X}$, $\hat{Y}$, $\hat{Z}$ (vectors of unit length) coordinates is

$$\hat{X}_R = \sin(EL)\frac{dx}{dh} + (\cos(AZ)\cos(EL))\frac{dx}{d\phi} + (-\sin(AZ)\cos(EL))\frac{dx}{d\lambda}$$

$$\hat{Y}_R = \sin(EL)\frac{dy}{dh} + (\cos(AZ)\cos(EL))\frac{dy}{d\phi} + (-\sin(AZ)\cos(EL))\frac{dy}{d\lambda}$$

$$\hat{Z}_R = \sin(EL)\frac{dz}{dh} + (\cos(AZ)\cos(EL))\frac{dz}{d\phi} + (-\sin(AZ)\cos(EL))\frac{dz}{d\lambda}$$

where, in general, $\frac{da}{db}$ (a=x or y or z, b=h or ϕ or λ)

$$\frac{da}{db} = \frac{\frac{da}{db}}{\sqrt{\left(\frac{da}{dh}\right)^2 + \left(\frac{da}{d\phi}\right)^2 + \left(\frac{da}{d\lambda}\right)^2}}$$

Therefore, we can calculate the position of the site $(\hat{X}_s, \hat{Y}_s, \hat{Z}_s)$ and the possible points at which an azimuth, elevation reading point

$$\hat{X}_p = \hat{X}_s + B\hat{X}_r \tag{1a}$$

$$\hat{Y}_p = \hat{Y}_s + B\hat{Y}_r \tag{1b}$$

$$\hat{Z}_p = \hat{Z}_s + B\hat{Z}_r \tag{1c}$$

where B is a parameter.

Next we consider what value of B would explain an altitude A for the vapour trail. If the vapour trail is released at altitude A, it is assumed to be blown by constant winds (for the time interval considered) such that it stays at the same altitude above the earth. Thus, the position of the vapour trail is on an elipse which can be described as

$$\vec{r} = \hat{Z}\, b_r \sin s_2 + \hat{X}C + \hat{y}D \tag{2a}$$

with

$$C^2 + D^2 = a_r^2 \cos^2(s_2) \tag{2b}$$

where $a_r = a+A^2$, $b_r = b+A$ and s is arbitrary. Then we must have from (1) and (2)

$$b_r \sin(s_2) = Z_s + BZ_R \tag{3}$$

and

$$a_r^2 \cos^2(s_2) = (Y_s + BY_R)^2 + (Z_s + BZ_R)^2 \tag{4}$$

Assume we guess $s_2 = s^*$ $B = B^*$

Then

$$E_1 = b_r \sin(s_2^*) - Z_s - B^* Z_R \tag{3a}$$

$$E_2 = a_r^2 \cos^2(s_2^*) - (X_s + B^* X_R)^2 - (Y_s + B^* Y_R)^2 \tag{4a}$$

$$\frac{\partial E_1}{\partial s^*} = b_r \cos(s_2^*)$$

$$\frac{\partial E_1}{\partial B^*} = -Z_R$$

$$\frac{\partial E_2}{\partial s^*} = -2a_r^2 \sin(s_2^*) \cos(s_2^*)$$

$$\frac{\partial E_2}{\partial B^*} = -2 X_R(X_s + B^* X_R) - 2 Y_R(Y_s + B^* Y_R)$$

and using Newton-Raphson's method we can converge to a solution for B and s_2.

We also know the original position of the rocket so $s_1 = \tan^{-1}$ $(\frac{b_r}{a_r} \tan \phi_s)$ where ϕ_s is the latitude of the rocket at altitude A.

Then assume constant latitudinal winds $K_1(A)$ at altitude A or

$$K_1(A) = \sqrt{a_r^2 \sin^2 s + b_r^2 \cos^2 s} \ \frac{ds}{dt}$$

$$\Rightarrow \quad K_1(A)\ (t-t_R) = \int_{s_1}^{s_2} a_r \sqrt{1 + \frac{(b_r^2-a_r^2)}{a_r^2} \cos^2(s)}\ ds$$

and since $b_r \sim ar$

$$K_1(A)\ (t-t_R) \sim \int_{s_1}^{s_2} ar\left(1 + \frac{1}{2}\left(\frac{b_r^2-a_r^2}{a_r^2}\right) \cos^2(s)\right) ds$$

or

$$K_1(A)\ (t-t_R) \sim a_r \left[s + \frac{1}{4}\left(\frac{b_r^2-a_r^2}{a_r^2}\right) (s + \sin(s)\ \cos(s)\right]_{s_1}^{s_2}$$

and

$$K_1(A) \sim \frac{1}{(t-t_R)}\ a_r\left[s_2 - s_1 + \frac{1}{4}\left(\frac{b_r^2-a_r^2}{a_r^2}\right)\ (s_2 - s_1 + \sin(o_2)\ \cos(s_2) - \sin(o_1)\ \cos(o_1)\right]$$

Then since we assume the longitudinal winds are constant $K_2(A)$ at altitude A

$$\frac{d\lambda}{ds}\, b_r \sin s = K_2(A)$$

or from

$$\frac{d\lambda}{ds} = \frac{d\lambda}{dt}\,\frac{dt}{ds}$$

$$\frac{d\lambda}{ds} = \frac{K_2(A)\sqrt{a_r^2 \sin^2(s) + b_r^2 \cos^2(s)}}{K_1(A)\, b_r \sin s}$$

$$d\lambda = \frac{K_2(A)}{b_r K_1(A)} \sqrt{a_r^2 + b_r^2 \frac{\cos^2(s)}{\sin^2(s)}}\, ds$$

Using

$$a_r^2 = a_r^2 \sin^2(s) + a_r^2 \cos^2(s)$$

$$\Rightarrow \frac{a_r}{\sin^2(s)} = a_r^2 + a_r^2 \frac{\cos^2(s)}{\sin^2(s)}$$

$$d\lambda = \frac{K_2(A)\, a_r}{b_r K_1(A) \sin(s)} \sqrt{1 + \frac{(b_r^2 - a_r^2)\cos^2 s}{a_r^2}}\, ds$$

$$d\lambda \sim \frac{a_r K_2(A)}{b_r K_1(A) \sin(s)} \left(1 + \frac{1}{2}\left(\frac{b_r^2 - a_r^2}{a_r^2}\right) \cos^2 s\right) ds$$

Now since

$$\int \frac{ds}{\sin s} = \ln\left(\tan\left(\frac{s}{2}\right)\right) + \text{Constant}$$

and

$$\int \frac{\cos^2 s\, ds}{\sin s} = \int \frac{ds}{\sin s} - \int \sin s\, ds = \log\left(\tan\left(\frac{s}{2}\right)\right) + \cos s + \text{Constant}$$

This yields

$$(\lambda_p - \lambda_r) \sim \frac{a_r K_2(A)}{b_r K_1(A)} \int_{s_1}^{s_2} \left[\log(\tan(\tfrac{s}{2})) \left(1 + \frac{1}{2}\left(\frac{b_r^2 - a_r^2}{a_r^2}\right) + \frac{1}{2}\left(\frac{b_r^2 - a_r^2}{a_r^2}\right) \cos(s)\right)\right]$$

where λ_p, λ_r is the longitude of the vapour trail at time t, rocket at time t_R with

$$\lambda_p = \tan^{-1}\left(\frac{Y_s + BY_R}{X_o + BX_R}\right)$$

Let

$$S = \left(\log(\tan(\tfrac{s_2}{2})) - \log(\tan(\tfrac{s_1}{2}))\right)\left(1 + \frac{1}{2}\,\frac{b_r^2 - a_r^2}{a_r^2}\right)$$

$$+ \frac{1}{2}\left(\frac{b_r^2 - a_r^2}{a_r^2}\right)\left(\cos(s_2) - \cos(s_1)\right)$$

Then finally

$$K_2(A) \sim \frac{b_r(\lambda_p - \lambda_r)\, K_1(A)}{a_r\, s}$$

Using this analysis many velocity versus altitude curves were calculated, plotted and compared. The results for one group of data lead to an estimate of a wind velocity versus altitude profile. The results of another set of data seem to indicate some inconsistency in the data.

This work is continuing.